2016

Examination of the cellular stress response and post-transcriptional regulation of RNA during Ebola virus infection

BOSTON UNIVERSITY

SCHOOL OF MEDICINE

Dissertation

EXAMINATION OF THE CELLULAR STRESS RESPONSE AND POST-TRANSCRIPTIONAL REGULATION OF RNA DURING EBOLA VIRUS INFECTION

by

EMILY VICTORIA NELSON

B.S., The George Washington University, 2010

Submitted in partial fulfillment of the

requirements for the degree of

Doctor of Philosophy

2016

Approved by

First Reader _____

Elke Mühlberger, Ph.D.

Associate Professor of Microbiology

Second Reader _____

Rachel Fearns, Ph.D.

Associate Professor of Microbiology

DEDICATION

For my family, especially my sisters April and Elizabeth, who have unfailingly supported me in all my endeavors.

.

ACKNOWLEDGMENTS

I am indebted to the scientists who performed the BSL-4 work contained within this dissertation: Dr. Kristina Schmidt, Dr. Judith Olejnik, Dr. Adam Hume and Dr. Laure Deflubé-Owen in the Mühlberger lab, as well as Dr. Logan Banadyga at Rocky Mountain Laboratories in Hamilton, MT. In addition, all of the fluorescence in-situ hybridization experiments and data were done by Dr. Sultan Doganay in the lab of Dr. Taekjip Ha at the University of Illinois Urbana Champaign. I am also indebted to Dr. Nancy Kedersha at Brigham and Women's Hospital for all her advice and reagents.

I would like to thank the members of the Mühlberger lab, past and present, for all their kindness and support. Importantly, they taught me so much over the years but still always treated me as a peer. Their friendship and respect in both the lab and the real world made coming to lab every day more than just a job. Importantly, I would like to thank Elke for her mentorship and for all of the things she has taught me over the years. Her strength of character and utter fearlessness have been an invaluable influence on my development as a scientist.

My thesis committee has also been an incredibly important source of help and advice and I cannot thank them enough for their support. In particular, they have taught me how to communicate my science to the best of my capability and I am a better scientist because of them. The brilliant women on my thesis committee have been inspirational examples of strong female scientists, and I am thankful for their unique perspectives and positive influences on my scientific growth. I would also like to especially thank Dr. Greg "Big G" Viglianti for not only serving as my committee chair,

but also for being one of the most encouraging and understanding people in my graduate school career. Additionally, I would like to thank Dr. Rachel Fearns for being my second reader, and Dr. Susan Winandy and Dr. Paul Duprex for being valuable members of my thesis committee.

I am grateful for all the guidance and support that I have received through the department of Microbiology and the NEIDL. Dr. Ron Corley in particular has made my time in the department and at the NEIDL an incredible learning experience and provided me with a number of opportunities to enjoy science outside of the lab and give back to my community. Importantly, the graduate students and other members of the department have been an indispensable source of comfort and friendship, without which I would have truly been unable to survive graduate school. This particularly applies to all of the following goofballs: Kristie Hilliard, Ken Barth, Kate Sawatzki, Greg Wasserman, Munir Mosaheb, Daniel Cary, Fadie Coleman, Nicole Stauffer, and Nora Ramirez. I cannot express how fortunate I am to have them all in my life.

EXAMINATION OF THE CELLULAR STRESS RESPONSE AND POST-TRANSCRIPTIONAL REGULATION OF RNA DURING EBOLA VIRUS INFECTION

EMILY VICTORIA NELSON

Boston University School of Medicine, 2016

Major Professor: Elke Mühlberger, Ph.D., Associate Professor of Microbiology

ABSTRACT

Ebola virus (EBOV) causes severe disease in humans characterized by high case fatality rates and significant immune dysfunction. A hallmark of EBOV infection is the formation of viral inclusions in the cytoplasm of infected cells. These inclusions contain the EBOV nucleocapsids and are sites of viral replication and nucleocapsid maturation. Although there is growing evidence that viral inclusions create a protected environment that fosters EBOV gene expression and genome replication, little is known about their role in the host response to infection. The cellular stress response is an antiviral strategy that leads to stress granule (SG) formation and translational arrest mediated by the phosphorylation of the alpha subunit of eukaryotic translation initiation factor 2 (eIF2α). Related to this response is the post-transcriptional regulation of RNA mediated by stability elements called AU-rich elements (AREs) and their associated binding proteins (ARE-BPs), many of which are found in SGs. Because these processes have antiviral implications, many viruses have evolved strategies to interfere with SG formation, or

appropriate ARE-BPs to benefit viral replication. However, it is unknown if EBOV interacts with these cellular systems. Here, we show that SG proteins were sequestered within EBOV inclusions where they formed distinct granules that colocalized with viral RNA. The inclusion-bound aggregates were not canonical SGs, and did not lead to translational arrest in infected cells. EBOV did not induce cytoplasmic SGs at any time post infection, but was unable to overcome SG formation induced by additional stressors. Despite the sequestration of SG proteins, canonical SGs did not form within inclusions. At high levels of expression, viral protein 35 (VP35), the viral polymerase co-factor that also mediates various immune evasion functions, disrupted SGs formation independently of eIF2α phosphorylation. Finally, we found that the cellular ARE-BP tristetraprolin (TTP) specifically targeted the 3'untranslated region (UTR) of the viral nucleoprotein (NP) mRNA and promoted its degradation. Interestingly, TTP was not found within viral inclusions, leading us to speculate that inclusions might serve to prevent viral RNA from encountering TTP. These results indicate that EBOV interacts with the cellular stress response and associated RNA regulatory proteins in ways that promote viral replication.

TABLE OF CONTENTS

LIST OF TABLES

LIST OF FIGURES

LIST OF ABBREVIATIONS

ARE..... AU Rich Element

ARE-BP ..... AU Rich Element Binding Protein

ARS.....Arsenite

B-gal .....Beta-Galactosidase

BDBV .....Bundibugyo Virus

BRF1 ..... Butyrate Response Factor 1

BSA ..... Bovine Serum Albumin

BSL .....Biosafety Level

CD .....Cluster of Differentiation

CDC .....Centers for Disease Control and Prevention

CHX .....Cycloheximide

CLB .....Cell Lysis Buffer

DMEM .....Dulbecco's Modified Eagle Medium

DMSO.....Dimethyl Sulfoxide

DNA..... Deoxyribonucleic Acid

DOXY.....Doxycycline

DRC ..... Democratic Republic of Congo

dsRNA .....Double Stranded RNA

EBOV..... Ebola Virus

eGFP .....Enhanced Green Fluorescent Protein

eIF .....Eukaryotic Translation Initiation Factor

ELAV ..... Embryonic Lethal Abnormal Vision

EM ..... Electron Microscopy

ER ..... Endoplasmic Reticulum

EtOH ..... Ethanol

EVD ..... Ebola Virus Disease

FBS ..... Fetal Bovine Serum

FISH ..... Fluorescence In-situ Hybridization

g ..... Gram

G3BP ..... Ras-GTPase Activating Protein Binding Protein 1

GCN2 ..... General Control Nonderepressible 2

GFP ..... Green Fluorescent Protein

GM-CSF ..... Granulocyte Macrophage Colony Stimulating Factor

HCl ..... Hydrochloric Acid

HCV ..... Hepatitis C Virus

HIPP ..... Hippuristanol

HIV ..... Human Immunodeficiency Virus

hnRNP ..... Heterogeneous Nuclear Ribonucleoprotein D

h ..... Hour

HRI ..... Heme-regulated Inhibitor Kinase

HuR ..... Human Antigen R

IAV ..... Influenza Virus

IDR ..... Intrinsically Disordered Region

IFA .....Immunofluorescence Analysis

IFN .....Interferon

IID .....Interferon Inhibitory Domain

IG .....Immunoglobulin

IKBα Nuclear Factor Of Kappa Light Polypeptide Gene Enhancer in B Cells Inhibitor Alpha

IL .....Interleukin

IRF .....Interferon Regulatory Factor

L-HPG..... L-homopropargylglycine

LB .....Lysogeny B

LPS.....Lipopolysaccharide

MAPK.....Mitogen Activated Protein Kinase

MCS .....Multiple Cloning Site

mg .....milligram

min .....Minute

MK2 .....Mitogen Activated Protein Kinase Activate Protein Kinase 2

ml .....Milliliter

mM..... Millimolar

MOI.....Multiplicity of Infection

mRNA .....Messenger RNA

NaCl ..... Sodium Chloride

NC .....Nucleocapsid

NFKB..... Nuclear Factor Kappa Light Chain Enhancer of Activated B cells

ng.....Nanogram

NIAID .....National Institute of Allergy and Infectious Disease

NIH .....National Institutes of Health

NP .....Nucleoprotein

NNS .....Nonsegmented Negative Sense

ORF..... Open Reading Frame

P-body .....Processing Body

p-value..... Probability Value

p.i. ..... Post-infection

PABP .....Poly A Binding Protein

P-Body ..... Processing body

PBS .....Phosphate Buffered Saline

PCR..... Polymerase Chain Reaction

PFA ..... Paraformaldehyde

PFU .....Plaque Forming Unit

PKR..... Protein Kinase R

PMA..... Phorbol Myristate Acetate

Pol .....Polymerase

PVDF .....Polyvinylidene Difluoride

qRT-PCR .....Quantitative Real Time Polymerase Chain Reaction

RBP .....RNA Binding Protein

RDRP .....RNA Dependent RNA Polymerase

REBOV ..... Reston Virus

RIG-I ..... Retinoic Acid Inducible Gene 1

RNA ..... Ribonucleic Acid

RNP ..... Ribonucleoprotein

RPMI ..... Roswell Park Memorial Institute Media

RSV ..... Respiratory Syncytial Virus

RT-PCR ..... Reverse Transcription Polymerase Chain Reaction

SDS ..... Sodium Dodecyl Sulfate

SDS-PAGE ..... Sodium Dodecyl Sulfate Polyacrylamide Gel Electrophoresis

SEBOV ..... Sudan Virus

SG ..... Stress Granule

siRNA ..... Small Interfering RNA

ssRNA ..... Single Stranded RNA

STAT ..... Signal Transducers and Activators of Transcription

TAFV ..... Taï Forest Virus

TBS ..... Tris-buffered Saline

TCID ..... Tissue Culture Infective Dose

TEM ..... Transmission Electron Microscopy

TIA-1 ..... T-cell Restricted Intracellular Antigen 1

TLR ..... Toll-like Receptor

TNF ..... Tumor Necrosis factor

tRNA ..... Transfer RNA

TTP ..... Tristetraprolin

USP10 ..... Ubiquitin Carboxyl-Terminal Hydrolase 10

UTR..... Untranslated Region

VP ..... Viral protein

VRC ..... Vanadyl Ribonucleoside Complex

VSV ..... Vesicular Stomatitis Virus

WB ..... Western Blot

ZAP ..... Zinc Finger Antiviral Protein

ZEBOV ..... Zaire Ebola virus

μg ..... microgram

μl ..... microliter

μm ..... micrometer

CHAPTER ONE: INTRODUCTION

Ebolaviruses

History and Epidemiology

The first documented cases of Ebola virus disease (EVD) occurred in 1976 from two simultaneous outbreaks of a hemorrhagic fever described in southern Sudan and northern Zaire, or what is now the Democratic Republic of the Congo (DRC) (Bowen et al., 1977; Kuhn, 2008). The outbreak in Sudan reported 284 cases with 151 deaths (Team, 1978), while the outbreak in Zaire reported 318 cases and 280 deaths (Commission, 1978). The unidentified disease presented similar illness to that of Marburg virus disease, which had been discovered only nine years previously (Kissling, Robinson, Murphy, & Whitfield, 1968; Slenczka & Klenk, 2007). It was later determined that these two outbreaks were caused by two distinct species of ebolavirus, named after the Ebola river in the DRC. According to the Centers for Disease Control and Prevention (CDC), since the initial outbreaks of EVD in 1976, there have been approximately 30 additional documented human outbreaks, of varying size and severity (CDC, Outbreaks Chronology, 2016). The most complex and widespread outbreak began at the end of 2013 in the West African nation of Guinea (Baize et al., 2014). Although the outbreak began in Guinea, there were 10 countries in total with reported cases, including four nations outside the continent of Africa. The greatest burden of disease fell upon only three countries however, Guinea, Liberia and Sierra Leone. According to the World Health Organization, as of January 20th, 2016 there were 28,638 total reported cases (this number includes suspected, probable and confirmed cases) with 11,301 reported deaths

(World Health Organization, 2016). On January 14th 2016, Guinea, Liberia and Sierra Leone were declared Ebola free, as each country had completed the requisite 90 day surveillance period (World Health Organization, 2016). However, since this declaration a number of residual cases continue to appear, indicating that ending the outbreak will be difficult. The number of cases and fatalities reported for this outbreak far exceeds the total of all previous outbreaks combined. Even taking into considering the scale of the West African outbreak, the global health burden of EVD remains quite low. Prior to 2014, there were only about 2,000 reported EVD cases with about 1500 deaths (CDC, Outbreaks Chronology, 2016), although under reporting due to the remote nature of most outbreaks is likely. The severity of disease and lack of viable treatment or vaccine options classify ebolaviruses as biosafety level 4 (BSL-4) pathogens and Category A priority pathogens by the United States Government (NIAID, 2015).

Taxonomy

Ebolaviruses belongs to the order *Mononegavirales*, a taxonomic grouping of viruses that possess a nonsegmented, negative-sense (NNS) RNA genome. This order is comprised of five virus families, including the family *Filoviridae*. Within the filovirus family there are three separate genera: *Cuevavirus*, of which no full-length viruses have been successfully isolated (Negredo et al., 2011), *Marburgvirus*, and *Ebolavirus*. There are five *Ebolavirus* species in total that all differ in their disease severity (Kuhn, Bào, et al., 2014b). *Zaire ebolavirus* (EBOV) is the most pathogenic, with case fatalities rates ranging from 40-90%, followed by *Sudan ebolavirus (*SUDV*), Bundibugyo ebolavirus*

(BDBV), *Taï Forest ebolavirus* (TAFV), and finally *Reston ebolavirus* (RESTV), of which there have been no documented human cases (Feldmann, 2014; Feldmann & Geisbert, 2011a). Most outbreaks of EVD are caused by either EBOV or SUDV, with the most recent 2014 West African outbreak caused by the Makona strain of EBOV (Baize et al., 2014; Kuhn, Andersen, et al., 2014a). There has been only one documented non-fatal case of TAFV(Le Guenno et al., 1995). BDBV is the most recently discovered ebolavirus, identified from an outbreak in Uganda in 2007 (Towner et al., 2008). There have been no human cases of RESTV, but reported epidemics in nonhuman primates and pigs (Barrette et al., 2009; Editorial team, 2009; T. W. Geisbert, Jahrling, Hanes, & Zack, 1992; M. E. G. Miranda & Miranda, 2011; Rollin et al., 1999).

Ecology

With the exception of RESTV, ebolaviruses are endemic to Africa, with outbreaks typically occurring in equatorial regions of the continent. Prior to the 2014 outbreak in West Africa, only one case of a natural EVD infection had ever been documented in humans outside of this central African region. This incident involved only one case of TAFV in Cote d'Ivoire, which the patient survived (Le Guenno, Formenty, & Boesch, 1999). Interestingly, RESTV was the first documented natural infection of an ebolavirus in nonhuman primates in the Philippines, as well as the only virus in this family with origins outside of Africa (M. E. G. Miranda & Miranda, 2011).

Due to the severity of disease and high case fatality rates in both humans and nonhuman primates associated with many ebolaviruses, it is thought that these species do

not represent a suitable reservoir. Combined with the notion that a majority of emerging infectious diseases are zoonotic in nature (K. E. Jones et al., 2008), considerable effort has been made attempting to identify a host species or arthropod vector. An extensive sampling study of wildlife in areas near outbreaks of chimpanzee and gorilla populations in Gabon and the DRC suggested that fruit bats might represent a potential reservoir. This conclusion was based on the presence of virus specific IgG in serum collected from three different bat species, as well as viral nucleotide sequences detected by PCR (Leroy et al., 2005). However, in this study viral RNA was never isolated from any bat, making it difficult to conclude with certainty that they are in fact the reservoir. Intriguingly, it was later discovered that the fruit bat *Rousettus aegyptiacus* might be the reservoir species for Marburg virus (Towner et al., 2007). Bats are encountered quite frequently in filovirus endemic areas, and represent a common food source for many people in these regions (Leroy et al., 2009). While it is still unclear what the precise animal reservoir(s) may be, evidence strongly points to fruit bats as hosts.

Clinical Course of Disease

Clinical Manifestations

The severity of EVD is dependent upon on the species or strain and can vary considerably. It is important to note that outbreaks typically occur in geographically remote locations in populations with a high prevalence of comorbidities. This has made it difficult to study the clinical course of disease in humans. However, it is generally thought that the course of disease occurs quite rapidly with symptoms that are often

severe and complex. The viral incubation period ranges from 2-21 days followed by the abrupt onset of non-specific symptoms including fever and malaise. These symptoms quickly develop into more severe and systemic symptoms including nausea, vomiting, anorexia, and diarrhea. Signs of hemorrhage, attributed in part by disseminated intravascular coagulation, are present in less than half of patients but typically present at the height of infection and are characterized by mucosal hemorrhage and uncontrollable bleeding from venipuncture sites (T. W. Geisbert, Young, et al., 2003b). A macropapular rash is also often a characteristic at later stages of infection. Those who succumb to fatal infection typically die from complications associated with hypovolemic shock, multi-organ failure, and severe metabolic dysfunction (Bah et al., 2015; Lyon et al., 2014; T. W. MD et al., 2015b; Zaki & Goldsmith, 1999). Recent data collected from survivors during the 2014 West African outbreak indicate that convalescence is associated with a number of sequelae, many of which are still poorly understood. Common among these include severe headaches and other neurological symptoms, joint pain, and ocular degeneration ("Examination of the Retina," 2015; Mattia et al., 2015). The complications of what is being termed "post-Ebola syndrome" are of increasing interest to both researchers and clinicians alike.

Transmission

As zoonotic pathogens, ebolaviruses can spread between and among animals and humans. Animal to human transmission typically occurs through the hunting and consumption of infected animals, or the handling of animal carcasses. Successful human-

to-human transmission also only occurs via close contact with bodily fluids of an infected individual. Outbreaks are often initiated by a single introduction of virus from wildlife, either the reservoir species or another end host species (Baize et al., 2014; Feldmann & Geisbert, 2011). Sites of exposure typically include mucosal surfaces or breaks in the skin barrier. Laboratory exposure, although rare, has also been reported, and was due to needlestick injury or improper handling of blood (Emond, Evans, Bowen, & Lloyd, 1977; "ProMED-mail post," 2016; rpt4, 2008).

Although not exhaustively studied, evidence indicates that EBOV can remain in certain areas of the body for extended periods of time, even after the apparent clearance of virus from the blood. These sites include the central nervous system, the eye, breast milk and semen (Akerlund, Prescott, & Tampellini, 2015; Heeney, 2015; Kelly, Richardson, & Barry, 2015). A recent study examined the persistence of EBOV in the semen of male survivors and found that viral RNA could be detected in seminal fluid up to nine months after the onset of illness (G. F. Deen et al., 2015; Mate et al., 2015). This finding is therefore indicative of spread through sexual contact. Other evidence suggestive of viral persistence or latency includes the reports from one survivor who was found to harbor EBOV within his eye after discharge from the hospital and in spite of negative blood and urine tests (Varkey et al., 2015; Yeh, Varkey, & Crozier, 2015). These examples of viral persistence despite disease recovery highlight the need to examine latency more closely.

Treatments and Vaccines

As of January 2016 there are no licensed vaccines or therapeutic options available for EVD. Currently, treatment is limited to intensive supportive care, with particular emphasis on rehydration, nutritional support and treatment of comorbidities (J. Deen, Dondorp, & White, 2015b; Mehta, Lyon, & Varkey, 2015). A number of experimental treatments have been employed during the 2014 West African outbreak (Hoenen & Feldmann, 2014) including the use of convalescent serum or plasma (van Griensven, De Weiggheleire, et al., 2016; van Griensven, Edwards, et al., 2016), small interfering RNAs (siRNAs) (Kraft et al., 2015), and monoclonal antibody cocktails (Lyon et al., 2014; Marzi et al., 2012; Qiu et al., 2013). Many of these potential therapeutics are undergoing testing in clinical trials but their efficacy remains inconclusive. Similarly, testing and clinical trials of a number of experimental vaccines were also made a priority during the 2014 outbreak. While a number of vaccines have been developed and tested in animal models of EVD (Hoenen, Groseth, & Feldmann, 2012; Marzi & Feldmann, 2014), not all have been approved for use in humans. A number of promising candidates have emerged however, and include a recombinant vesicular stomatitis virus (VSV) based vaccine (Agnandji et al., 2015; Huttner et al., 2015; Marzi et al., 2015) and chimpanzee adenovirus 3-based vaccine(M. D. T. MD et al., 2015a; Stanley et al., 2014). Phase II and III clinical trials of each vaccine are currently underway in West Africa (World Health Organization, 2015).

Viral Components and Pathogenesis

Genome and Viral Proteins

As a member of the order *Mononegavirales*, EBOV possesses a non-segmented negative-sense RNA genome that is roughly 19 kilobases in length. The single stranded genome, depicted in Figure 1, encodes seven genes that produce seven structural proteins. At the terminal 3' and 5' ends of the genome are extragenic regions termed the leader and trailer, that contain promoters for replication and transcription (Mühlberger, 2007; Neumann, Watanabe, & Kawaoka, 2009). The seven structural proteins produced include the nucleoprotein (NP), the polymerase cofactor viral protein 35 (VP35), the matrix protein VP40, the glycoprotein (GP), transcriptional cofactor VP30, the minor matrix protein VP24, and the polymerase L. Viral replication and transcription take place in the cytoplasm of infected cells and are carried out by the RNA-dependent RNA polymerase (RDRP) L, in conjunction with VP35 and VP30. Like other NNS viruses, the EBOV polymerase complex initiates transcription at a single transcription promoter at the 3' end of the genome then proceeds towards the 5'end to transcribe each gene sequentially. The polymerase is thought to occasionally dissociate from the genome, predominantly at the gene borders, forcing it to reinitiate transcription back at the 3' transcription promoter. This creates a gradient of transcribed viral mRNAs, with a higher abundance of transcripts produced from genes found closer to the transcription promoter compared to those more distally located (Brauburger et al., 2014; Shabman et al., 2013; Whelan, Barr, & Wertz, 2004). The seven resulting monocistronic mRNAs are all 5'-capped and 3'-polyadenylated. Replication leads to the production of a positive-sense replication

intermediate called the antigenome. This intermediate serves as a template for genome replication. Both the genome and the antigenome are encapsidated by the nucleocapsid complex, composed of NP, VP35, VP30 and VP24 (genome replication and transcription reviewed in (Messaoudi, Amarasinghe, & Basler, 2015; Mühlberger, 2007; Neumann et al., 2009).

Figure 1. Schematic of the EBOV genome.

The EBOV negative sense ssRNA genome is approximately 19 kb in length and contains seven genes. Each gene, represented by a green box, contains an open reading frame (ORF) that is flanked by long untranslated regions (UTRs). At each end of the genome are short extragenic regions, the leader and the trailer. The leader and the trailer compliment, which is found on the antigenome, contain cis-acting elements required for replication and transcription. Figure is not drawn to scale.

Pathogenesis

EBOV entry into the body typically occurs though a mucosal surface or a breach in the skin barrier. Primary targets of infection include monocytes, macrophages and dendritic cells (T. W. Geisbert, Hensley, et al., 2003a; Ryabchikova et al., 1996). These cells presumably contribute to the widespread dissemination of the virus from initial sites of infection to nearly every tissue in the body, particularly the liver and spleen, via the blood and lymphatic system. EBOV infection leads to significant immune dysfunction, starting with the release of inflammatory cytokines and chemokines (Baize et al., 2002; Mohamadzadeh, Chen, Olinger, Pratt, & Schmaljohn, 2006). Fatal infection is characterized by an uncontrolled inflammatory response that contributes to a state of sepsis-like shock (Baize et al., 2002; 1999; Feldmann & Geisbert, 2011a). Infection studies using monocyte-derived dendritic cells showed that EBOV infection prevents their maturation and subsequent interaction and antigen-presenting function to T cells (Bosio et al., 2003; Lubaki et al., 2013; Mahanty et al., 2003). Further contributing to an impaired immune response is the development of lymphopenia targeting $CD4^+$ and $CD8^+$ T cells, as well as natural killer cells (Baize et al., 1999; Bradfute et al., 2010; Gupta, Spiropoulou, & Rollin, 2007; Reed, Hensley, Geisbert, Jahrling, & Geisbert, 2004). Additionally, EBOV encodes several proteins that are involved in the inhibition and antagonism of the innate immune response (reviewed in (Basler, 2015)). This is primarily mediated by VP35, which serves many immune evasion functions. These functions include but are not limited to blocking type I interferon (IFN) production by preventing the phosphorylation of interferon regulatory factor 3 (IRF-3)(Basler et al.,

2003), impairing retinoic acid-inducible gene 1 (RIG-I) signaling (Cárdenas et al., 2006; Luthra et al., 2013), and protein kinase R (PKR) antagonism (Feng, Cerveny, Yan, & He, 2007a; Schümann, Gantke, & Mühlberger, 2009). Similarly, VP24 has been shown to block IFN signaling by preventing the nuclear translocation of signal transducers and activators of transcription 1 (STAT1) (Mateo, Reid, Leung, Basler, & Volchkov, 2010; Reid et al., 2006; W. Xu et al., 2014). Overall, significant immune evasion and dysfunction combined with widespread viral dissemination and cellular pantropism contribute to the relatively uninhibited viral amplification and high levels of viremia observed during EBOV infection.

Viral Nucleocapsid Complexes and Inclusions

Concurrent with viral RNA synthesis is the encapsidation and packaging of EBOV genomic and antigenomic RNAs by NP. Mediated through the interaction with the other nucleocapsid proteins (VP35, L, VP30 and VP24), either directly or via linker proteins, NP serves as a nucleating factor for the formation of ribonucleoprotein complexes (RNPs) or nucleocapsids (NCs). Within the cytoplasm these NCs aggregate into highly ordered structures called viral inclusions, which are the sites of viral replication and nucleocapsid maturation (Hoenen et al., 2012b; Nanbo, Watanabe, Halfmann, & Kawaoka, 2013a; Schudt et al., 2015). The first morphological sign of EBOV inclusion formation, as visualized by electron microscopy (EM), is the presence of viral granular material, composed of viral proteins and RNA, at about 9 hours post infection (Ryabchikova & Price, 2004). This appearance of granular material is followed

by the development of highly organized inclusions, consisting of tubular structures roughly 50 nm in diameter (Noda, Aoyama, Sagara, Kida, & Kawaoka, 2005; Noda et al., 2006). NP, in the absence of the other nucleocapsid components, oligomerizes into loose helices that serve as drivers of NC-like structure formation in the cytoplasm (Nanbo, Watanabe, Halfmann, & Kawaoka, 2013b; Noda et al., 2006). Co-overexpression of NP, VP24 and VP35 yields inclusions that are morphologically indistinguishable from those observed during EBOV infection (Huang, Xu, Sun, & Nabel, 2002; Noda et al., 2005; 2006).

EBOV Proteins VP35 and VP30

During EBOV infection, the virus employs a number of immune evasion strategies, many of which are mediated by the multifunctional protein VP35. This protein is considered to be the filovirus analog to the phosphoproteins (P) of other NNS viruses, which are part of the ribonucleoprotein complexes required for viral replication (Conzelmann, 1998; Rahmeh et al., 2012; Whelan et al., 2004). In addition to its role as a nucleocapsid component and polymerase cofactor, VP35 counteracts type I interferon induction (Bale et al., 2013; Basler et al., 2003; 2000; Cárdenas et al., 2006; Hartman, Towner, & Nichol, 2004; D. W. Leung, Prins, Basler, & Amarasinghe, 2010; Prins, Cárdenas, & Basler, 2009), blocks RNA interference pathways (Fabozzi, Nabel, Dolan, & Sullivan, 2011; Haasnoot et al., 2007; Zhu et al., 2012) and antagonizes the activation of the dsRNA sensor PKR (Feng, Cerveny, Yan, & He, 2007b; Schümann et al., 2009). VP35's IFN inhibition function can be traced to a C-terminal domain, the interferon

inhibitory domain (IID), that contains a stretch of basic residues and binds dsRNA (Kimberlin et al., 2010; D. W. Leung et al., 2009). A single mutation to either arginine 309 or lysine 312 in the has been shown to abrogate dsRNA binding (Cárdenas et al., 2006; Hartman et al., 2004; D. W. Leung et al., 2009). The IID shares sequence similarity to the amino-terminal dsRNA binding domain of the influenza A virus (IAV) NS1 protein, a well characterized IFN antagonist (Hartman et al., 2004). NS1 is also able to antagonize PKR and disrupt the type I IFN response via dsRNA binding and IRF-3 inhibition (García-Sastre, 2001; Krug, Yuan, Noah, & Latham, 2003; Shoudong Li, Min, Krug, & Sen, 2006), and has been shown to prevent stress granule (SG) formation during IAV infection (Khaperskyy et al., 2014; Khaperskyy, Hatchette, & McCormick, 2012; Mok et al., 2012). These two viral proteins are thus functionally very similar.

In addition to its ability to bind dsRNA, VP35 also has a number of protein binding partners. As part of nucleocapsid complexes and viral inclusions, VP35 interacts with both L (Prins et al., 2010; Trunschke et al., 2013) and NP (Noda, Hagiwara, Sagara, & Kawaoka, 2010; Noda, Kolesnikova, Becker, & Kawaoka, 2011) directly, and is thought to act as a bridge between the two (Becker, Rinne, Hofsäss, Klenk, & Mühlberger, 1998; Boehmann, Enterlein, Randolf, & Mühlberger, 2005). Co-expression of VP35 and NP in cells leads to the formation of inclusion bodies that are similar to those found in infected cells. With the addition of VP24 these inclusions are structurally identical to those found in infected cells (Huang et al., 2002; Noda et al., 2006). VP35 binds to NP via two unique binding sites, which independently localize VP35 to viral inclusions, or maintain NP in a monomeric, RNA free state (Kirchdoerfer, Abelson, Li,

Wood, & Saphire, 2015; D. W. Leung et al., 2015). When expressed in excess of NP, VP35 is able to disrupt the structure of viral inclusions, indicating that the NP to VP35 ratio is important for efficient viral replication (Noda et al., 2010; 2011). A number of cellular proteins have also been shown to bind VP35, including protein activator of the interferon-induced protein kinase (PACT), a key component of RNA interference and IFN pathways,(Fabozzi et al., 2011; Luthra et al., 2013; Zhu et al., 2012), DRP76, a regulator of PKR activation (Shabman et al., 2011) and the light chain of the molecular motor dynein (Luthra, Jordan, Leung, Amarasinghe, & Basler, 2015). It is presumably through these diverse RNA and protein interactions that VP35 mediates its functions during EBOV infection.

Similar to VP35, VP30 is a component of EBOV nucleocapsid complexes and can be found in viral inclusions (Hoenen et al., 2012b; Nanbo, Watanabe, Halfmann, & Kawaoka, 2013b). However, while VP35 is required for viral genome replication, VP30 is dispensable for this function, and is instead a critical transcription activator and reinitiation factor (Martinez et al., 2008; Mühlberger, Weik, Volchkov, Klenk, & Becker, 1999). The function of VP30 during viral transcription has not been precisely defined, however it has been shown that if the RNA hairpin loop secondary structure found in the transcription start signal of the first viral gene, *NP*, is destroyed, transcription no longer requires VP30 (Weik, Modrof, Klenk, Becker, & Mühlberger, 2002). It is thus thought that VP30 plays a role at early stages of viral transcription.

VP30 is able to bind the other nucleocapsid components NP (Modrof, Mühlberger, Klenk, & Becker, 2002), VP35 (Biedenkopf, Hartlieb, Hoenen, & Becker,

2013), and L (Groseth et al., 2009). It also forms homo-oligomers, which are required for viral transcription, but are dispensable for its interaction with EBOV nucleocapsids (Hartlieb, Modrof, Mühlberger, Klenk, & Becker, 2003). The phosphorylation of VP30 at two N-terminal serine clusters has been shown to also regulate its various functions (Modrof et al., 2002). Phosphorylation of VP30 led to decreased transcription and enhanced viral replication, while the unphosphorylated form of VP30 promoted viral transcription and repressed viral replication, suggesting that VP30 influences the balance between replication and transcription, depending on its phosphorylation state (Biedenkopf et al., 2013; Ilinykh et al., 2014; Martinez et al., 2011; Modrof et al., 2002). The cellular phosphatases protein phosphatase 1 (PP1) and 2A (PP2A) have been shown to dephosphorylate VP30, and are thus able to influence its activity during viral infection (Ilinykh et al., 2014; Modrof et al., 2002). Furthermore, it was shown that targeting PP1 with a small molecular inhibitor lead to an increase in VP30 phosphorylation, which inhibited viral transcription and suppressed viral replication in Vero-E6 cells (Ilinykh et al., 2014). These data suggest that VP30 is a promising target for antivirals.

Unlike VP35, VP30 binds to ssRNA, a function that can be mapped to a stretch of basic amino acids located in the N-terminus, and requires Zn^{2+} ions (John et al., 2007). Also located in the N-terminus is a Cys_3His (CCCH) zinc finger domain, which is required for VP30's transcriptional activity, but has no effect on its interaction with NP and viral inclusions (John et al., 2007; Modrof, Becker, & Mühlberger, 2003). The respiratory syncytial virus (RSV) homolog of VP30, M2-1, also contains this unique CCCH zinc finger motif, which was shown to be required for M2-1's function in RSV

transcription (Hardy & Wertz, 2000; Tang, Nguyen, Cheng, & Jin, 2001). Interestingly, the CCCH motif is found almost exclusively in cellular proteins that mediate the post-transcriptional regulation of mRNA stability, such as tristetraprolin (TTP) and butyrate response factor 1 (BFR1) (Lai, Carballo, Thorn, Kennington, & Blackshear, 2000; Lai, Kennington, & Blackshear, 2002). Another cellular protein containing four CCCH motifs is zinc-finger antiviral protein (ZAP) which has been shown to target viral mRNAs and promote their degradation, including the EBOV and MARV L mRNA (Gao, Guo, & Goff, 2002; Jeong, Kim, & Jang, 2010; Müller et al., 2007; Wang, Lv, & Gao, 2010). The presence of this unique CCCH motif in VP30 thus suggests that it might be involved in regulating mRNA stability.

The Cellular Stress Response and mRNA Regulation

The regulation of mRNA stability and translation represents an important post-transcriptional checkpoint leading to appropriate yet dynamic protein expression and is particularly important for quickly fine-tuning cellular responses to changes in the environment or returning cells to a state of homeostasis. The availability and abundance of mRNA transcripts to the host translation machinery are two important factors that influence the outcome of a cellular response to changes in the environment. These can be controlled by the integrated stress response and the regulation of mRNA stability, respectively.

The Integrated Stress Response

Exogenous environmental stress such as heat, nutrient deprivation, ultraviolet radiation and viral infection can trigger the cellular stress response, which acts as a form of mRNA triage to prioritize the translation of those mRNAs that are essential for cell survival. Four cytoplasmic kinases sense these various forms of stress and initiate the signaling cascade that eventually leads to a state of translational arrest (Anderson & Kedersha, 2008; 2009a). These kinases include PKR, heme-regulated inhibitor kinase (HRI), PKR-like endoplasmic reticulum kinase (PERK), and general control nonderepressible 2 (GCN2), which sense dsRNA, oxidative stress, ER stress, and amino acid deprivation, respectively. Upon activation, these kinases phosphorylate the α-subunit of eukaryotic translation initiation factor 2 (eIF2α), thereby preventing the assembly of the ternary pre-initiation complex, which is required to bring $tRNA^{met}$ to the 40S ribosomal subunit. This leads to the accumulation of stalled translation initiation complexes on mRNAs and triggers the aggregation of other RNA binding proteins (Anderson & Kedersha, 2009b; Kedersha & Anderson, 2009). These complex and highly dynamic aggregates of mRNA and protein are referred to as stress granules (SGs). SGs are non-membranous granules that form exclusively in the cytoplasm and are typically 1-2 μm in diameter (Souquere et al., 2009). A schematic of eIF2α-induced SG formation is depicted in Figure 2.

The protein composition of SGs can vary depending on the type of stress present, but many SG proteins, such as Ras GTPase-activating protein-binding protein 1 (G3BP) and T-cell restricted intracellular antigen 1 (TIA-1) are consistent across all SG types and

are therefore considered canonical SG components. These proteins are also critical drivers of the nucleation of SGs, and can even induce SG formation at sufficiently high levels of cytoplasmic protein expression in the absence of stress (Anderson & Kedersha, 2009a; Buchan & Parker, 2009; Thomas, Loschi, Desbats, & Boccaccio, 2011). In addition to mRNA and translation factors, SGs include other protein components such as scaffold proteins, RNA helicases, RNA binding proteins involved in mRNA stability, and components of other signaling pathways (Kedersha, Ivanov, & Anderson, 2013).

SGs can persist for many hours, but they are highly dynamic structures that depend on microtubule networks for assembly and disassembly (Bartoli, Bishop, & Saunders, 2011; Loschi, Leishman, Berardone, & Boccaccio, 2009). Live cell imaging studies have shown that SG components, including TIA-1 and poly-A binding protein (PABP) can shuttle into and out of SGs continuously (Kedersha et al., 2000; 2005), however it is unknown if all SG components behave as such. Further evidence suggesting that SGs are highly dynamic is the observation that mRNA, another canonical component of SGs, can shuttle between polysomes, SGs, and processing bodies (P-bodies), which are another type of cellular RNA granule (Anderson & Kedersha, 2006; Kedersha et al., 2005). While SGs focus on diverting translational energy towards the expression of proteins involved in cell survival, P-bodies are enriched in mRNA decay machinery suggesting they are important for the degradation and processing of mRNAs (Anderson & Kedersha, 2009a). Unlike SGs, P-bodies are constitutively present in cells but can increase in size and number under conditions of stress (Eulalio, Behm-Ansmant, & Izaurralde, 2007; Teixeira, Sheth, Valencia-Sanchez, Brengues, & Parker, 2005).

Because of their dynamic nature and complex compositions, P-bodies and SGs are difficult to study and methods for their characterization are limited to mainly microscopy and other forms of cellular imaging (Brielle, Gura, & Kaganovich, 2015; Panas, Kedersha, & McInerney, 2015a).

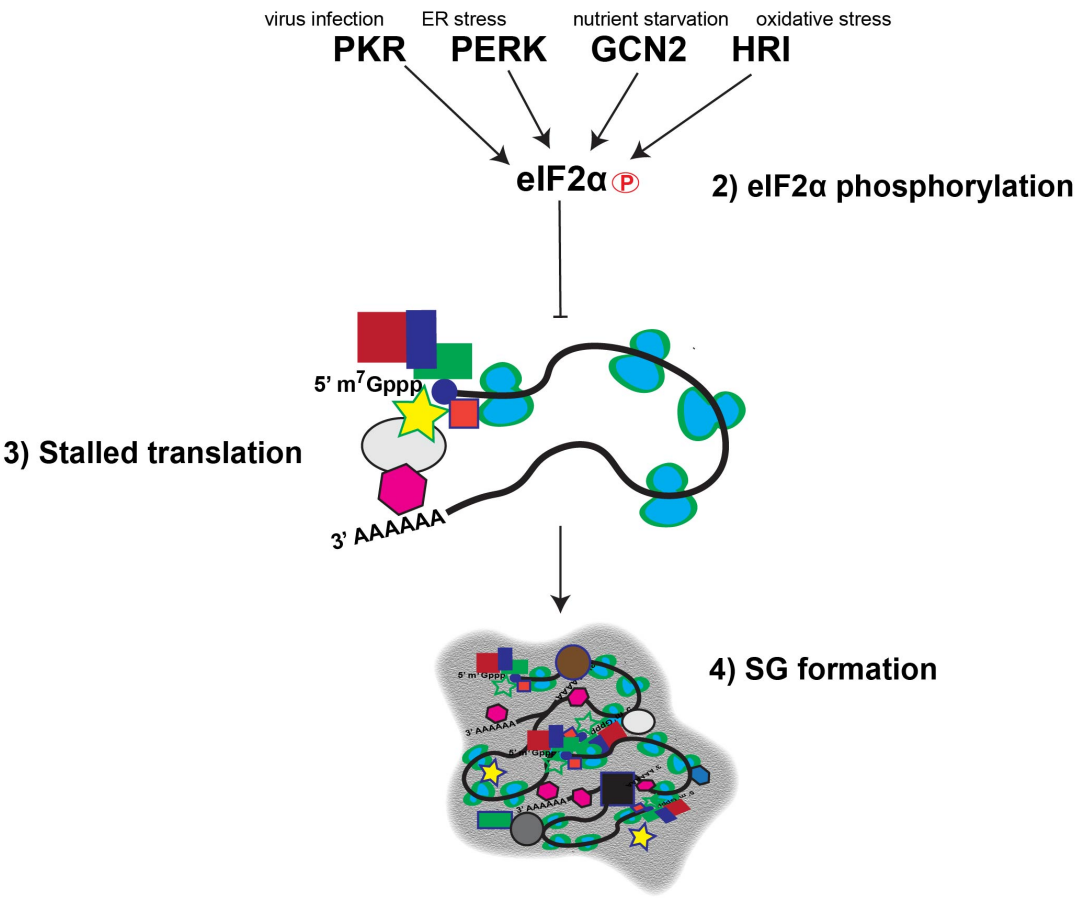

Figure 2. Basic scheme of SG induction.

Cellular stress is sensed by the four cytoplasmic kinases, PKR, PERK, GCN2, and HRI, which sense viral infection, ER stress, nutrient deprivation and oxidative stress, respectively. Upon activation, these kinases phosphorylate the alpha subunit of eIF2, which ultimately prevents the formation of complete translation initiation complexes. Stalled translation leads to the accumulation of a number of translation initiation factors, RNA binding proteins, mRNA and 40S ribosomal subunits, ultimately resulting in the formation of SGs and translational arrest.

Stress Granule Formation and Viral Infection

The global decrease in protein translation associated with SG formation is unsustainable for viral replication, which requires the host translational machinery to synthesize viral proteins. Therefore, many viruses have evolved strategies to antagonize the stress response. Few viruses have been shown to co-exist with fully formed SGs over the entire course of infection. Hepatitis C virus (HCV) is one of the few examples of such viruses, and has been shown to induce eIF2α phosphorylation and SG formation during infection and use the associated host translational arrest to block interferon production, thus using the stress response to its own advantage (Garaigorta & Chisari, 2009). HCV is able to maintain the translation of its own polyprotein via an internal ribosome entry site (IRES), which is an eIF2α independent translation strategy (Garaigorta, Heim, Boyd, Wieland, & Chisari, 2012; Thakor & Holcik, 2012). A majority of viruses however, have been shown to either induce SGs early during infection, but disrupt SG formation later when viral protein levels are high, or to suppress SG formation during the entirety of the infection (Montero & Trujillo-Alonso, 2011; J. P. White & Lloyd, 2012). A number of viruses, including EBOV, have been shown to prevent PKR activation (Feng, Cerveny, Yan, & He, 2007b; Schümann et al., 2009; J. P. White & Lloyd, 2012). IAV does not induce SG formation at any time during infection and is able to prevent PKR activation via its viral protein NS1 (Khaperskyy et al., 2012). Similarly, the arenavirus Junín virus was shown to inhibit SG formation by impairing eIF2α phosphorylation, via an undetermined mechanism (Linero, Thomas, Boccaccio, & Scolaro, 2011). Other viruses are able to prevent SG formation through the cleavage of important SG components.

During poliovirus infection, SGs are induced early but are later disrupted via the cleavage of G3BP by the viral protease 3C (J. P. White & Lloyd, 2011; J. P. White, Cardenas, Marissen, & Lloyd, 2007). Finally, other viruses have been shown to sequester or subvert critical SG components. The alphavirus chikungunya virus represses SG formation through the recruitment of G3BP by the viral protein nsp3 to cytoplasmic foci that resemble SGs. These aggregates are compositionally distinct from canonical SGs however, and were shown to enhance viral replication (Fros et al., 2012; Scholte et al., 2015). Similarly, the flaviviruses West Nile virus and dengue virus do not induce SG formation during infection but show strong interaction with SG proteins TIA-1 and TIAR (Courtney, Scherbik, Stockman, & Brinton, 2012; B. Jain, Chaturvedi, & Jain, 2014; W Li et al., 2002; Xia et al., 2015). Dengue virus was also shown to induce the formation of G3BP1 granules in lung epithelial cells. These granules did not contain TIA-1, distinguishing them from canonical SGs (Xia et al., 2015). The increasing number of studies demonstrating an interaction between SGs and viruses highlights the significance of this response during viral infection. Furthermore, viruses employ a range of different mechanisms to prevent or exploit SGs and their components, which emphasizes the complex and unique interactions between them.

Regulation of mRNA Stability via AU-Rich Elements

AU-rich elements (AREs) are cis-acting elements located within the 3'-untranslated region (3'UTR) of mRNAs. AREs are able to modulate mRNA stability and subsequent protein translation via their interaction with associated RNA binding proteins

(RBPs). The function of AREs as mechanisms of mRNA decay was first discovered in 1986, when an AT-rich region from the 3'UTR of the granulocyte-macrophage colony stimulating factor (GM-CSF) gene, which would become an AU rich region in the transcribed mRNA, was fused to the rabbit β-globin gene. In this experiment, the recombinant β-globin gene, which produces a generally stable mRNA, instead resulted in a highly unstable mRNA that was rapidly degraded (Shaw & Kamen, 1986). It has now been established that many mRNAs, particularly those of cytokine and growth factors, possess AREs in the 3'UTRs (Beisang & Bohjanen, 2012; Kafasla, Skliris, & Kontoyiannis, 2014; Vlasova-St Louis & Bohjanen, 2014).

AREs are highly variable and are therefore difficult to define precisely. They have been loosely classified into three main groups. However, there are many known AREs that do not fall into these three categories. Class I AREs contain 1-3 copies of the pentameric sequence AUUUA throughout the UTR and are often surrounded by areas that are U-rich. Class II AREs typically contain 5-8 overlapping copies of the AUUUA motif. Finally, Class III AREs are comprised of predominately U-rich sequences and may lack the AUUUA motif altogether (C. Y. Chen & Shyu, 1995; Roretz, Marco, Mazroui, & Gallouzi, 2010; Vlasova-St Louis & Bohjanen, 2014; Wu & Brewer, 2012). The developers of an online database of ARE-containing transcripts found in different species (ARED Organism) introduced a second classification system. This new grouping contains five different categories of ARE, and distinguishes them based on the number of overlapping AUUUA pentamers, from one to five, respectively (Halees, El-Badrawi, &

Khabar, 2008). The different classification schemes are useful but are ultimately not sufficient to fully categorize the spectrum of observed AREs.

ARE-Binding Protein Tristetraprolin (TTP)

AREs are recognized by various RBPs that comprise complex regulatory networks and promote mRNA stability or degradation (Barreau, Paillard, & Osborne, 2005; C. Y. Chen & Shyu, 1995; Wu & Brewer, 2012). TTP is a canonical and well-characterized ARE-BP) that contains a CCCH zinc finger motif and targets mRNAs for degradation (Brooks & Blackshear, 2013; Lai et al., 2000). TTP was first functionally characterized in studies examining TTP knock out mice. It was found that these mice exhibited severe inflammation, cachexia and autoimmunity (Taylor et al., 1996). This paper established that TNF-α was a target of TTP, and mice deficient in TTP demonstrated unrestricted TNF-α expression, resulting in the immunological pathologies observed. It was later determined that TTP binds to ssRNA via its two tandem CCCH zinc finger motifs. A single mutation to any one of the Cys or His residues of the zinc finger domains was sufficient to ablate RNA binding (Lai et al., 2000). The list of TTP targets continues to expand since the initial studies examining TTP's effect on TNF-α in 1996 and includes many cytokine and growth factors. Interestingly, TTP has been shown to regulate the stability of its own mRNA, as well as various viral mRNAs (Brooks, Connolly, & Rigby, 2004; Maeda et al., 2006). TTP is also known to interact with a number of cellular proteins, particularly those involved in mRNA decay. These include decapping, deadenylating and exosome proteins (Brooks & Blackshear, 2013). Important

to its function is the phosphorylation of TTP. The p38 mitogen activated protein kinase (MAPK) pathway seems to be primarily responsible for controlling TTP function. Both MAPK-activated protein kinase 2 (MK2) and p38 can phosphorylate TTP, which promotes binding of the chaperone protein 14-3-3 and thereby inactivates TTP (Mahtani et al., 2001; Stoecklin et al., 2004; L. Sun et al., 2007).

Because TTP is a potent regulator of mRNA stability, it is also involved in the cellular response to stress. TTP has been shown to localize to SGs upon energy deprivation but is excluded from arsenite-induced SGs (Roretz et al., 2010). This difference is thought to be due to the p38-MAPK mediated phosphorylation of TTP and subsequent binding to 14-3-3, induced during oxidative stress (Stoecklin et al., 2004). TTP can also be found in P-bodies, which are known to be enriched in RNA decay machinery (Brooks & Blackshear, 2013; L. Sun et al., 2007). The precise mechanisms that determine the localization of specific ARE-BPs and their associated mRNAs to SGs or P-bodies under conditions of stress are still poorly understood.

Evidence also suggests that TTP, like many other ARE-BPs, can interact with viral RNA and thus influence the outcome of viral infection. TTP has been shown to bind to human immunodeficiency virus 1 (HIV-1) genomic RNA, which is AU-rich (Graf et al., 2000; Maeda et al., 2006). TTP skews the ratio of HIV RNA splicing products, thereby altering the expression of certain HIV proteins which leads to reduced HIV virion production (Maeda et al., 2006). It remains to be determined if TTP functions as an antiviral protein in EBOV infection.

ARE-Binding Protein Human antigen R (HuR)

Human antigen R (HuR) is another well-studied ARE-BP that promotes mRNA stability and protein translation (Brennan & Steitz, 2001; Simone & Keene, 2013). HuR mediates a number of biological functions aside from post-transcriptional regulation of mRNA. It is involved in the cellular stress response (Yamasaki & Anderson, 2008) is thought to be anti-apoptotic and regulates cellular differentiation (Cherry, Karschner, Jones, & Pekala, 2006; Hinman & Lou, 2008; Lal, Kawai, Yang, Mazan-Mamczarz, & Gorospe, 2005). A complete knock out is embryonic lethal in mice, highlighting its important contributions to cellular growth and differentiation (Antic & Keene, 1997; Ghosh et al., 2009; Lebedeva et al., 2011). HuR is predominately located in the nucleus but shuttles to the cytoplasm under conditions of stress (Brennan & Steitz, 2001). It shares many mRNA targets with TTP, including TNF-α, and as such, competition exists between them, adding another layer of regulation to their respective functions (Anderson, 2010; Vlasova-St Louis & Bohjanen, 2014). It is thought that one contribution of HuR to mRNA stability is through the competitive binding with other destabilizing ARE-BPs (Garneau, Wilusz, & Wilusz, 2007; Lal et al., 2004; Roretz et al., 2010). HuR can be activated by a number of different stresses including ultraviolet radiation, heat shock, and oxidative stress and can be found in cytoplasmic SGs (Anderson & Kedersha, 2009a; Gallouzi et al., 2000; Masuda, Abdelmohsen, & Gorospe, 2009; Roretz et al., 2010). Similar to other ARE-BPs, HuR can be phosphorylated at various sites, which influence HuR's function, and can determine its cellular localization (Brennan & Steitz, 2001; Simone & Keene, 2013).

As a promoter of mRNA stability, HuR is an attractive cellular target during viral infection, and has been shown to interact with a number of different viruses. The 3'UTR of the classic swine fever virus genome was identified as a target of HuR. However, the contribution of HuR to viral replication remains undetermined (Nadar et al., 2011). Similarly, HuR was shown to bind to the 3'UTR of Sindbis virus mRNA during infection, thus promoting productive infection (Sokoloski et al., 2010). RSV, which forms inclusion bodies similar to those observed during EBOV infection, was also shown to sequester HuR within these inclusions. However, the precise function of HuR during RSV infection remains unclear (Lindquist, Lifland, Utley, Santangelo, & Crowe, 2010). The appropriation of HuR by different viruses suggests a proviral function for HuR and as such makes it an appealing target for examination during EBOV infection.

Scientific Proposal

The majority of studies dealing with the innate immune evasion strategies employed by EBOV focus on the type I IFN response. Little is known regarding the interaction of EBOV with the host RNA regulatory machinery and the influence this has on viral replication. By defining the cellular events that take place during EBOV infection, we improve our understanding of EBOV pathogenesis. Furthermore, by identifying antiviral mechanisms that the virus is unable to disturb or evade we can identify putative targets for antiviral interventions and improve the development of therapeutic strategies. Here, investigated two mechanisms of host RNA regulation with antiviral implications during EBOV infection. These include the cellular stress response

mediated by SG formation and the post-transcriptional control of mRNA stability. This dissertation is divided into two main research topics based on these separate but related research aims.

Part I: The Cellular Stress Response

While type I IFNs and cytoplasmic pattern recognition receptors are thought of as prototypical components of the host innate antiviral response, the cellular stress response is becoming increasingly appreciated as an important antiviral strategy (Montero & Trujillo-Alonso, 2011; J. P. White & Lloyd, 2012). Central to this response is the rapid repression of cellular translation to prioritize the production of proteins important for cell survival. Because viral protein synthesis relies on the host translation machinery, translational arrest mediated by SG formation is an efficient strategy for inhibiting viral replication and as such, many viruses have evolved mechanisms to overcome this block. To date, no studies have examined the cellular stress response and potential antiviral implications it might have during EBOV infection. While it has been shown that EBOV is able to antagonize the dsRNA sensor PKR, these studies did not examine PKR's function as an inducer of SG formation. Furthermore, PKR antagonism was only examined late in infection, providing no insight into whether EBOV may be able to prevent SG formation and avoid translational repression early in infection. Therefore, it is undetermined if SG formation occurs at any point during EBOV infection, or whether the stress response influences EBOV replication. Additionally, it is unknown if EBOV is able to prevent the activation of the other eIF2α kinases, which could represent

alternative mechanisms for inducing the stress response and thereby repressing viral translation. In Chapter 3 we investigated whether SG formation occurs at any time during the course of infection, and if EBOV is able to block this response. Furthermore, we aimed to determine if EBOV interferes with SG formation induced by other forms of stress, aside from viral infection, to identify potential antiviral pathways that the virus is unable to evade.

Part II: Post-transcriptional control of mRNA stability

Fatal EBOV infection is characterized by an uncontrolled inflammatory response and cytokine storm (Baize et al., 2002; Feldmann & Geisbert, 2011b; Wauquier, Becquart, Padilla, Baize, & Leroy, 2010). It is still unclear, however, what the mechanisms are that lead to such a discordant and dysfunctional immune response. Cytokines and chemokines make up a significant portion of cellular proteins that can be regulated at the mRNA level by AREs and ARE-BPs (Anderson, 2010). The viral protein VP30 is an RNA-binding protein that shares many similarities, including a CCCH zinc finger motif, to cellular proteins known to function as mRNA destabilizing factors (John et al., 2007; Modrof et al., 2003). TTP, BRF1 and ZAP all contain CCCH zinc finger motifs and mediate the degradation of their targets via AREs (Lai et al., 2000). Therefore, in Chapter 4 we investigated whether VP30 functions as an ARE-BP and contributes to the dysregulation of cytokines observed during infection.

The EBOV genes contain unusually long 5' and 3' UTRs flanking the open reading frames. Four of the seven EBOV genes contain putative AREs within the 3'UTRs of the

corresponding mRNAs. It is not known whether these 3'UTRs influence viral mRNA stability. Here, we aim to elucidate the function of the putative AREs on viral mRNA stability and determine their impact on viral protein translation. It is conceivable that VP30 targets ARE-containing viral mRNAs to regulate their stability and translation, and to control the amount of viral mRNA that is present in cells. The putative AREs within viral 3'UTRs might also influence mRNA stability independently of VP30 and instead be targeted by cellular ARE-BPs, a phenomenon that has been observed for a growing number of viruses (Dickson & Wilusz, 2011; Sokoloski et al., 2010). Therefore, we aimed to identify whether VP30 functions as an ARE-BP and regulates the stability of potential viral and cellular mRNA targets, such as cytokines known to be dysregulated during EBOV infection. We also aimed to determine whether VP30, which is required for viral transcription, regulates the stability of EBOV mRNAs by targeting the putative AREs in their 3'UTRs.

CHAPTER TWO: MATERIALS AND METHODS

Cell Culture

Cells were maintained in Dulbecco's modified Eagle medium (DMEM) supplemented with 10% fetal bovine serum (FBS), penicillin (50 units/ml), and streptomycin (50 mg/ml) and L-glutamine (200 mM) unless otherwise noted. U2OS-USP10-eGFP cells were treated with 200 ng/ml doxycycline (Sigma) 24 hours prior to infection or transfection to induce USP10-eGFP expression. THP-1 cells were grown in suspension in RPMI media. Prior to use, cells were matured by seeding 5 x 10^5 cells per well in a 6 well plate in 2 ml RPMI media supplemented with 100 nM phorbol myristate acetate (PMA). Cells were matured over 2 days at 37 ^{o}C. Two days after incubation with PMA, media was replaced with 2 ml fresh RPMI media and incubated for 2 more days at 37 ^{o}C. A list of all eukaryotic cells lines used is outlined in Table 1.

Table 1. Eukaryotic Cells Lines

Name	**Cell type**	**From**
HEK293T	Human embryonic kidney, epithelial	G. Viglianti, Boston University
HuH7	Human hepatocellular carcinoma, epithelial	J. Alonso, Texas Biomedical Research Institute, San Antonio, TX
HeLa	Cervical adenocarcinoma, epithelial	ATCC CCL-2
VeroE6	African green monkey kidney cells,	ATCC CRL-1586
U2OS	Human osteosarcoma, epithelial	ATCC HTB-96

U2OS-USP10-eGFP	Human osteosarcoma, epithelial, doxycycline inducible USP10-eGFP overexpression	N. Kedersha, Division of Rheumatology, Immunology and Allergy. Brigham and Women's Hospital
U2OS-G3BP-eGFP	Human osteosarcoma, epithelial, stably overexpressing G3BP-eGFP	N. Kedersha Division of Rheumatology, Immunology and Allergy. Brigham and Women's Hospital
THP-1	Monocyte	R. Gummuluru, Boston University

Viruses

Zaire ebolavirus (EBOV; Kikwit or Mayinga isolate, Table 2) was grown in Vero or VeroE6 cells and virus titers were determined by TCID50 or plaque assay. All work with EBOV was done under biosafety level 4 conditions at the Integrated Research Facility in the Rocky Mountain Laboratories, Division of Intramural Research, NIAID, NIH, Hamilton, MT, or the Texas Biomedical Research Institute San Antonia, Texas. BSL-4 infections were performed by: Dr. Judith Olejnik, Dr. Adam Hume, Dr. Kristina Schmidt, Dr. Laure Deflubé-Owen, or Dr. Logan Banandyga

Table 2. Virus Isolates

Virus	**Source**	**Genbank #**
Zaire ebolavirus (Mayinga 1976 isolate)	Center for Disease Control and Prevention (CDC), Atlanta GA, USA	AF086833.2
Zaire ebolavirus (Kikwit 1995 isolate)	National Institutes of Allergy and Infectious Disease (NIAID), Rocky Mountain Laboratories, Hamilton MT	KR867676.1

Molecular Cloning of 3'UTRs into pMIR-Luciferase Reporter

To insert the individual 3'UTRs (positive-sense orientation) from the four viral nucleocapsid mRNAs into the pMIR-luciferase reporter plasmid (Origene), the 3'UTRs from the NP, VP30 and VP35 genes were excised from existing pTM1 expression plasmids using appropriate restriction enzymes. The 3´ UTR specific regions were then amplified by PCR using the primers outlined in Table 4. All PCR reactions were performed using the PfuUltra Hotstart DNA polymerase (Agilent, #600390) and were performed as recommended by the manufacturer. The 3'UTR of the VP24 gene derived from EBOV Mayinga genomic RNA. For RNA isolation, VeroE6 cells were infected with EBOV and cell supernatants containing EBOV particles were collected four days post infection and cleared of debris by a low-speed centrifugation step. Viral genomic RNA was purified using the Qiagen QIAamp viral RNA mini kit. The 3'UTR of the VP24 gene was then reverse transcribed and amplified using the specific primers listed in Table 4, with the Qiagen OneStep RT-PCR kit. All viral 3'UTRs were PCR-amplified a second time to add terminal restriction sites for the restriction enzymes SpeI and HindIII (primers outlined in Table 5). The newly amplified DNA of all 3'UTRs were purified using a PCR purification kit (Qiagen) and then individually ligated into the pMIR-luciferase reporter plasmid. The resulting plasmids were transformed into high efficiency competent *E.coli* (New England Biolabs) and cloned and amplified using standard procedures. For insertion of the 3'UTRs of IL-10 and TNF-α genes into the pMIR-luciferase reporter plasmid, cellular mRNA was isolated from THP-1 cells, matured with 100 nM PMA. Cells were matured for 2 days at 37 ^{o}C, and then treated with 200 ng/ml

LPS (InvivoGen) for 2 hours. RNA was isolated using RNAzol (Molecular Research Center Inc.) following the manufacturer's protocol for mRNA isolation. Insertion of these 3'UTRs and cloning of the resulting plasmids was performed as described for the VP24 3'UTR.

Table 3. Plasmids

Name	**Source**
3E-5E-Luciferase	Mühlberger Lab
3E5E-eGFP	Mühlberger Lab
3E5E-mCherry	Mühlberger Lab
pCAGGS-eGFP	Mühlberger Lab
pCAGGS-L synth minus	Mühlberger Lab
pCAGGS-L	Mühlberger Lab
pCAGGS-NP full 3'UTR	Generated by E.V.Nelson
pCAGGS-NP no 3'UTR	Generated by E.V.Nelson
pCAGGS-NP	Mühlberger Lab
pCAGGS-T7 (RNA-dependent DNA T7 polymerase)	Y. Kawaoka, University of Wisconsin, Madison, WI
pCAGGS-VP24	Mühlberger Lab
pCAGGS-VP30	Mühlberger Lab
pCAGGS-VP35-HA	Mühlberger Lab
pCAGGS-VP35	Mühlberger Lab
pCDNA3- HuR	Kindly provided by N. Kedersha
pCDNA3-VP35-3A	Mühlberger Lab
pCDNA3-VP35-Del3	Mühlberger Lab
pCDNA3-VP35-Del4	Mühlberger Lab
pCDNA3-VP35-Del7	Mühlberger Lab
pCDNA3.1- TTP-Myc/His	Generated by E.V.Nelson,

pCMV-SPORT-TTP	Purchased from Harvard Plasmid Repository
pMIR-Beta-galactosidase	Purchased from Origene
pMIR-IKB-α	Purchased from Origene
pMIR-IL-10	Generated by E.V.Nelson
pMIR-IL-6	Generated by E.V.Nelson
pMIR-Luciferase	Generated by E.V.Nelson
pMIR-NP	Generated by E.V.Nelson
pMIR-TNF-α	Generated by E.V.Nelson
pMIR-VP24	Generated by E.V.Nelson
pMIR-VP30	Generated by E.V.Nelson
pMIR-VP35	Generated by E.V.Nelson

Table 4. 3'UTR Cloning Primers Initial RT-PCR

3'UTR	**Forward**	**Reverse**
IL-10	GACATCAGGGTGGCGACTCTATAGAC	GATGTGAATAAGATACATTTATTTATTC
NP	CGTACTAGTTGAATGAGCATGGAACAATGGGATGAT	GACAAGCTTTTTTCTTAATTATAAAACGATCGTGTA
TNF-α	GGAGGACGAACATCCAACCT	TTCTTTTCTAAGCAAACTTTATTT
VP24	GGATCCTCGACACGAATGCAAAGTTTG	CTGCTTCATCTAAAACACGGAAAGACCC
VP30	CGTACTAGTTAATAAGGCTGACTAAAACACTATATAACC	GACAAGCTTTTTCTTAATATTTTAAGAGATCATTAGTAAG
VP35	CGTACTAGTTGAGCCAATCTCCCTTCCCTCCGAAAG	GACAAGCTTTTTCTTAATCTTCATCACTTTTGGTTTGGG

Table 5. 3'UTR Cloning Primers

3'UTR	Forward	Reverse
IL-10	CGTACTAGTGACATCAGGGTG GCGACTCTATAGAC	CGTACTAGTGACATCAGGGT GGCGACTCTATAGAC
IL-6	CGTGCTAGCGGGCACCTCAGA TTGTTGTTGTTAATGGGC	GACTCTAGATGAATTTTTTAA AATGCCATTTATTGGT
TNF-α	CGTGAGCTCGGAGGACGAAC A TCC	GACACTAGTTTCTTTTCTAAG CAAACT
VP24	CGTGCTAGCTAACTAAGGTAG AATACTTC	GACTCTAGATTTTTTCTTAAT CTACTTATCTAATG
VP30	CGTGCTAGCTAATAAGGCTGA CTAAAACACTATATAACC	GACTCTAGATTTCTTAATATT TTAAGAGAT
VP35	CGTGCTAGCTGAGCCAATCTC CCT TCCCTCCGAAAG	GACTCTAGATCTTAATCTTCA T CACTTTTGGTTTGGG

Table 6. Primers: Altering NP 3'UTR Lengths in pCAGGS Backbone

3'UTR	Forward	Reverse
Full length	GATGTCTAAGGTGTGAAT TATTATCAC	GACAGCTAGCCTTAATTATAAAA CGATCGTGTAAATG
No 3'UTR	GCTCAACCAGCCCTCGCA TGCTGAC	GACAGCTAGCTCACTGATGATGT TGCAGGATTGCC

Table 7. Sequencing Primers

Target	Forward	Reverse
IKB-α 3'UTR	CAGCAAGGAGGTAGGTGAGG	ATTTGGTATCTGCGCTCTGC
Luciferase	AATTGCTAGCGCACTGCAGCGCTTAAGCCG	GGCCCGGCTTAAGTCGCTCAGTGCGCTAGC
pCAGGS backbone	CCTTCTTCTTTTTCCTACAG	CCTTTATTAGCCAGAAGTCAG
TTP	CTCGGCCGACACCCCTCATG	GGGTGGTGGAGGTTGCAGTGGG

Quantitative reverse transcription-PCR (qRT-PCR)

Total cellular RNA was isolated from 293T cells using RNAzol (Molecular Research Center, Inc), as directed by the manufacturer. Five ng of RNA were then analyzed by qRT-PCR using the QuantiFast SYBR green RT-PCR kit (Qiagen) following the manufacturer's protocol. Validated primers by Qiagen were used (QuantiTect primer assays) to detect and quantify IL-6, TNF-α, HuR, TTP, or β-2-microglobin RNA. Primers designed by E.V. Nelson were used to detect and quantify luciferase, eGFP, NP and IL-6 RNA levels (Table 8). β-2-microglobin was used as an endogenous control for normalization. Data was collected and analyzed using the $\Delta\Delta C_T$ method with Bio-Rad CFX Manager 1.5 software.

Table 8. qRT-PCR Primers Designed by E.V. Nelson

Target	Forward	Reverse
eGFP	GACGTAAACGGCCACAAGTT	AAGTCGTGCTGCTTCATGTG
IL-6	CATCACTCGAGCAATTTGGA	TGTTTGTGGACGAAGTACCG
Luciferase	GTGGTGTTGTGTTCGTGGAC	CGATCTTTCCGCCCTTCT
NP	CCCAGTCAGAACACTCTTTTGAGG	GACATCAAAAATTCTTCCTGTTTTC

Transfections

All transfections were performed using the lipid based transfection reagents, transIT-LT1 (Mirus), Lipofectamine LTX with Plus reagent (Invitrogen), or Lipofectamine 2000 (Invitrogen) following the manufacturer's protocols. Cells were transfected at between 60-70% confluency. For those transfections done using with transIT-LT1, media was removed before transfection and replaced with DMEM supplemented with 2% FBS and L-glutamine (200 mM).

Luciferase Assay

pMIR-luciferase reporter plasmids along with a beta-galactosidase (B-gal) expression plasmid (see below) were transfected into 293T cells seeded at a density of 3x10^5 cells per well in 6-well or 1.5X10^ 5 cells per well in 12-well plates using the transIT LT1 transfection reagent as described above. Cells were harvested two days post transfection using 1X cell lysis buffer (CLB) (Promega, catalog #E1500). Prior to lysis,

cells were washed once with 1 ml of PBS at room temperature. For lysis in a 6-well plate, 600 of µl 1X CLB per well were added onto the cells and incubated for 20 minutes at room temperature with gentle shaking. For lysis in 12-well plates, 300 µl 1X CLB were added per well. After lysis, samples were transferred to 2 ml Eppendorf tubes and subjected to centrifugation at 12,000 x g at 4^{o}C for 5 minutes. Supernatants were then transferred to 1.5 ml Eppendorf tubes and either immediately assayed for luciferase activity, or stored at -20^{o}C until ready for use. The luciferase assay was performed in 96-well format with a LUMIstar Omega luminometer (BMG Labtech) using 20 µl of the lysate, or appropriate dilution of the lysates, and 50 µl of the luciferase assay reagent (Promega).

Beta-galactosidase Assay

All luciferase assay samples were normalized to B-gal activity (B-gal). 50 µl of cell lysates were used for a B-gal enzyme system assay (Promega) in 96-well format following the manufacturers protocol. Samples were read on Molecular Devices Spectra Max M2 plate reader.

Minigenome System

The EBOV minigenome assay was performed in 293T or U2OS cells as previously described (Mühlberger et al., 1999; Trunschke et al., 2013). 293T cells were transfected with a pCAGGS-T7 plasmid, along with T7 RNA polymerase-driven pTM1 plasmids encoding the EBOV *NP*, *VP35*, *VP30* and *L* genes. In addition, cells were also

transfected with a T7-driven plasmid expressing the EBOV 3E-5E minigenome containing the reporter genes *eGFP* or *luciferase*, in negative sense. U2OS cells were transfected with support plasmids in the pCAGGS backbone, and a 3E-5E-eGFP minigenome under the control of a Pol II promoter.

Western Blot Analysis

Preparation of EBOV-Infected Cell Lysates

At the indicated time points post infection, EBOV-infected and mock-infected cells were scraped into 5 ml ice cold PBS, transferred into a 15 ml tube and subjected to centrifugation for 10 min at 500 x g. All liquid was removed and the pellet was frozen at -20^{o}C until ready for lysis. For cell lysis, the frozen pellet was resuspended in 25 µl cell extraction buffer (Invitrogen) supplemented with 1 µl protease inhibitor (Roche) and 0.25 µl phosphatase inhibitor (HALT, Pierce). The lysates were transferred to a 1.5 ml tube and left on ice for 20 minutes, vortexing every 5-7 minutes during this incubation period. Samples were centrifuged for 8 min at 10,600 x g and 25 µl of the lysates were transferred into fresh tubes containing 4x SDS sample buffer and incubated for 10 min at 99°C to inactivate EBOV.

Preparation of Transfected Cell Lysates

Transfected cells were harvested for Western blot analysis at the indicated times post transfection. Cells were scraped into cell culture media, transferred to 2 ml tubes,

and spun down at 15,000 x g for 3 minutes at 4°C. Supernatants were discarded and the pellet was resuspended in 50 µl cell extraction buffer (Biosource) complemented with 1 mM protease inhibitor mix (Complete; Roche) and 0.1 µM serine/threonine phosphatase inhibitor (calyculin A; Cell Signaling Technologies). Lysates were incubated for 20 minutes on ice, vortexing briefly during this time. The lysates were then centrifuged for 10 minutes at 15,000 x g at 4°C. Supernatants were transferred to 1.5 ml tubes containing 50 µl 2X SDS-sample buffer (Laemmli Buffer) and either used for Western blot analysis immediately or stored at -20°C until ready for use.

Detection of Proteins

To detect proteins of interest by Western blot analysis, SDS-PAGE gels were prepared as outlined in Table 9. Prior to loading, samples were incubated for 5 minutes at 95°C. SDS gels were then loaded with the appropriate volume of sample and run at 100-140 volts until sufficient separation of proteins occurred. After separation, the proteins in the SDS-PAGE gel were transferred to a polyvinylidene fluoride (PVDF) membrane. The membrane was activated by incubating it for 30 seconds in 100% methanol. Transfer was performed by placing the SDS-PAGE gel and PVDF membrane between separate layers of Whatman blotting paper soaked in three separate transfer buffers (anode I, anode II, and cathode buffers, respectively). Proteins were transferred at 30 volts for 30 minutes. After transfer, the membrane was incubated in blocking buffer (Odyssey Blocking Reagent) for 1 hour at room temperature, or 4°C overnight, then washed 3 times in TBS + 0.1% Tween, for ten minutes per wash. The membrane was

then incubated with the appropriate primary antibodies, diluted in Odyssey Blocking Reagent supplemented with 0.1% Tween for either 1 hour at room temperature or 4^{o}C overnight. Primary antibodies used are outlined in Table 10. After the membrane was washed three times with TBS supplemented with 0.1% Tween, 10 minutes per wash, it was incubated with the appropriate secondary antibodies diluted in Odyssey Blocking Reagent with 0.1% Tween for either 1 hour at room temperature or 4^{o}C overnight. The membranes were protected from light and washed twice in TBS with 0.1% Tween, followed by two washes with TBS alone. Blots were then scanned on the Odyssey Infrared Imaging system, and analyzed using Image Studio software.

Table 9. Preparation of SDS-PAGE Gels

	Stacking gel	**Separating gel**		
	4%	**8%**	**10%**	**12%**
H_2O	2.9 ml	4.7 ml	4 ml	3.3 ml
30% acrylamide/bisacrylamide	750 µl	2.6 ml	3.3 ml	4 ml
10% SDS	50 µl	100 µl	100 µl	100 µl
1.5 M Tris pH 8.8	-	2.5 ml	2.5 ml	2.5 ml
0.5 M Tris pH 6.8	1.25 ml	-	-	-
10% APS	50 µl	100 µl	100 µl	100 µl
TEMED	5 µl	5 µl	5 µl	5 µl

Table 10. Western Blot Primary Antibodies

Target	Species	Source	Dilution
β-actin	Mouse	Abcam (ab8226-100)	1:1000
eIF2α phospho	Rabbit	Life Technologies (44-728G)	1:1000
eIF2α total	Mouse	Biosource (AHO802)	1:500
Flag (M2)	Mouse	Sigma (F1804)	1:25,000
HA	Mouse	Covance (MMS-101P)	1:2000
HuR	Mouse	Santa Cruz Biotechnology, Inc (sc-5261)	1:600
Lamin B	Rabbit	Abcam (ab16048)	1:3000
NP	Mouse	G. Olinger USAMRIID	1:5000
TTP	Rabbit	P. Anderson, Division of Rheumatology, Immunology and Allergy. Brigham and Women's Hospital	1:1500
Tubulin	Mouse	Sigma (T6199)	1:5000
VP35	Mouse	C. Basler, Department of Microbiology, Icahn School of Medicine at Mount Sinai	1:200

Immunofluorescence Analysis

Fixation of EBOV-Infected Cells

At the indicated times post infection, EBOV-infected cells grown on chamber slides (Thermo Scientific) or chambered glass slides (Fisher Scientific) were fixed and inactivated for at least 24 hours with 4% paraformaldehyde (PFA, v/v) at 4^{o}C following

the inactivation SOPs of the respective BSL-4 facility. Once inactivated, all samples were treated as non-infectious and any subsequent immunofluorescence analysis (IFA) was performed at BSL-2 conditions.

Fixation of Non-Infected or Transfected Cells

At the indicated times post transfection, and after any appropriate drug treatments, media was removed from cell culture plates, and cells were washed once with PBS. Enough 4% PFA to cover the cells was then added, and cells were incubated at room temperature for 20 minutes, or 4^{o}C overnight. Transfection experiments intended for IFA were performed using glass coverslips.

Immunofluorescence Analysis

After fixation, PFA was removed and cells were washed with PBS. Cells were then permeabilized with 0.1% Triton X 100 (Boston Bioproducts) for 5 minutes at room temperature, using just enough Triton X to cover the cells on the slides or on the coverslips. Samples were then washed three times with PBS and subsequently incubated with 0.1 M glycine in PBS for 5 minutes at room temperature. Samples were again washed three times with PBS and then incubated with blocking reagent for 10 minutes at room temperature. Chamber slides or coverslips were then incubated at 4^{o}C overnight with the appropriate primary antibodies diluted in 25 µl blocking solution. All primary antibodies and their working dilutions are outlined in Table 11. After overnight

incubation with primary antibodies, samples were washed three times with PBS, and incubated with the applicable secondary antibodies (Table 12) diluted in 25 µl blocking solution for 1 hour at room temperature, protected from light. All chamber slides or coverslips were then washed three times in PBS dipped in Ultrapure water and dried slightly before fixing to glass microscope slides using mounting reagent (Calbiochem). Coverslips were sealed using nail polish around the edges.

Table 11. Primary Antibodies for Immunofluorescence

Target	Species	Source	Dilution
EBOV serum	Goat	S. Becker, University of Marburg, Marburg, Germany	1:500
eIF3	Goat	Santa Cruz Biotechnology Inc., (sc-16377)	1:50
eIF4G	Rabbit	Santa Cruz Biotechnology, Inc. (sc-11373)	1:100
G3BP	Mouse	BD Biosciences (611126)	1:50
HA	Mouse	Covance (MMS-101P)	1:50
HA	Rabbit	Covance (PRB-101P)	1:100
HuR	Mouse	Santa Cruz Biotechnology Inc., (3A2)	1:50
NP	Mouse	G. Olinger USAMRIID	1:100
PABP	Mouse	Santa Cruz Biotechnology, Inc. (sc-32318)	1:50
TIA-1	Goat	Santa Cruz Biotechnology, Inc. (sc-1751)	1:50
TTP	Rabbit	P. Anderson, Division of Rheumatology, Immunology and Allergy. Brigham and Women's Hospital	1:750
USP10	Rabbit	J. Connor, Boston University	1:200
VP35	Mouse	C. Basler, Department of Microbiology, Icahn School of Medicine at Mount Sinai	1:1000

Table 12. Secondary Antibodies for Immunofluorescence

Fluorescence conjugate	Species	Target Species
Alexa Fluor 350	Donkey	Mouse
Alexa Fluor 488	Chicken	Mouse
Alexa Fluor 488	Goat	Rabbit
Alexa Fluor 488	Donkey	Goat
Alexa Fluor 488	Goat	Rabbit
Alexa Fluor 350	Donkey	Rabbit
Alexa Fluor 594	Donkey	Goat
Alexa Fluor 594	Chicken	Mouse
Alexa Fluor 647	Donkey	Goat
Alexa Fluor 647	Goat	Mouse
Alexa Fluor 647	Donkey	Rabbit

Induction of Stress Granule Formation

For the induction of stress granule formation, cells were treated with 0.5 to 2 mM sodium arsenite (Ars) for 30 minutes at 37°C and then fixed in 4% PFA. For EBOV infection experiments, Ars treatment was performed by replacing media with fresh media either containing the indicated amount of Ars, or media without Ars for mock-treated cells. For transfection experiments, the indicated amount of Ars or PBS (mock-treated) was added dropwise onto the cells. Hippuristanol (kind gift from J. Pelletier, McGill University, Montreal, Canada) was also used to induce SGs. 1.25 μM Hippuristanol (Hipp) or the same volume of PBS (mock-treated) was added dropwise onto the cells. Cells were then incubated for 30 minutes at 37°C.

Cycloheximide Treatment

U2OS cells were infected with EBOV at an MOI of 1.5 PFU per cell. At 24 hours p.i., cell supernatants were removed and replaced with DMEM supplemented with 2% FBS and 0.5 mM Ars or DMEM and FBS alone for mock treated cells. After a 30 minute incubation period at 37°C, supernatants were removed and replaced with media containing either 100 µg/ of cycloheximide (CHX) or DMSO. Cells were incubated for one hour at 37^{o}C, washed once with PBS and fixed with DMEM containing 4% PFA.

Fluorescence In-situ Hybridization (FISH)

All FISH experiments were performed by Dr. S. Doganay at the Department of Physics, University of Illinois at Urbana-Champaign, IL. FISH probes were designed using Stellaris FISH Probe Designer software from Biosearch Technologies. A total of 48 probes, each 20 nucleotides in length and labeled with Alexa Fluor 594 or Cy5 were used to target the EBOV NP mRNA or genomic RNA sequence. U2OS cells were infected at an MOI of 1 as described above in the IFA section. Cells were fixed with 4% PFA for 48 hours and stored in 70% EtOH at -20°C until usage. Cells were rehydrated in PBS and subsequently subjected to FISH or IFA followed by FISH. For immunofluorescence analysis (IFA), all reagents were supplied with 2 mM of vanadyl ribonucleoside complex (VRC). For permeabilization and blocking, the IFA protocol described above was used. Primary antibodies were incubated for 3 hours and secondary antibodies for 2 hours at room temperature. After antibody incubation, cells were treated with 3% PFA for 10

minutes at room temperature for post-fixation and subjected to FISH. For FISH, cells were washed in 2x SSC (0.3 M NaCl, 0.03 M sodium citrate) containing 10% formamide for 5 minutes. Hybridization was performed at 37˚C overnight in 100 µl of hybridization buffer (10% dextran sulfate, 2 mM VRC, 0.02% RNAse-free BSA, 50 µg *E.coli* tRNA, 2x SSC, 10% formamide) containing labeled FISH probes targeting EBOV NP mRNA.

Click-iT Metabolic Labeling Assay

For fluorescence-based detection of nascent proteins, the Click-iT L-homopropargylglycine (L-HPG) metabolic labeling system (Invitrogen) was used. U2OS cells were infected as described above. At 25 hours p.i., cells were washed with D2-Met/Cys depletion medium (Sigma Gibco) and incubated in D2-Met/Cys depletion medium for one hour. Cell supernatants were removed and replaced with D2-Met/Cys depletion medium supplemented with 100 µM Click-iT L-HPG. After a 30-minute incubation period at 37^{o}C, cells were fixed with 4% PFA as described above, permeabilized with methanol for 15 minutes at -20^{o}C and blocked with 5% donkey serum for one hour. The Click-iT reaction buffer containing Alexa Fluor 488 detection reagent was added for 30 minutes at room temperature, protected from light. The cells were washed with 5% donkey serum, and then placed in PBS at 4^{o}C until ready for further IFA processing and imaging, which was performed as described above.

Imaging and Processing

Confocal imaging was performed using a Zeiss 710 confocal microscope with a Plan-Apochromat primary objective (63x; NA, 1.4). All images were taken using multi-track scanning for each fluorophore to prevent bleed-through. Z-dimension (z-) stacks, pinholes were set to an Airy unit of 1. Images were also acquired with a Zeiss Axiovert 200 M inverted microscope and a Plan-Apochromat primary objective (63x; NA, 1.4). Image acquisition and processing software used includes the Zeiss Zen (confocal microscope), Zeiss AxioVert (inverted microscope) and ImageJ (http://imagej.nih.gov/ij/).

Statistical Analysis

For quantitative analysis of SG-containing cells, cells were counted by two independent researches. One researcher was unbiased to the experiment and blinded to the drug conditions. An unpaired two sample t-test was performed using the GraphPad Prism version 5.04 for Windows, GraphPad Software, La Jolla California USA, www.graphpad.com.

Buffer Recipes

Blocking Reagent for IFA

20 g Bovine Serum Albumin (BSA), 2 ml Tween-20, 30 ml glycerin, 10 ml sodium azide (NaN_3, 5% solution), 1 L sterile PBS, sterile filtered

0.1 M Glycine for IFA

3.75 g glycine and 500 ml Ultrapure H_2O

0.1% Triton for IFA

0.1 ml Triton-X-100 and 100 ml PBS

4% Paraformaldehyde for IFA

71.25 ml 32% PFA solution and 500 ml DMEM

SDS-PAGE Running Buffer (10x)

10 g SDS, 30 g Tris, 144 g glycin, and 1 L H_2O

10% SDS for Western Blot

50 g SDS and 500 ml H_2O

TBS (10x) for Western Blot

24.2 g Tris, 80 g NaCl, 1 L H_2O, the pH was adjusted to 7.6 with HCl

1.5 M Tris for SDS gels

181.71 g Tris and 1 L H_2O, the pH was adjusted to to 8.8 or 6.8 with HCl

Anode Buffer I for Western Blot

36.34 g Tris, 200 ml EtOH, and 1 L H_2O

Anode Buffer II for Western Blot

3.06 g Tris, 200 ml EtOH, and 1 L H_2O

Cathode Buffer for Western Blot

6.25 g E-amino-capronic acid, 3.03 g Tris, 200 ml EtOH, and 1 L H_2O

CHAPTER THREE: EXAMINING THE CELLULAR STRESS RESPONSE DURING EBOLA VIRUS INFECTION

Rationale

During EBOV infection, the virus employs many immune evasion strategies, most notably via multiple layers of type I interferon (IFN) inhibition. VP35 is a key player in this innate immune evasion but also acts as a nucleocapsid component and a polymerase cofactor (Audet & Kobinger, 2015; Basler, 2015). By binding to and masking dsRNA, VP35 is able prevent the activation of viral nucleic acids sensors such as retinoic acid inducible gene 1 (RIG-I) (Cárdenas et al., 2006). Furthermore, VP35 has been shown to antagonize both PKR and IRF-3 activity, contributing to IFN inhibition (Feng, Cerveny, Yan, & He, 2007a; Hartman et al., 2004; Prins et al., 2009; Schümann et al., 2009). While type I IFNs and cytoplasmic nucleic acid pattern recognition receptors are thought of as prototypical components of the host innate antiviral response, the cellular stress response has also been implicated as an important mechanism for halting viral protein translation and thereby limiting viral replication (Montero & Trujillo-Alonso, 2011; Onomoto, Yoneyama, Fung, Kato, & Fujita, 2014). The global decrease in protein translation associated with SG formation is unsustainable for viral replication, which requires the host translational machinery to synthesize viral proteins. Therefore, many viruses have evolved strategies to antagonize the induction of the stress response. This often involves a disruption in the signaling pathways leading to eIF2α phosphorylation, primarily via PKR antagonism (Montero & Trujillo-Alonso, 2011; Valiente-Echeverría,

Melnychuk, & Mouland, 2012). Other mechanisms observed include the degradation or sequestration of key SG nucleation proteins such as G3BP or TIA-1(Matthews & Frey, 2012; J. P. White & Lloyd, 2011).

While many viruses have been shown to disrupt SG formation at various times during infection, little is known about the induction of a stress response during EBOV infection and whether the virus possesses putative SG antagonizing functions to prevent SG formation. It has been shown previously that PKR activation, the main trigger for SG induction during viral infection, is suppressed in EBOV-infected cells by VP35 through an undefined mechanism (Feng, Cerveny, Yan, & He, 2007a; Schümann et al., 2009). Furthermore, eIF2α is not phosphorylated during EBOV infection, suggesting that SG formation is not induced (Olejnik et al., 2013). However, the inhibitory effects of VP35on PKR activation were observed late in infection when the amount of VP35 was presumably high. It is thus unknown if PKR activation and eIF2α phosphorylation occur early in infection, when the VP35 levels are still low. Vulnerability of EBOV to exogenous stress might reveal novel strategies toward the development of antivirals. Therefore, we aimed to examine the cellular stress response mediated by SG formation more thoroughly during EBOV infection.

Results

3.1 Stress granules do not form during EBOV infection.

To determine if SG formation is induced during EBOV infection, particularly at early time points, we analyzed the distribution of the SG proteins eIF4G (Figure 3) and

TIA-1 (Figure 4) in EBOV-infected U2OS cells at different time points post infection (p.i.) by IFA. In non-infected cells, both eIF4G and TIA-1 were homogenously distributed in the cytoplasm at all time points examined, but were redistributed into typical punctate SGs when sodium arsenite (Ars) was used to induce oxidative stress (Figures 3 and 4, right panels). In EBOV-infected cells at early time points p.i. eIF4G and TIA-1 showed similar homogenous distribution in the cytoplasm and SGs were not observed. EBOV infection, visualized by staining for the nucleocapsid protein VP35, could only be detected at 17 and 24 hours p.i. when viral protein expression was high. At these late time points VP35 staining denoted typical viral inclusion formation, while eIF4G and TIA-1 were homogenously distributed throughout the cytoplasm of infected cells. Staining for another canonical SG protein eIF3 (data not shown) also indicated that SG formation did not occur at any time examined during EBOV infection. Collectively, the homogenous distribution of these canonical SG proteins in the cytoplasm of EBOV infected cells indicate that SGs do not form during infection.

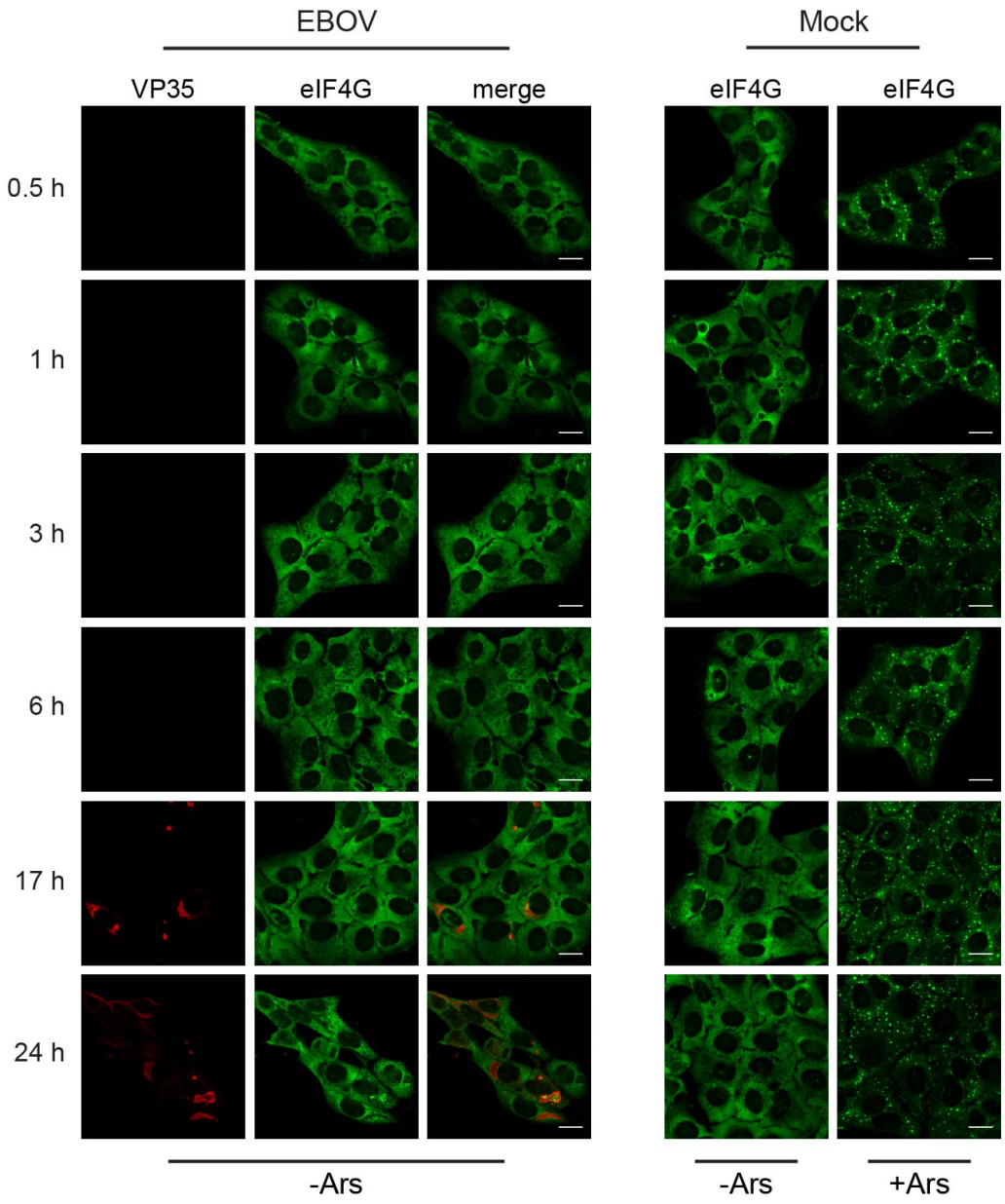

Figure 3. EBOV infection does not induce eIF4G containing canonical SGs.

U2OS cells were infected with EBOV at an MOI of 1 or mock-infected. At the indicated time points p.i. mock-infected cells were treated with 0.5 mM Ars (+Ars) for 30 minutes to induce SG formation or left untreated (-Ars). IFA was performed using antibodies against VP35 (red) and eIF4G (green). Scale bars = 20 μM.

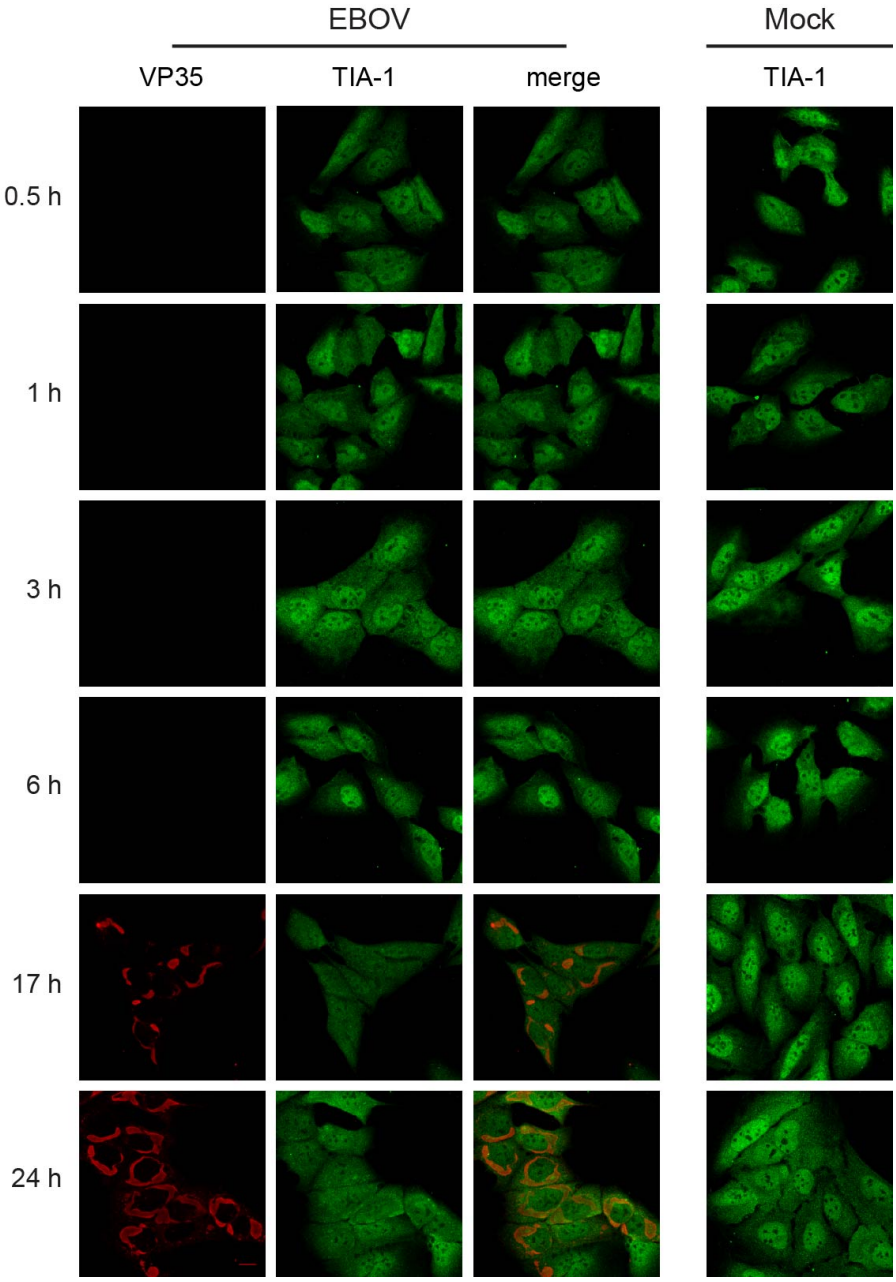

Figure 4. EBOV infection does not induce TIA-1 containing canonical SGs.

U2OS cells were infected with EBOV at an MOI of 1 or mock-infected. At the indicated time points p.i. mock-infected cells were treated with 0.5 mM Ars (+Ars) for 30 minutes to induce SG formation or left untreated (-Ars). IFA was performed using antibodies against VP35 (red) and TIA-1 (green).

3.2 SG proteins are sequestered within viral inclusions late during infection.

Although eIF4G was homogenously distributed throughout the cytoplasm of infected cells, indicating that SGs do not form, it was found aggregated within the viral inclusions starting at 17 hours p.i. in EBOV infected cells (Figure 3). This accumulation of eIF4G was more pronounced at 24 hours p.i. when viral inclusions were larger and more prominent (Figure 3). Many other SG proteins, including eIF4G (Figure 5A i), eIF3 (Figure 5A ii), poly-A binding protein (PABP Figure 5A iii) and human antigen R (HuR, Figure 5A iv), were found sequestered within viral inclusions by 24 hours p.i. but otherwise remained homogenously distributed throughout the cytoplasm. While a number of SG proteins were found aggregated within viral inclusions, the homogenous distribution of TIA-1 in both the nucleus and cytoplasm of EBOV-infected cells demonstrated that not every canonical SG protein was sequestered in viral inclusions. TIA-1 distribution looked similar to that found in non-infected cells, and showed little accumulation within viral inclusions (Figure 5B). There were however, small clusters that appeared to show minor aggregation similar to that observed for other proteins (Figure 5B, white arrows). Similar to TIA-1, ubiquitin carboxyl-terminal hydrolase 10 (USP10) did not aggregate within viral inclusions, although there were also minor areas of weak colocalization (Figure 5C, white arrows). Finally, the SG protein TTP, which is an important regulator of mRNA stability, was also absent from viral inclusions (data not shown). However, TTP showed no minor aggregation or colocalization with viral inclusions, suggesting that it is entirely excluded from inclusions. Collectively these data indicate that many, but not all, SG proteins are sequestered within viral inclusions at late

times during infection. Furthermore, these SG protein granules are compositionally different from fully formed canonical SGs and might represent a distinct species of protein granules.

To further examine the distribution of the SG proteins within viral inclusions, optical sectioning was performed in order to obtain Z-stack images of multiple focal planes within a single EBOV inclusion. This type of analysis allows users to examine protein colocalization in three dimensions, as depicted in (Figure 6, top panel), which helps remove some of the limitations of examining 3D structures images in two dimensions. When EBOV infected U2OS cells were examined using this technique, we observed that the SG proteins sequestered within viral inclusions showed no direct colocalization with any nucleocapsid protein, and that viral proteins were excluded from these aggregates (VP35 examined in red, eIF4G in green, Figure 6 bottom panel). Together, these results indicate that the nucleocapsid proteins fully encompass, but are excluded from, the SG protein aggregates within viral inclusions.

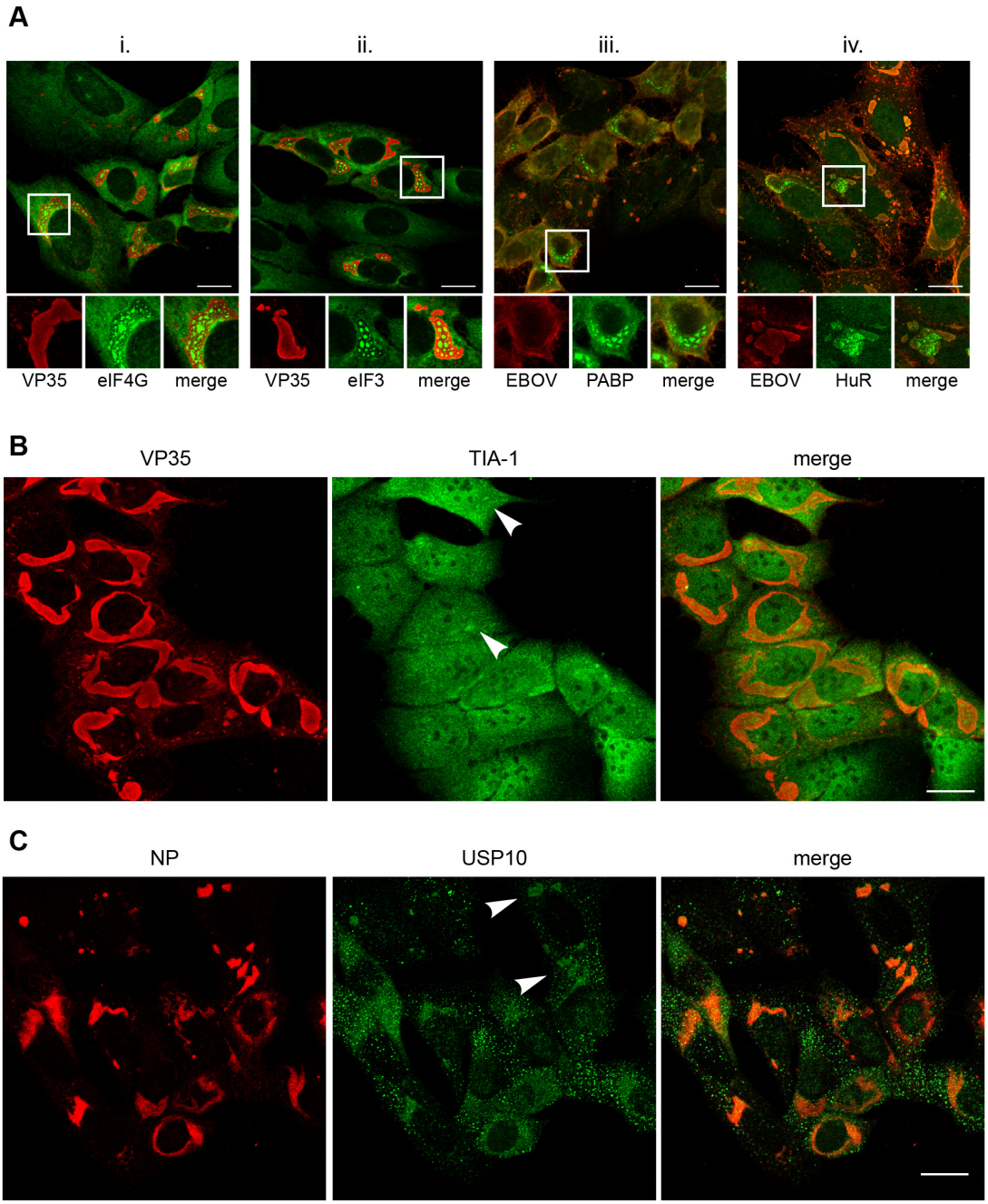

Figure 5. SG proteins are sequestered within viral inclusions.

A) U2OS cells were infected with EBOV at an MOI of 1.5, fixed at one day p.i. and analyzed by IFA. The SG proteins (green) eIF4G (i), eIF3 (ii), PABP (iii) or HuR (iv) were examined using antibodies specific for each protein. EBOV inclusions (red) were

detected using either an antibody against VP35 (i, ii) or an anti-EBOV serum that recognizes both GP and NP (iii, iv). B) U2OS cells were infected as in (A) but were stained for the viral protein VP35 (red) or the SG protein TIA-1 (green). White arrows indicate areas of TIA-1 minor colocalization with viral inclusions. C) U2OS cells were infected as in (A) but were stained for the viral protein NP (red) or the SG protein USP10 (green). White arrows indicate areas of USP10 minor colocalization with viral inclusions. Scale bars = 20 μM

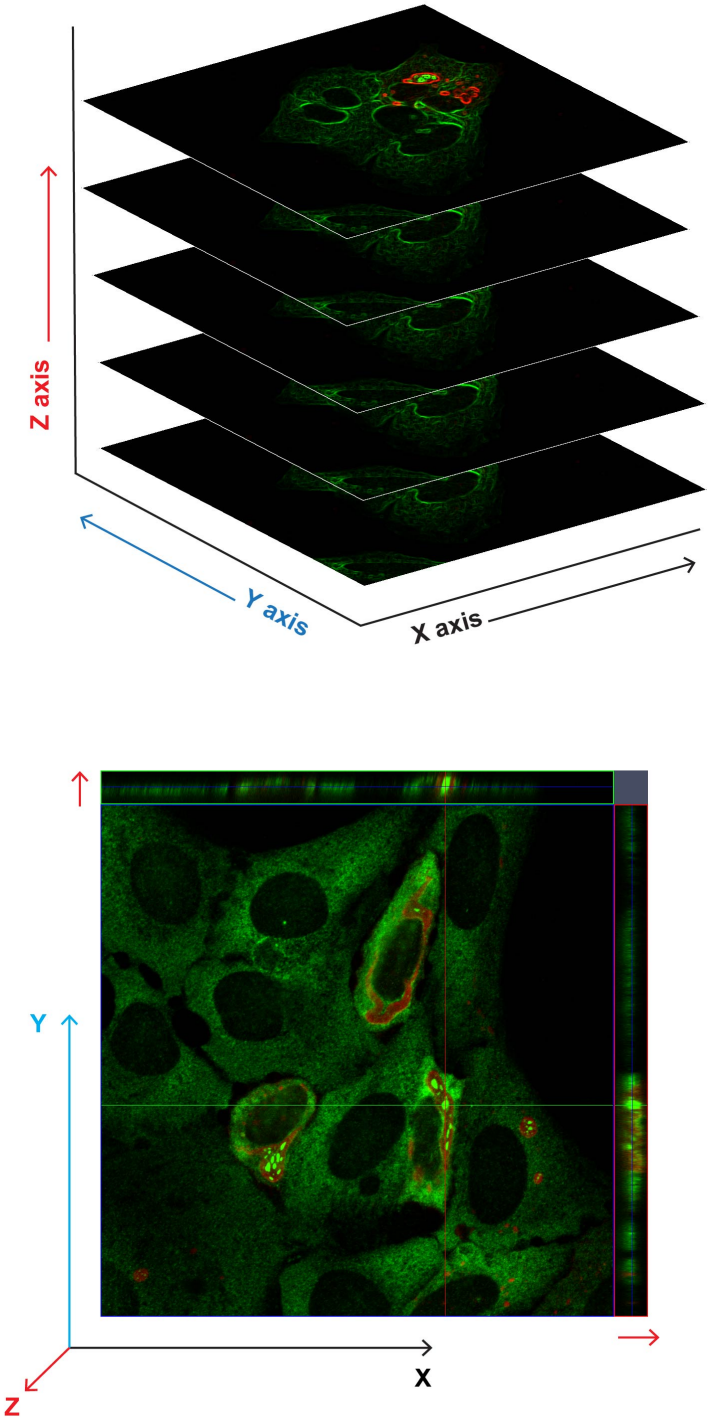

Figure 6. Three-dimensional analysis of sequestered proteins in viral inclusions.

U2OS cells were infected with EBOV at an MOI of 1 and fixed at one day p.i. and stained for the viral protein VP35 (red) and SG protein eIF4G (green). Optical sectioning using confocal z-stack analysis was performed. Schematic representation of the orientation of axes during optical sectioning is outlined in the top panel. Bottom panel indicates the X,Y, and Z axes of one z-stack, with the Z axis represented by red arrows.

3.3 Sequestered SG proteins analyzed colocalize within viral inclusions.

To address whether the sequestered SG proteins colocalized within EBOV inclusions or if they formed discrete aggregates, EBOV-infected U2OS cells were fixed at one day p.i. and co-stained for different combinations of SG proteins. The proteins eIF3 and eIF4G colocalized within viral inclusions, suggesting that they were both part of the same inclusion-bound aggregates (Figure 7A, top panels). Likewise, PABP and eIF4G also colocalized within inclusions (Figure 7A, bottom panels). Interestingly, although HuR was found sequestered within viral inclusions, it showed a distinct aggregation pattern compared to the other SG proteins present (Figure 5A iv). Compared to the eIF3 and eIF4G-containing granules, HuR clusters were significantly smaller and exhibited more irregular and less punctate aggregation within inclusions. Co-staining for eIF3 and HuR in EBOV-infected U2OS cells confirmed that these proteins formed distinct granules in EBOV inclusions and did not colocalize (Figure 7B). The HuR aggregates found in inclusions in EBOV-infected cells were in close proximity to, but separate from eIF3 granules. Thus, while a majority of the SG proteins sequestered within inclusions were found to be components of the same aggregates, this did not hold true for all SG proteins examined.

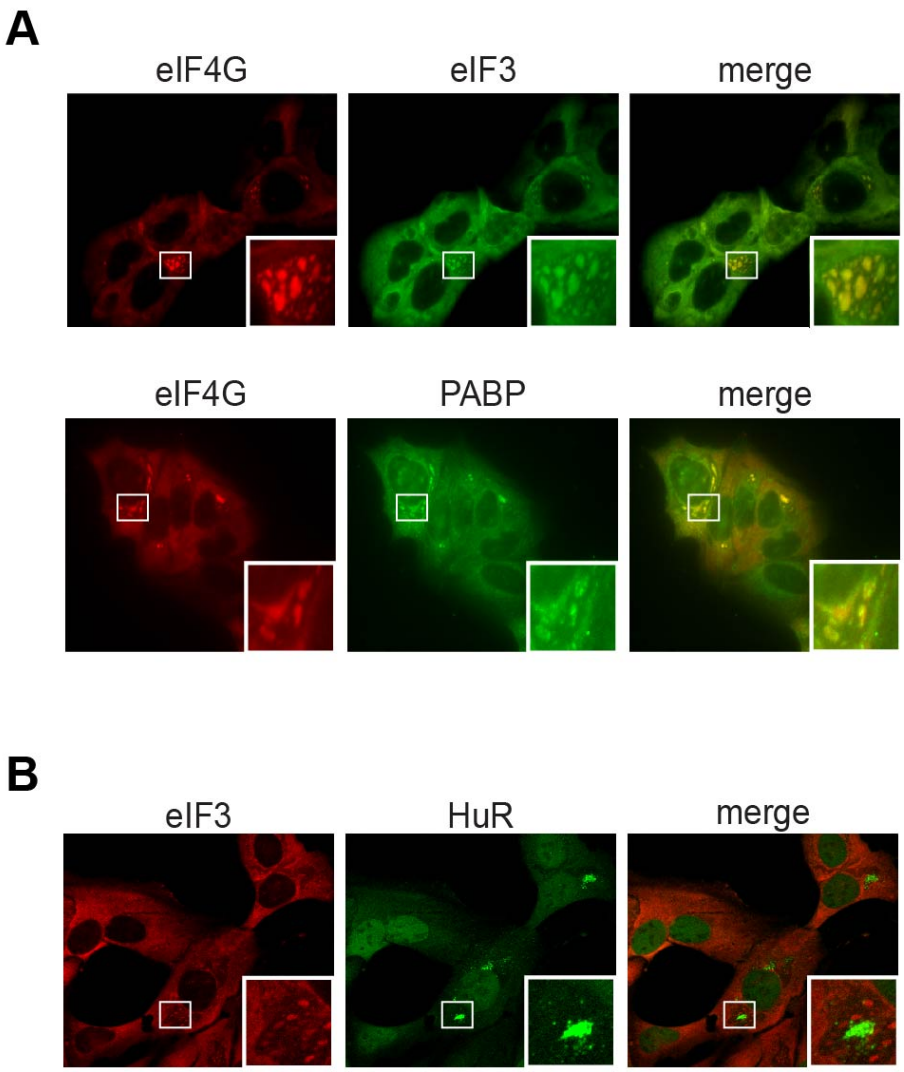

Figure 7. SG proteins colocalize within inclusions.

U2OS cells were infected with EBOV at an MOI of 1.5, fixed at one day p.i. and analyzed by IFA. A) Colocalization of SG proteins within inclusions was examined using antibodies against eIF4G (red) and eIF3 (green), or eIF4G (red) and PABP (green) respectively. C) Cells were examined as in (B) but stained for eIF3 (red), and HuR (green).

3.4 Inclusion formation is not sufficient to sequester SG proteins within inclusions.

To understand the driving force behind the accumulation of cellular proteins within viral inclusions, we next examined whether inclusion formation alone was sufficient to sequester SG proteins. U2OS cells were transfected with different combinations of plasmids expressing EBOV nucleocapsid proteins to induce inclusion formation in the absence of viral replication. In cells expressing NP alone, although inclusion formation was observed, eIF4G remained homogenously distributed in the cytoplasm and did not form aggregates within the inclusion-like structures (Figure 8). When NP was co-expressed in combination with the other nucleocapsid proteins, inclusions were reflective of those that form during infection, but eIF4G was never found aggregated within inclusions. Therefore, inclusion formation alone is not sufficient to sequester SG proteins within inclusions.

To examine if viral RNA synthesis or polymerase activity is required to redistribute SG proteins into inclusions, we next employed the minigenome system (outlined in Figure 9). This system can be used to mimic EBOV replication and transcription in a BSL-2 setting. The EBOV minigenome consists of a reporter gene flanked by the 3'leader and 5'trailer regions of the EBOV genome. The minigenome contains all required sequence elements to be accepted as a template for replication and transcription by the EBOV polymerase (Mühlberger et al., 1999). Briefly, cells are transfected with an expression plasmid containing the minigenome along with support plasmids encoding the EBOV proteins required for replication and transcription, which include the nucleocapsid proteins NP, VP30 and VP35, and the polymerase L. Reporter

gene expression is indicative of proper viral replication and transcription (Hoenen et al., 2012b; Mühlberger et al., 1999). Using this system, U2OS cells were transfected with a 3E5E-GFP minigenome driven by a pol II promoter, and the appropriate support plasmids, which were expressed from the pCAGGs backbone. Cells transfected in the absence of L showed no GFP expression as expected, and the SG proteins examined (HuR, G3BP and eIF4G) were all homogenously distributed in the cytoplasm, similar to their distribution in untransfected cells (data not shown). Similarly, when L was co-transfected with the minigenome and support plasmids, although GFP expression signified efficient minigenome activity, HuR, G3BP and eIF4G were not observed within viral inclusions and remained diffusely spread throughout the cytoplasm (Figure 10). These data indicate that inclusion formation and polymerase activity were not sufficient to redistribute and aggregate SG proteins within inclusions.

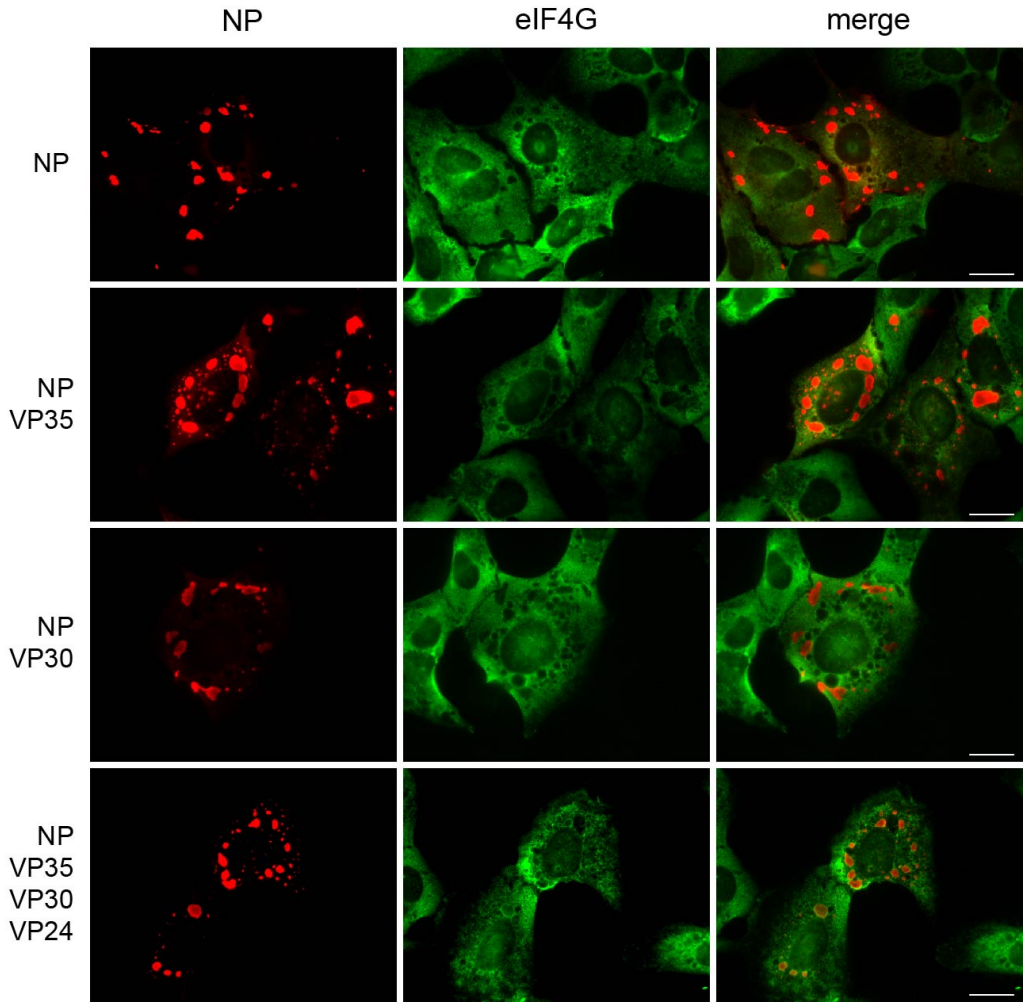

Figure 8. Inclusion formation is not sufficient to sequester SG proteins.

U2OS cells were transfected with the indicated combinations of the expression plasmids containing the viral genes *NP*, *VP30*, *VP35* or *VP24* and examined 2 days post-transfection by IFA using antibodies against NP (red) and eIF4G (green). Scale bars = 20 μM

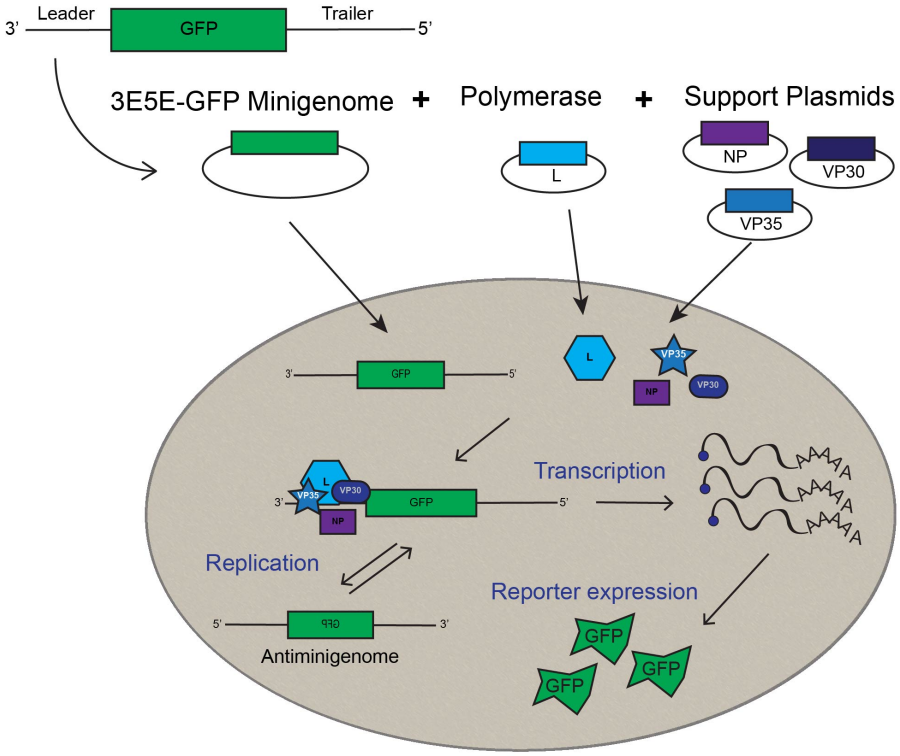

Figure 9. EBOV minigenome system.

The 3' and 5' leader and trailer regions of the EBOV genome are cloned into a pol II-driven expression plasmid where they flank a reporter gene. This expression plasmid is transfected into cells along with additional support plasmids, which encode the nucleocapsid proteins that are required for EBOV replication and transcription and include NP, VP35, L and VP30. In the transfected cells, an RNA minigenome template is generated and the nucleocapsid proteins are expressed. This then leads to initial rounds of replication, producing anti-minigenome, which is used as a template for additional minigenome production. Transcription of the minigenome leads to reporter gene mRNA production, followed by protein expression, which is the readout for successful minigenome replication and transcription.

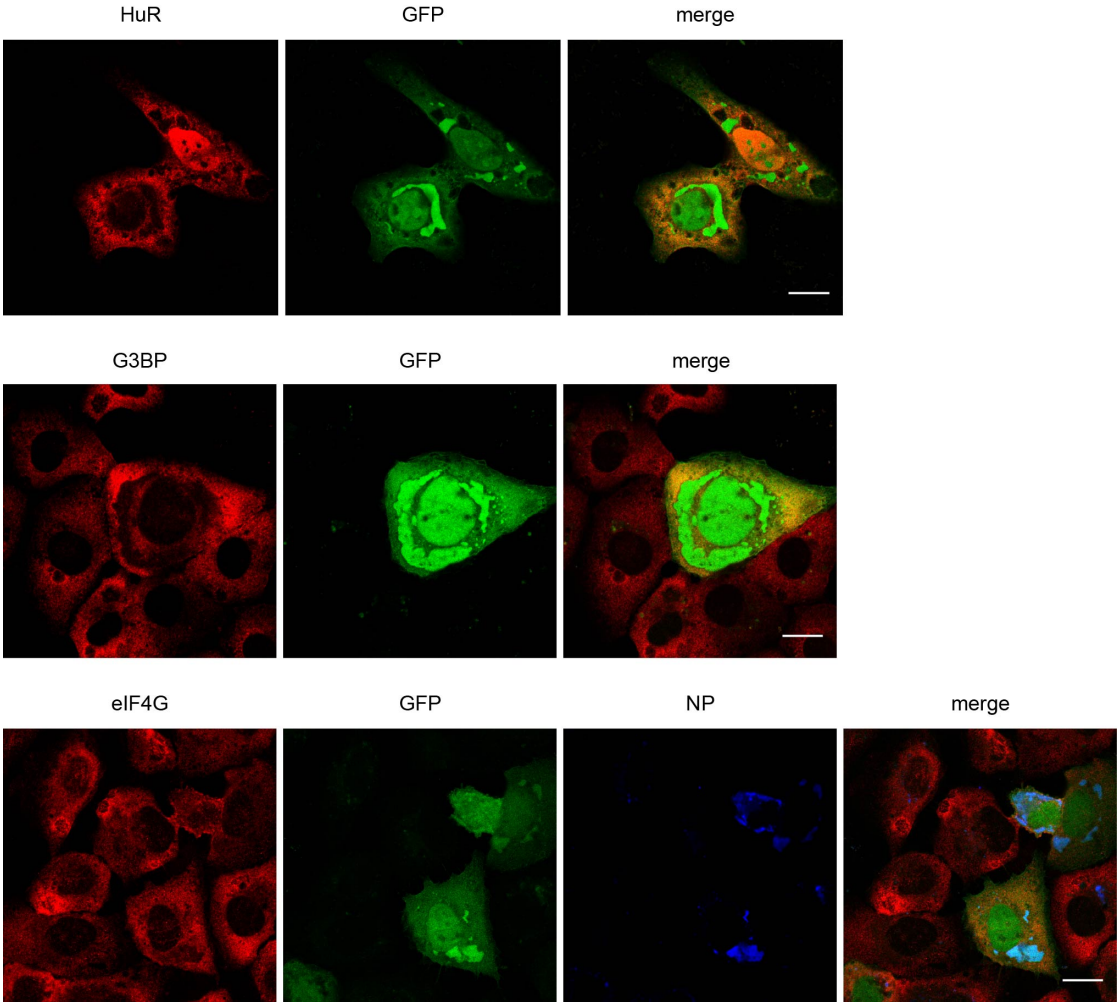

Figure 10. EBOV minigenome replication and transcription are not sufficient to sequester SG proteins.

U2OS cells were transfected with the 3E-5E-eGFP minigenome, driven by a pol II promoter along with EBOV support plasmids. Cells were fixed 2 days post transfection and examined by IFA. Staining was performed for the SG proteins HuR, G3BP or eIF4G (red). GFP expression indicates minigenome replication and transcription. Cells stained for eIF4G were also stained for the viral protein NP (blue) to identify viral inclusions. Scale bars = 20 μM

3.5 Sequestered SG proteins colocalize with viral RNA in inclusions

Many of the proteins involved in SG formation are RNA binding proteins important for mRNA stability and translation initiation (Kedersha & Anderson, 2002). Because EBOV inclusions are the sites of viral RNA synthesis and contain viral RNA (Hoenen et al., 2012), we next examined if there was any interaction between the inclusion-bound SG proteins and viral RNAs within inclusions. To visualize the intracellular distribution of viral RNA species during infection, we performed fluorescent in-situ hybridization (FISH). U2OS cells were infected with EBOV and 24 hours p.i, examined by FISH analysis using probes specific for NP positive-sense mRNA or negative-sense genomic RNA. While the probes designed to target NP mRNA also recognize positive sense antigenome RNA, this RNA species is much less abundant in infected cells than the viral mRNA (Shabman et al., 2014; Weik, Enterlein, Schlenz, & Mühlberger, 2005). Therefore, we assume that FISH probes for NP positive-sense RNA are predominately targeting NP mRNA. At 6 hours p.i., NP positive-sense RNA was diffusely distributed throughout the cytoplasm of infected cells, but demonstrated clustered aggregation at 24 hours p.i. (Figure 11A). These aggregates resembled those observed for the SG proteins sequestered within inclusions. The distribution of negative-sense genomic RNA showed similar aggregated distribution in a majority of cells examined at 24 hours p.i. (Figure 11B, left panel yellow arrows). However, it was also found in more inclusion-like patterns, with little to no aggregation apparent (Figure 11B, right panels, white arrows). When examined concurrently at 24 hours p.i., both positive-sense NP RNA and negative-sense genomic RNA were found to colocalize in distinct

areas of infected cells, presumed to be inclusions (Figure 11C). Staining for both negative-sense RNA and the viral protein NP confirmed that these RNA species were in fact found within viral inclusions (Figure 11D).

To examine if SG proteins colocalized with viral RNA, the SG protein eIF3 was stained for in addition to viral RNA. At 24 hours p.i., both NP positive-sense RNA (Figure 12A) and negative-sense genomic RNA (Figure 12B) showed colocalization with eIF3. Positive-sense NP RNA showed no colocalization with TTP, however (Figure 12C), suggesting that only the SG proteins found within inclusions colocalized with the viral RNA, and excluding the possibility of fluorescence bleed through. Collectively, these data indicate that viral RNA colocalizes with inclusion-bound aggregates and may be responsible for their sequestration.

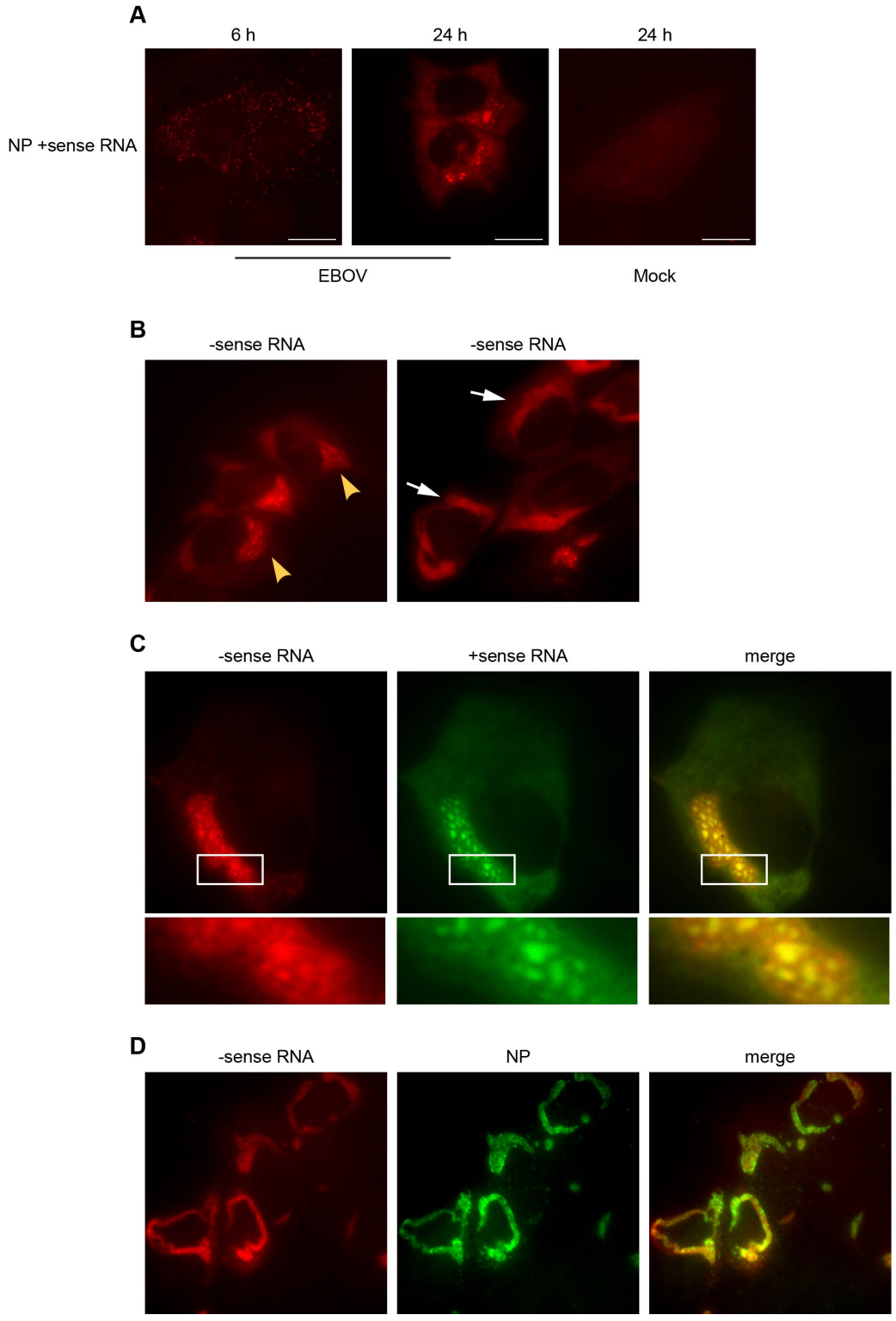

Figure 11. NP mRNA and genomic RNA colocalize within viral inclusions.

U2OS cells were infected with EBOV at an MOI of 1, fixed at 6 hours (A) or 24 hours p.i. (A-D) and analyzed by FISH using RNA probes specific for NP positive-sense RNA (A) or negative-sense genomic RNA (B). Yellow arrowheads in (B) indicate viral RNA with aggregated distribution similar to the distribution observed for inclusion bound SG aggregates. White arrows indicate viral RNA with a more inclusion like distribution. C) Distribution of EBOV RNA in infected cells at 24 hours p.i. Positive-sense NP RNA is shown in green and negative-sense genomic RNA in red. Areas shown in higher magnification are indicated by white rectangles. D) NP protein (green) was co-stained for with negative-sense genomic RNA (red) at 24 hours p.i. Scale bars = 20 μM

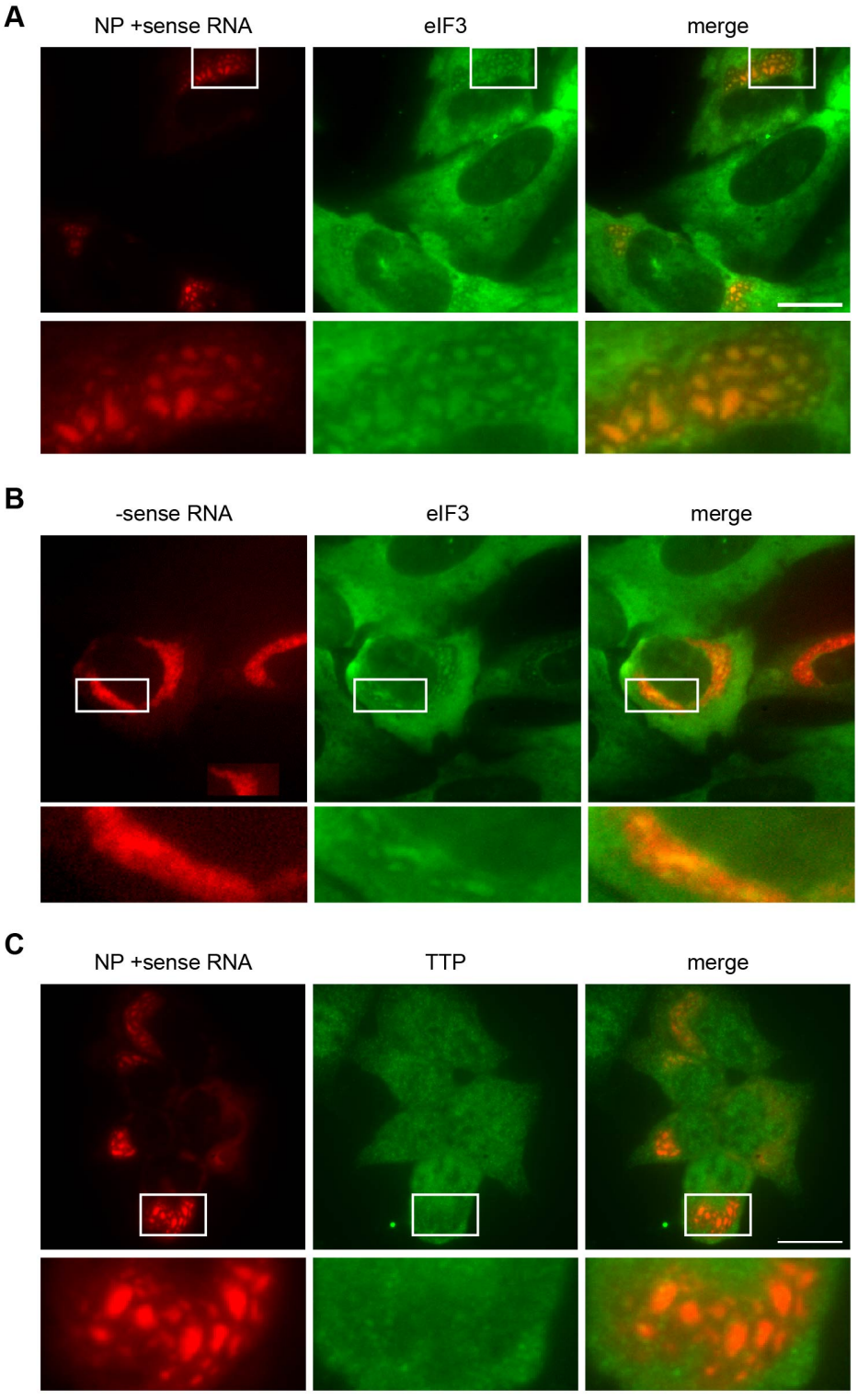

Figure 12. Inclusion-bound SG proteins colocalize with viral RNA species.

U2OS cells were infected with EBOV at an MOI of 1, fixed at 24 hours p.i. and analyzed by FISH using RNA probes specific for NP positive-sense RNA (A, red) or negative-sense genomic RNA (B, red). Distribution of the SG protein eIF3 (green) was analyzed by IFA. C) U2OS cells were infected and fixed as in (A) but stained for the SG protein TTP (green) and NP positive-sense RNA (red). Scale bars = 20 μM

3.6 HuR does not colocalize with viral RNA.

Because the distribution of HuR within viral inclusions was different from that of the other SG proteins we examined, we next sought to determine if HuR colocalized with viral RNA. U2OS cells were infected with EBOV and examined at 24 hours p.i. by FISH using probes binding to viral RNA, and IFA using an antibody against HuR. Although HuR was found aggregated in distinct locations in these cells, it did not colocalize with either genomic RNA or positive-sense NP RNA (Figure 13). Instead, HuR was found in very close proximity to or surrounding these viral RNA aggregates. These data further suggest that HuR may serve a distinct function from the inclusion-bound aggregates.

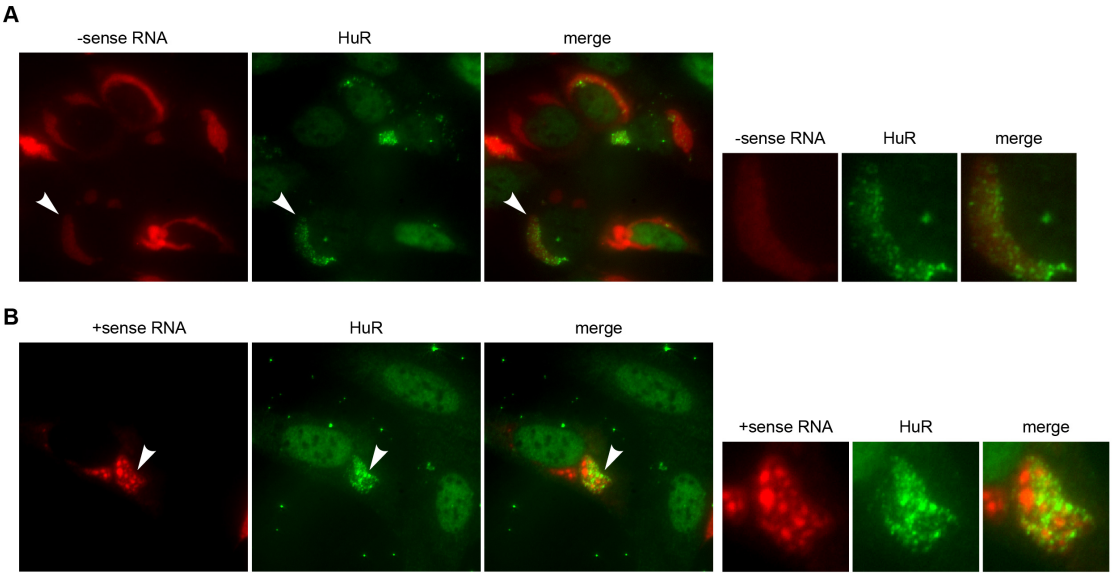

Figure 13. HuR does not colocalize with viral RNA.

U2OS cells were infected with EBOV at an MOI of 1 and fixed at 24 hours p.i. Negative-sense genomic RNA (A, red) or positive-sense NP mRNA (B, red) were examined for colocalization with HuR protein (green). White arrowheads indicate areas of higher magnification, shown on the right.

3.7 Inclusion-bound aggregates are distinct from canonical SGs.

While many SG proteins aggregated into distinct structures within viral inclusions, these structures were larger and less symmetrical in shape than typical SGs found in the cytoplasm. As shown in Figure 4, the canonical SG marker protein TIA-1 was not found as part of the aggregates in inclusions, suggesting that these structures are distinct from canonical SGs. Other viruses such as chikungunya virus, Semliki Forest virus and vaccinia virus have been shown to induce the formation of granules containing various SG components that are morphologically, structurally or functionally different from canonical SGs (Panas et al., 2012; Rozelle, Filone, Kedersha, & Connor, 2014; Scholte et al., 2015). To more thoroughly distinguish the inclusion bound aggregates observed during EBOV infection from canonical SGs, we used cycloheximide (CHX), an inhibitor of protein synthesis known to block polysome disassembly and dissolve SGs. Canonical SGs disperse upon exposure to CHX, while other virally induced SG-like aggregates do not (Kedersha et al., 2000; Rozelle et al., 2014; Scholte et al., 2015). EBOV-infected or mock-infected U2OS cells were treated with Ars to induce SG formation, and then subsequently treated with CHX. In mock-infected cells treated with Ars, SGs completely disassembled upon CHX treatment as expected (Figure 14). When EBOV-infected cells were treated with CHX alone, the SG protein aggregates within the inclusions, shown by eFI4G (green), persisted and did not disassemble (Figure 14, -Ars, +CHX). Ars treatment of EBOV-infected cells led to the formation of SGs in the cytoplasm, which dissolved upon CHX treatment. However, despite the dissolution of SGs seen within the cytoplasm after CHX treatment, the inclusion bound granules did not

disassemble under these conditions (Figure 14, +Ars, + CHX). Thus, while aggregates containing certain SG proteins were observed within the viral inclusions during EBOV infection, because of their distinct morphology, protein composition and insensitivity to CHX treatment, we propose that they represent a unique accumulation of cellular proteins that are not canonical SGs.

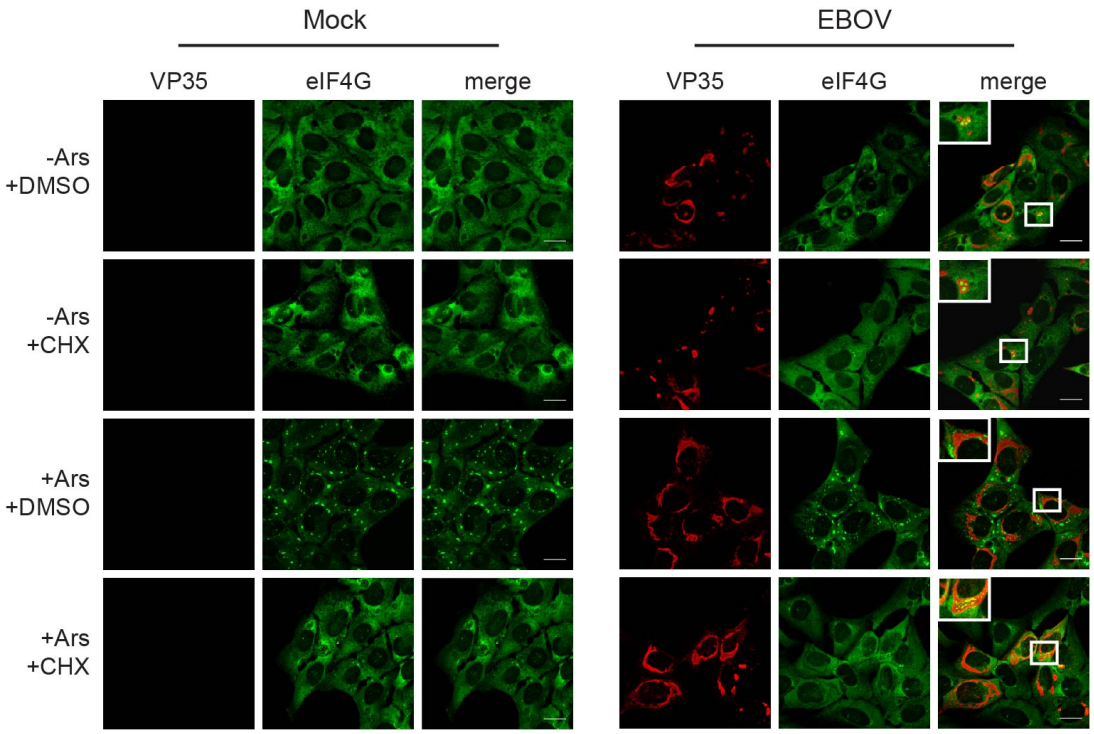

Figure 14. Inclusion-bound aggregates are not canonical SGs.

U2OS cells were infected with EBOV at an MOI of 1.5, incubated for 24 hours and then treated with 0.5 mM Ars for 30 minutes (+Ars) or left untreated (-Ars). Cells were subsequently treated with either DMSO or 100 µg/ml of CHX for 1 hour and analyzed by IFA using antibodies against VP35 (red) and eIF4G antibody (green). Scale bars = 20 µM.

3.8 Preventing SG formation does not impair inclusion-bound aggregate formation.

To further differentiate these SG like aggregates found in inclusions from canonical cytoplasmic SGs we used a doxycycline-inducible U2OS cell line that allows overexpression of eGFP-tagged USP10. USP10 is a deubiquitinase that binds to G3BP and prevents SG formation by blocking G3BP aggregation (Panas et al., 2015b). When left untreated, the U2OS-USP10-eGFP cells did not express USP10-eGFP, and formed SGs in the cytoplasm when treated with Ars, as reflected by the punctate distribution of HuR which was used as a SG marker (Figure 15A). When these cells were treated with doxycycline for 24 hours to induce USP10-eGFP overexpression, SGs formation did not occur after Ars treatment, and HuR remained diffusely distributed in cells expressing USP10-eGFP. Overexpression of USP10-eGFP had no effect on EBOV replication and allowed for normal inclusion formation in infected cells (Figure 15B). Interestingly, although SGs were unable to form in cells overexpressing USP10-eGFP, G3BP was still sequestered within viral inclusions (Figure 15C). This corroborates our findings that the aggregates of SG proteins found within viral inclusions during EBOV infection are distinct from canonical SGs. Furthermore, SG formation itself is not the impetus for the formation of inclusion bound SG-like aggregates.

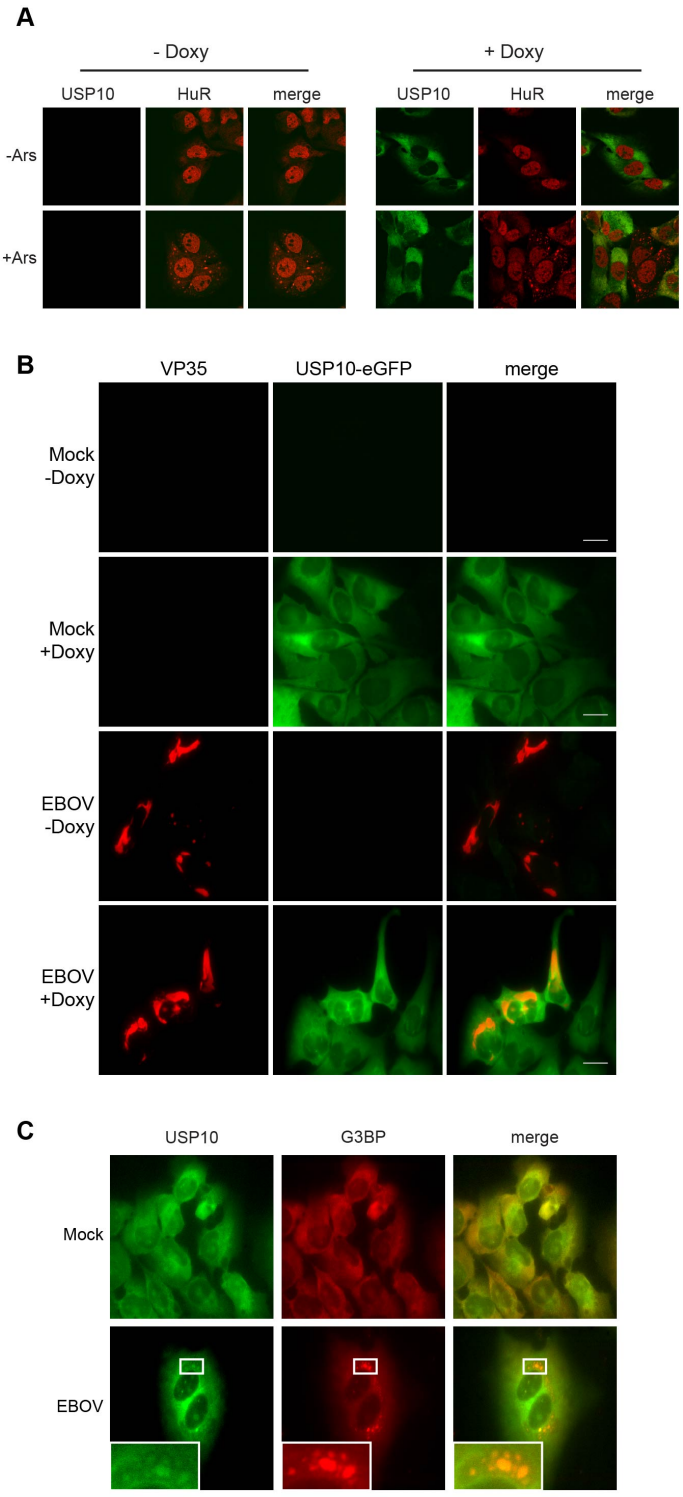

Figure 15. SG formation is not required for sequestration of SG proteins in viral inclusions.

U2OS-USP10-eGFP cells were treated with doxycycline for 24 hours to induce USP10-eGFP expression or left untreated. USP10 expression is shown in green by eGFP fluorescence. A) Untreated and doxycycline-treated cells were treated with 0.5 mM Ars for 30 minutes or left untreated. SGs were visualized using an antibody against HuR (red). B and C) U2OS-USP10-eGFP cells were infected with EBOV at an MOI of 1.5, fixed at 24 hours p.i. and analyzed by IFA using an antibody against VP35 (B, red) or G3BP (C, red). Infected cells in C were treated with doxycycline for 24 hours prior to infection.

3.9 Inclusion-bound aggregates do not impair protein translation

Next we addressed the question of whether inclusion bound granules exert antiviral activity in EBOV-infected cells. SG-like granules that are distinct from SGs but have antiviral activity have been observed for various viruses, including poxviruses and influenza virus (Onomoto et al., 2012; Rozelle et al., 2014; Simpson-Holley et al., 2011). Formation of antiviral granules during vaccinia virus infection interferes with protein translation, leading to decreased viral titers (Rozelle et al., 2014; Simpson-Holley et al., 2011). To determine if the inclusion bound granules blocked protein translation during EBOV infection, we examined nascent protein synthesis in EBOV-infected cells using Click-iT labeling technology. Using this system, newly synthesized proteins were labeled in EBOV-infected cells at 24 hours p.i., and viral inclusions and SG marker proteins were visualized by co-IFA. While nascent proteins (green) were distributed throughout the cytoplasm in mock-infected cells, newly synthesized proteins accumulated in the viral inclusions in EBOV-infected cells, despite the presence of SG proteins, suggesting that the SG aggregates within inclusions are not detrimental to protein translation (Figure 16A). Higher magnification images of EBOV infected cells recapitulate that newly synthesized proteins are found within viral inclusions and that these inclusions also contain sequestered SG proteins (Figure 16B). Transmission electron microscopy (TEM) analyses of EBOV-infected Vero cells showed that ribosomes were not present within viral inclusions, but were in close proximity (data not shown). Regardless of the size or density of viral inclusions, ribosomes were never found interspersed with nucleocapsids or viral granular material suggesting that the inclusions are not the sites of viral protein

translation. Rather, translation of viral proteins likely occurs in close proximity to inclusions with the newly synthesized proteins then transported into viral inclusions. Regardless of where viral protein synthesis occurs, the presence of SG proteins within viral inclusions did not impair the production or subsequent delivery of newly synthesized proteins to viral inclusions during EBOV infection.

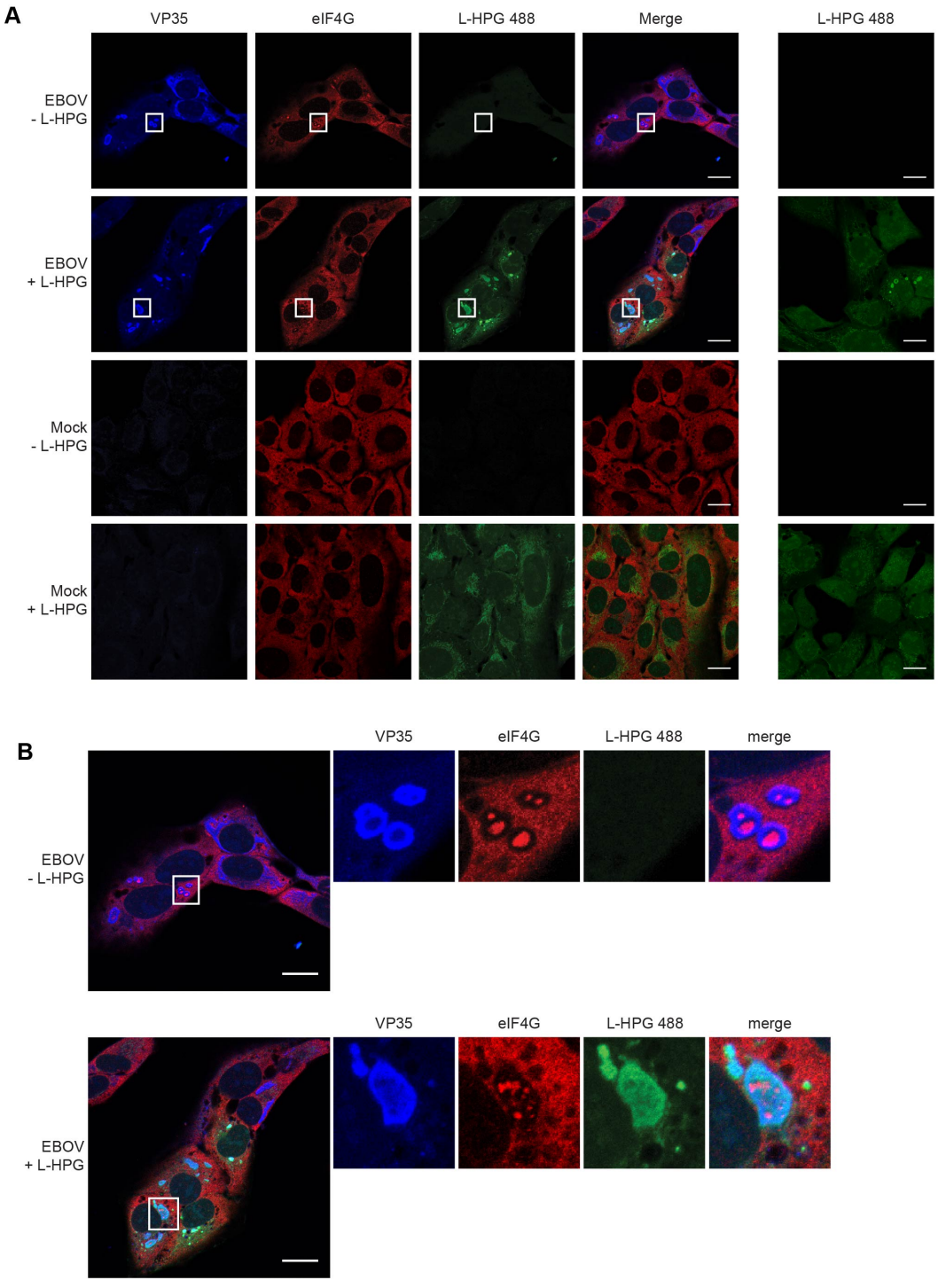

Figure 16. Inclusion-bound aggregates do not interfere with protein translation.

A) U2OS cells were mock-infected or infected with EBOV at an MOI of 1.5. At 24 hours p.i., cells were pulse-labeled with the amino acid analog L-HPG for 30 minutes. Nascent proteins were visualized with an Alex Flour 488 detection reagent specific for L-HPG, while virus infection was detected with a VP35 antibody (blue) and inclusion-bound aggregates with an eIF4G antibody (red). Right panels show EBOV-infected cells labeled with L-HPG 488 in the absence of VP35 and eIFG4 antibodies. B) Higher magnification images of the indicated conditions. Scale bars = 20 μM.

3.10 EBOV does not block SG formation induced by oxidative stress early during infection

Because the SG-like aggregates found within viral inclusions did not interfere with protein translation, we next investigated if their sequestration might play a more pro-viral role and prevent canonical SG formation in EBOV-infected cells. A number of viruses have been shown to not only avoid the induction of the cellular stress response, but also actively prevent SG formation during infection (Montero & Trujillo-Alonso, 2011; J. P. White & Lloyd, 2012). For example, Semliki Forest virus has been shown to sequester G3BP aggregates within viral replication centers, which ultimately prevents subsequent cytoplasmic SG formation (Panas et al., 2012). Likewise, IAV can suppress SG formation not only through PKR antagonism but also via an eIF2α independent mechanism mediated by the proteins NP and PA-X (Khaperskyy et al., 2012; 2014). To examine if EBOV was able to block SG formation induced by oxidative stress, EBOV-infected U2OS cells were treated with Ars at different time points p.i. and analyzed by IFA using antibodies against VP35 and a panel of SG proteins. SG formation was observed in the cytoplasm of EBOV-infected, Ars-treated cells at all time points p.i., as shown by staining for eIF4G (Figure 17). Staining for two other canonical SG proteins eIF3 and TIA-1 also verified the presence of SGs in EBOV-infected cells after Ars treatment (data not shown).

In contrast to the early time points p.i. when the majority of EBOV-infected, Ars-treated cells displayed canonical cytoplasmic SGs, at 24 hours p.i. eIF4G was homogenously distributed in a significant proportion of infected, Ars-treated cells (Figure

18A i). Furthermore, the SGs in many infected and Ars-treated cells appeared more diffuse and less punctate compared to Ars-treated, mock-infected cells (Figure 18A ii). However, there were infected cells that still possessed canonical SGs within the cytoplasm that appeared undisturbed (Figure 18A iii**)**. A quantitative analysis showed that while nearly 100% of the mock-infected, Ars-treated cells showed typical punctate eIF4G-containing SGs, there was a significant reduction in the number of cells positive for canonical SGs in EBOV infected cells at 24 hours p.i. (Figure 18B). Likewise, during infection the number of cells deficient in SGs increased by 30% compared to mock-infected, Ars-treated cells (Figure 18B). The reduction in SGs observed late during EBOV infection suggests that although EBOV does not induce SG formation, it might have evolved mechanisms to disrupt additional SG formation at late stages of infection.

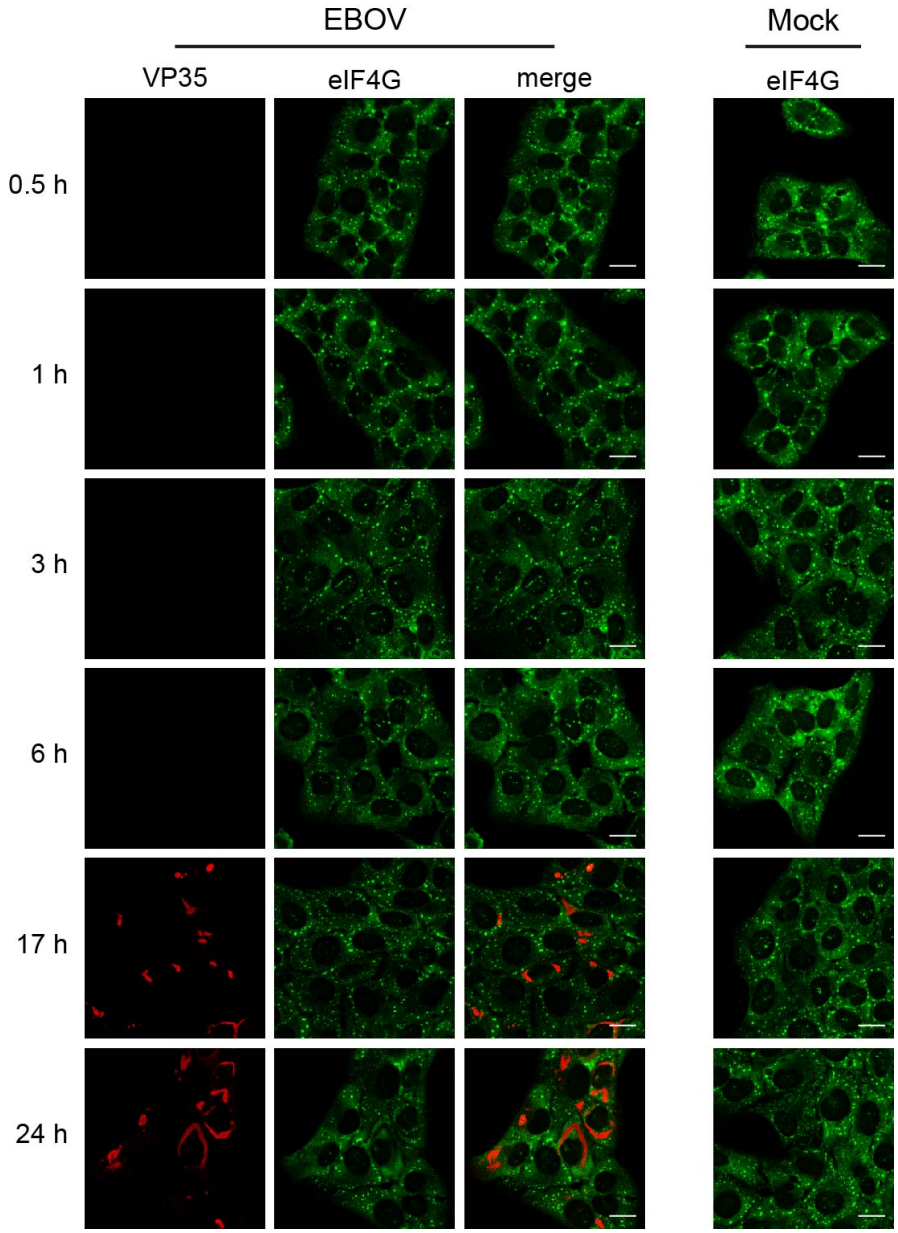

Figure 17. EBOV does not prevent Ars-induced SG formation early during infection.

U2OS cells were mock-infected or infected with EBOV at an MOI of 1.5. At the indicated time points p.i., cells were treated with 0.5 mM Ars for 30 minutes, fixed and examined by IFA using antibodies against eIF4G (green) and VP35 (red). Scale bars = 20 μM.

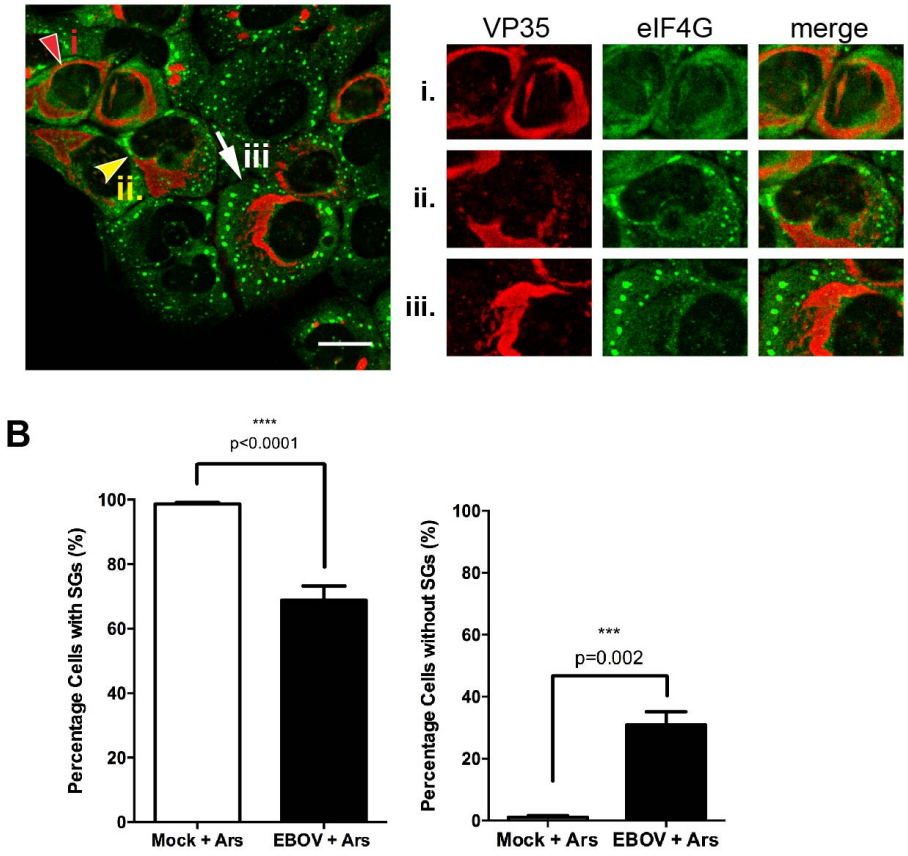

Figure 18. SGs are reduced late during infection.

A) U2OS cells were infected with EBOV at an MOI of 1.5, and treated with 0.5 mM Ars at 24 hours p.i. Arrows indicate representative images of the three outcomes of SG induction observed, shown at higher magnification on the right. Scale bars = 20 μM. B) Quantification of SG-containing cells was performed for three separate experiments. For each experiment, 24 fields were randomly chosen and counted. A total number of 290, 187 and 262 cells were counted, respectively. Counting was performed twice by two individual lab members. Statistical analysis was performed with Graphpad prism software, using an unpaired two sample t-test.

3.11 EBOV is unable to prevent Ars induced eIF2α phosphorylation

To dissect the underlying mechanism(s) for the observed reduction in the number of SGs in EBOV-infected, Ars-treated cells at 24 hours p.i (Figure 18), we first analyzed if EBOV was able to block eIF2α phosphorylation triggered by oxidative stress. We performed Western blot analysis to examine the phosphorylation state of eIF2α in EBOV-infected cells that were treated with Ars or left untreated at both early and late time points p.i. Because high cell density can trigger eIF2α phosphorylation (Savinova & Jagus, 1997), we used subconfluent HeLa cells for this experiment. Ars treatment led to eIF2α phosphorylation in mock-infected as well as EBOV-infected HeLa cells at all time points examined, indicating that although EBOV is able to block PKR signaling and does not induce eIF2α phosphorylation (Feng, Cerveny, Yan, & He, 2007b; Olejnik et al., 2013), it is unable to prevent Ars-induced activation of the signaling pathways leading to SG formation (Figure 19). eIF2α was not phosphorylated in EBOV-infected, untreated cells at any time examined, which corroborates our results showing that EBOV infection per se does not induce eIF2α-triggered SG formation (Figures 3 and 4). Importantly, robust eIF2α phosphorylation was observed in EBOV-infected, Ars-treated cells at 24 hours p.i., indicating that the observed impairment of SG formation cannot be attributed to the inhibition of eIF2α phosphorylation induced by oxidative stress.

To determine if the sequestration of SG proteins within inclusions impaired cytoplasmic SG formation and accounted for the reduction in SGs observed late in infection, EBOV-infected U2OS cells that were left untreated or treated with Ars at 24 hours p.i. were closely examined to determine if there was a correlation between the

presence of inclusion bound granules and the absence of cytoplasmic SGs. As expected, eIF4G was sequestered in a majority of viral inclusions in EBOV-infected, untreated cells (Figure 20). Surprisingly, EBOV-infected cells treated with Ars showed little to no aggregation of eIF4G within inclusions, and SGs could still form in the cytoplasm of most cells. This shows that the sequestration of SG proteins within viral inclusions is not sufficient to prevent SG formation induced by cellular stress. It also suggests that inclusion-bound SG proteins are not rigidly restrained by viral components and can be released into the cytoplasm upon the induction of stress. To understand if this was an Ars dependent effect, two other forms of stress were also tested. Similar to Ars, heat-induced formation of SGs requires phosphorylation of eIF2α by HRI (Ivanova, Velichko, Kantidze, & Razin, 2015; L. Lu, Han, & Chen, 2001). Hippuristanol however bypasses this step and induces SG formation by inhibiting activity of the RNA helicase eIF4A and preventing further translation initiation events (Bordeleau et al., 2006; Mazroui et al., 2006). EBOV-infected U2OS-G3BP-eGFP cells treated with heat or hippuristanol also demonstrated cytoplasmic SG formation (data not shown). We therefore propose that the sequestration of SG proteins during EBOV infection is not sufficient to prevent SG formation induced by additional stress.

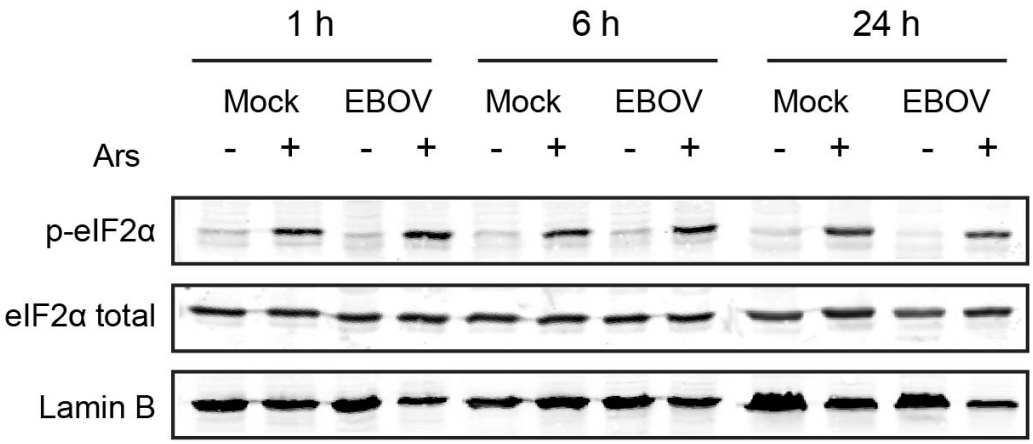

Figure 19. EBOV does not prevent Ars-induced eIF2α phosphorylation.

HeLa cells were mock-infected or infected with EBOV at an MOI of 1.5 and harvested for Western blot analysis at the indicated time points p.i. Prior to cell lysis, cells were treated with 0.5 mM Ars for 30 minutes to induce SG formation or left untreated. eIF2α phosphorylation was analyzed using a phospho-specific eIF2α antibody.

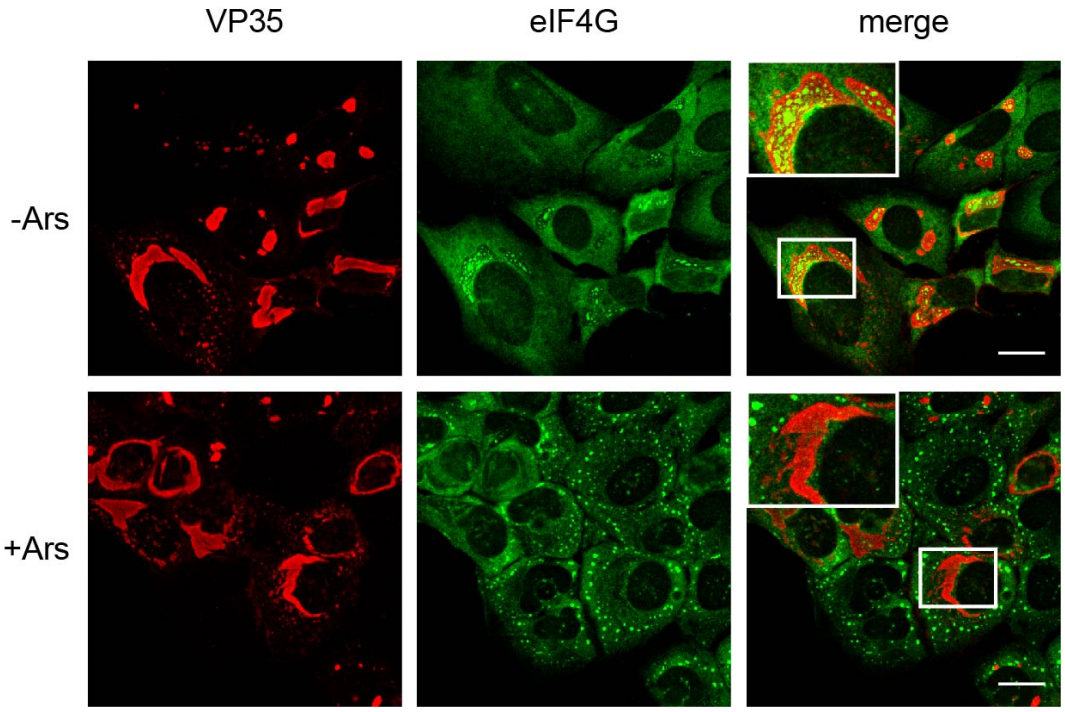

Figure 20. SG proteins are not present within inclusions after Ars treatment. U2OS cells were infected with EBOV at an MOI of 1.5. At 24 hours p.i., cells were mock-treated or treated with 0.5 mM Ars for 30 minutes. Accumulation of SG proteins within viral inclusions was visualized by staining for eIF4G (green). Inclusions are shown in red via VP35 staining. Scale bars = 20 μM.

3.12 Viral inclusions prevent canonical SG formation

Despite the ability of the inclusion-bound SG proteins to respond to cytoplasmic stress, canonical SGs were not present within viral inclusions in EBOV-infected, Ars-treated cells (Figure 21A). Rather, we observed assorted distributions of SG marker proteins and viral inclusions. In a majority of cells, the viral inclusions were completely devoid of SG proteins but were surrounded by cytoplasmic SGs (Figure 21A, i). A significant number of EBOV-infected cells contained no SGs within either the cytoplasm or viral inclusions (Figure 21A, ii). SG-like aggregates were rarely found within large viral inclusions (Figure 21A, iii**)** but were occasionally seen in very small viral inclusions (Figure 21B, left panel). Although canonical SGs were predominately absent in large inclusions, they were often seen in close proximity to, or surrounded by viral inclusions (Figure 21A, middle panel). Late stages of EBOV infection are characterized by large, more diffuse inclusions that eventually disperse (Nanbo, Watanabe, Halfmann, & Kawaoka, 2013b). In these instances, SGs were often scattered throughout dispersing inclusions, but did not colocalize with viral proteins (Figure 21B, right panel). Based on these observations we propose that while viral inclusions do not entirely insulate SG proteins from cytoplasmic stress signals, SG formation itself is prevented within inclusions.

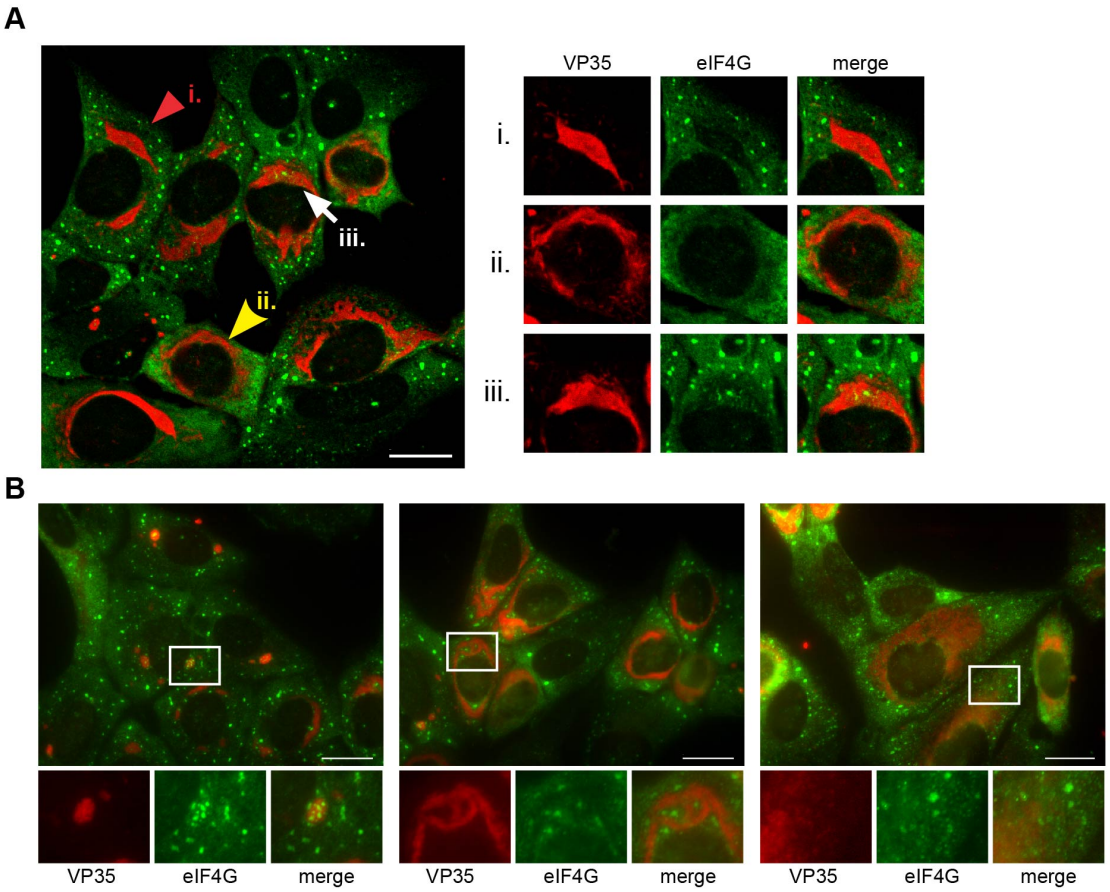

Figure 21. Stress granules do not form in viral inclusions.

A) U2OS cells were infected with EBOV at an MOI of 1.5. At 24 hours p.i., the cells were treated with 0.5 mM Ars for 30 minutes, fixed and analyzed by IFA. SGs are visualized by staining for eIF4G (green) and viral inclusions by VP35 (red). Images are representative of what was observed in infected cells. B) U2OS cells were infected as in A, but represent a wider array of SG and viral inclusion distributions in infected cells Scale bars = 20 μM

3.13 VP35 is able to disrupt SG formation

Because SG formation was not observed within in viral inclusions (Figure 21), we analyzed whether any of the EBOV nucleocapsid proteins were able to interfere with the formation of SGs. EBOV NP, VP35, VP30 and VP24 were individually expressed in Huh7 cells or U2OS-G3BP-eGFP cells. At 2 days post transfection, the cells were treated with Ars or left untreated and examined by IFA for the impact of individual viral proteins on SG formation. Of the proteins tested, VP35 was found to disrupt the intracellular aggregation of SG proteins under conditions of oxidative stress. To examine if the expression level of VP35 correlated with its ability to disrupt SG formation, Huh7 cells were transfected with either 0.5 μg or 1.5 μg of a VP35 expression plasmid and analyzed at 2 days post transfection. When transfected at a low level (0.5 μg), in untreated cells VP35 showed a predominately diffuse distribution in the cytoplasm, with some areas of minor clustering (Figure 22A, left panels). This distribution became more aggregated and resembled viral inclusions when VP35 was transfected at a much higher level (1.5 μg; Figure 22A, right panels). At both low and high levels of VP35 expression, eIF4G distribution remained homogenous in the absence of stress. When expressed at lower levels, VP35 colocalized with or was in close proximity to SGs in Ars-treated cells. While SGs could still form in these cells, they started to appear more diffuse and less punctate compared to those in Ars-treated cells lacking VP35 (Figure 22B, VP35 (0.5 μg); compare cells indicated by white arrow and red arrowhead). SGs were frequently surrounded by small, globular VP35 aggregates. At higher expression levels, VP35 was found in patch-like structures in the cytoplasm of both untreated and Ars-treated cells

(Figure 22A and B) and SG formation was strongly impaired in the Ars-treated cells (Fig 22B, VP35 (1.5 μg); compare cells indicated by white arrow and red arrowhead). Together, these data indicate that VP35 interacts with SGs and is able to disrupt SG formation when expressed at sufficiently high levels.

To determine if VP35 was able to disrupt SG formation induced by other forms of stress, we employed two additional methods for inducing SGs. These include Hipp treatment and G3BP overexpression. As described above, Hipp induces SG formation independently of eIF2α phosphorylation. Additionally, SGs can be induced through the overexpression of certain proteins that are important scaffolds for SG nucleation, including TIA-1 and G3BP (Anderson & Kedersha, 2008; Kedersha et al., 2013). When Huh7 cells were treated with 1.5 μM Hipp, eIF4G staining showed typical cytoplasmic SGs (Figure 23, mock). In Hipp-treated cells transfected with 0.5 μg of a VP35 expression plasmid, VP35 formed clusters around eIF4G with some areas of colocalization as it did after Ars treatment (Figure 23, top panels). SGs were almost entirely absent from Hipp-treated cells transfected with 1.5 μg of a VP35 expression plasmid (Figure 23, middle panels). To determine if VP35 was also able to disrupt SGs induced by the overexpression of G3BP, Huh7 cells were transfected with an expression plasmid containing an eGFP-tagged G3BP. Upon G3BP-eGFP expression in cells, G3BP formed large aggregates that were similar to SGs (Figure 24) and contained endogenous eIF4G. When these cells were co-transfected with high levels (1.5 μg) of a VP35 expression plasmid, the G3BP aggregates were reduced in size and became fragmented.

Collectively, these data indicate that VP35 is able to disrupt SG formation induced by diverse forms of stress.

VP35 is not diffusely distributed in the cytoplasm of EBOV-infected cells, but is directed into the viral inclusions via binding to NP-RNA complexes (Trunschke et al., 2013). It has been reported previously that the NP to VP35 ratio is crucial for NP-induced inclusion formation and that excess expression of VP35 prevents archetypal inclusion formation in cells co-expressing NP and VP35 (Noda et al., 2011). To examine if VP35 was still able to disrupt SG formation in the presence of NP, Huh7 cells were transfected with NP and VP35 plasmid DNA in a 1:1 ratio and 2 days after transfection, were treated with Ars or left untreated. As expected, VP35 was no longer diffusely distributed in the cytoplasm of untreated cells but was directed to NP-induced inclusions (Figure 25A, upper left panel; compare to VP35 distribution in Figure 22). Upon Ars treatment, VP35 remained bound to NP-induced inclusions and did not colocalize with eIF4G-containing SGs that formed in the cytoplasm (Figure 25A, upper right panel). When NP concentrations were kept low but VP35 was expressed at three fold higher amounts in excess of NP, inclusions were dispersed, confirming the previous observations by Noda and colleagues (Noda et al., 2011)(Figure 25B, bottom panels). In addition, SG formation was significantly reduced under these conditions (Figure 25A and B, bottom panels). This might recapitulate the disruption in SG formation seen late in EBOV infection, when VP35 expression is high. In summary, our data provide strong evidence that VP35 interacts with SGs and plays a role in preventing SG formation late in infection when concentrations of VP35 are high.

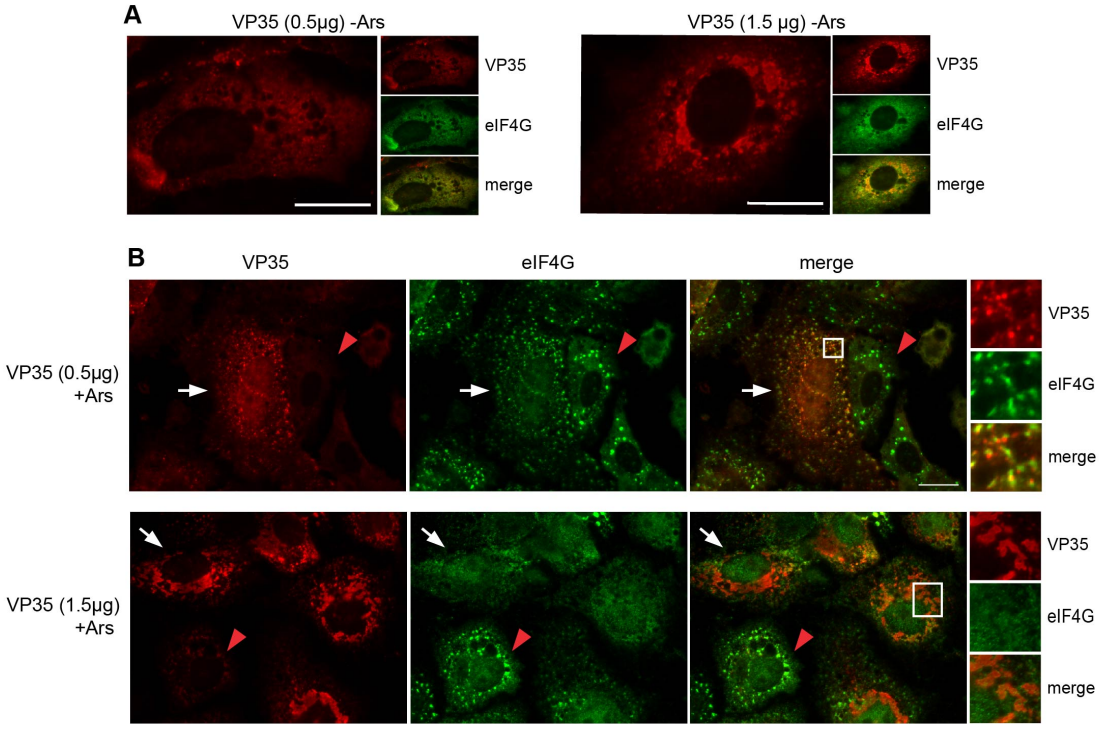

Figure 22. VP35 disrupts Ars induced SG formation at high levels of expression.

Huh7 cells were transfected with low (0.5 µg) or high (1.5 µg) amounts of an HA-VP35 expression plasmid. At two days post transfection, cells were left untreated (A) or treated with 0.5 mM Ars for 30 minutes (B), and fixed. IFA was performed using an HA-specific antibody to detect VP35 (red) and an anti- eIF4G antibody (green). White arrows in (B) indicate cells expressing VP35, with little to no SG formation. Red arrows indicate cells that do not express VP35 and show canonical SG formation.

Scale bars = 20 µM.

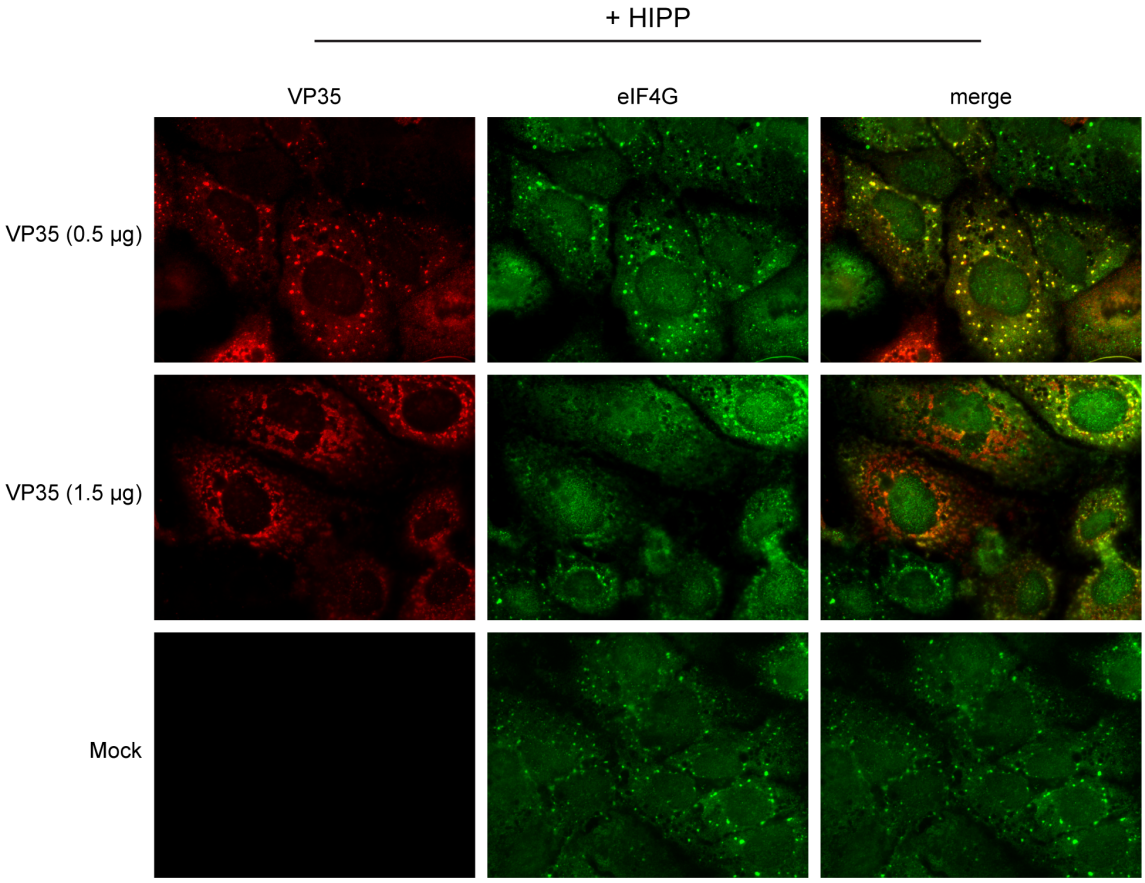

Figure 23. VP35 is able to disrupt Hipp induced SG formation.

Huh7 cells were transfected with increasing amounts of an HA-tagged VP35 expression plasmid. At two days post transfection, cells were treated with 1.5 mM Hipp or left untreated. Cells were then fixed and examined by IFA. VP35 was visualized with an HA-specific antibody (red), and SGs were observed with an eIF4G antibody (green).

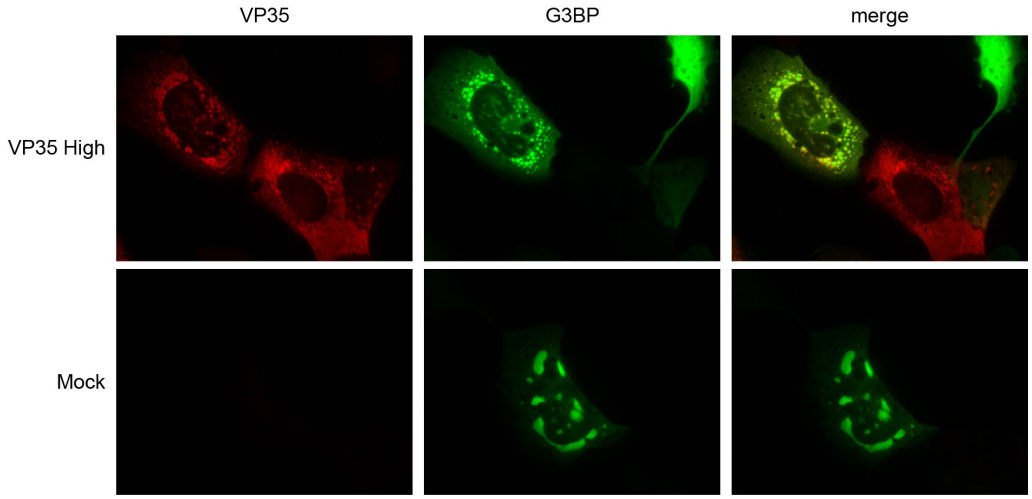

Figure 24. VP35 can disrupt G3BP aggregates.

Huh7 cells were transfected with 0.25 μg of a G3BP-eGFP expression plasmid either in the absence or presence of a high concentration (1.5 μg) of an HA-tagged VP35 expression plasmid or without additional plasmid DNA. VP35 was visualized with an HA-specific antibody. G3BP is shown via eGFP fluorescence.

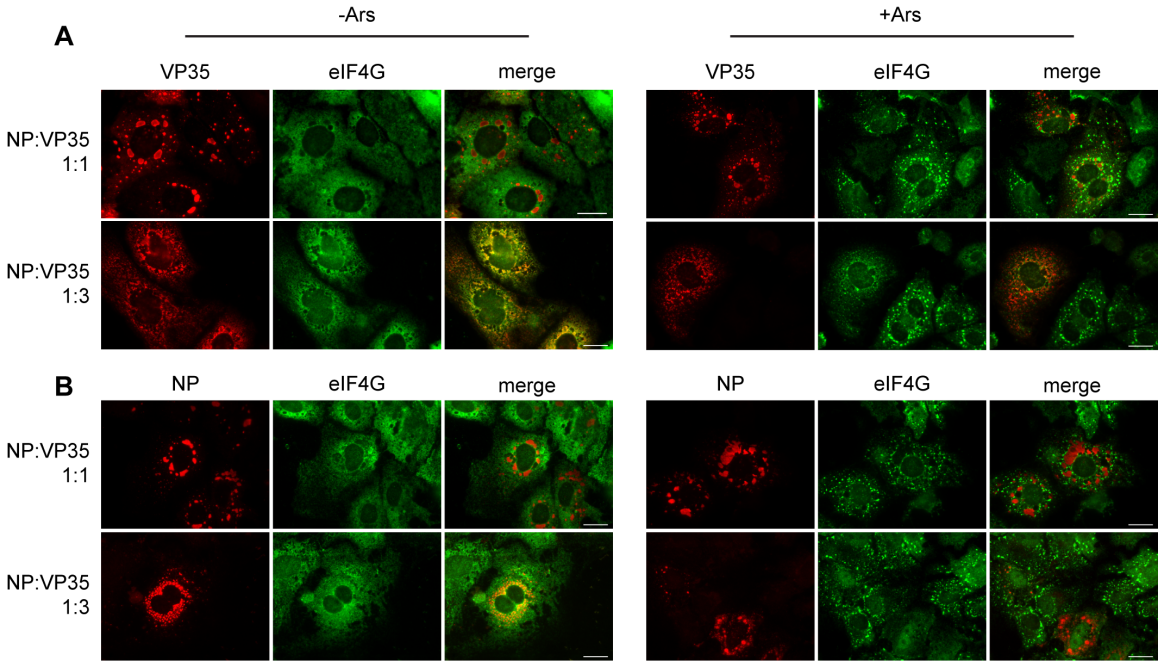

Figure 25. VP35 can still disrupt SG formation in the presence of NP.

Huh7 cells were transfected with expression plasmids expressing EBOV NP or HA-tagged VP35. Top panels show cells transfected in a 1:1 plasmid ratio of 0.5 µg each per well in a 6-well plate. Cells shown in bottom panels were transfected in a NP to VP35 plasmid ratio of 1:3 (0.5 µg NP DNA, 1.5 µg VP35 DNA). At two days post transfection, cells were treated with 0.5 mM Ars for 30 mins or left untreated, and then imaged by IFA. A) Staining was performed using antibodies targeting HA to visualize VP35 (red), and eIF4G (green). B) Staining was performed using antibodies targeting NP (red) and eIF4G (green). Scale bars = 20 µM.

3.14 Double-stranded RNA binding is not required for VP35's ability to disrupt SG formation

To further understand the mechanism underlying VP35's ability to disrupt SG formation, we used various VP35 variants (Figure 26) to determine which domains may be required for this function. Previous extensive mutational analyses of VP35 have shown that residues R305, K309 and R312 within the interferon inhibitory domain (IID) are essential for its ability to bind dsRNA, but have no effect on its polymerase cofactor functions. Substitution of either R312 or K309 alone is sufficient to ablate dsRNA binding (Bale et al., 2013; Cárdenas et al., 2006; Kimberlin et al., 2010). To determine if dsRNA binding is also important for VP35's capacity to disrupt SG formation, a previously described VP35 variant, referred to as VP35-3A, was used. This protein possesses the substitutions R305A, K309A, and R312A, which have no effect on NP binding or VP35 oligomerization. However this variant is significantly impaired in its ability to block both PKR activation and IFN induction (Schümann et al., 2009). When expressed in U2OS cells and examined by IFA, VP35-3A was homogenously distributed in the cytoplasm when transfected at a low level (0.5 μg), and more aggregated at a higher level (1 μg), similar to the wild type VP35 (Figure 27A). When cells transfected with 0.5 μg of VP35-3A plasmid were subsequently treated with Ars, the variant protein colocalized with the SG protein eIF4G. In cells transfected with a higher amount (1 μg) of VP35-3A plasmid, the variant protein did not colocalize with eIF4G upon Ars treatment, and there was a clear reduction in SG formation. When co-expressed in a 1:2 ratio with NP, VP35-3A colocalized with NP inclusions as expected (Figure 27B).

Furthermore, when NP and VP35-3A expression plasmids were co-transfected at a 1:5 ratio, NP inclusions began to disperse and resembled those disrupted by wild type VP35. The VP35-3A variant therefore behaved identically to the wild type, indicating that dsRNA binding is not required for VP35's function to disrupt SGs or NP-based viral inclusions.

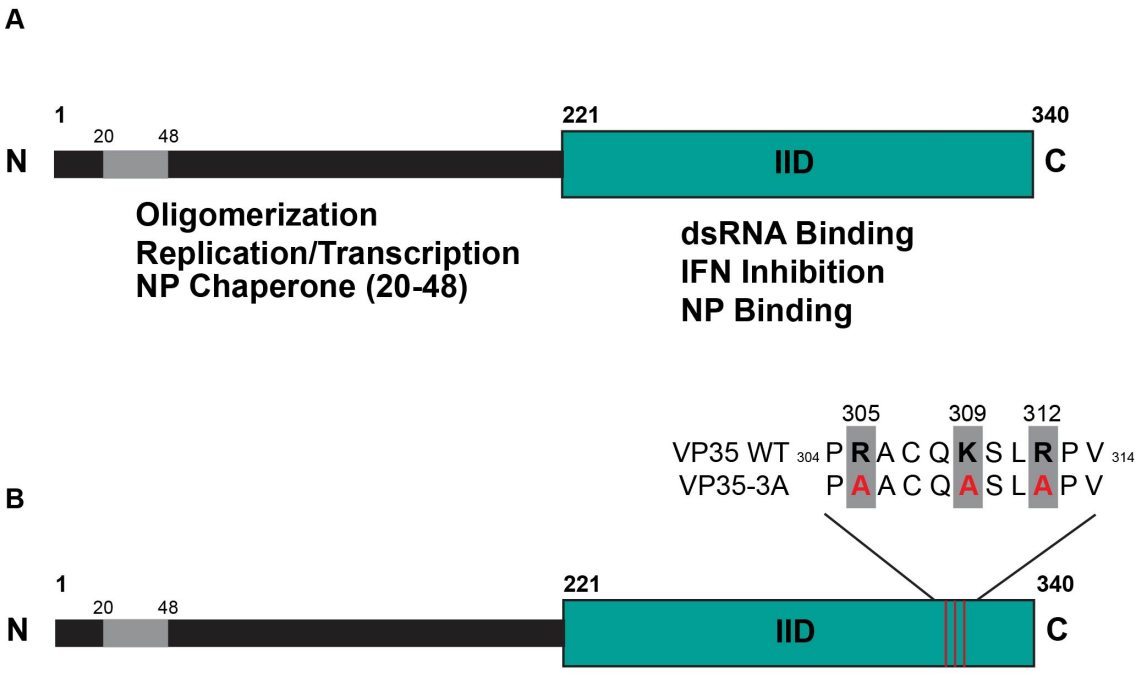

Figure 26. VP35 wild type and VP35-3A variant schematic.

A) Schematic of functional domains on wild type VP35. The N-terminus includes domains important for oligomerization, NP chaperone function, and replication/transcription. The C-terminus contains the interferon inhibitory domain (IID) and includes domains responsible for dsRNA binding and NP binding. B) In the IID domain of the VP35-3A variant 3 basic amino acids required for dsRNA binding are exchanged with alanine residues. Alanine substitutions are indicated in red.

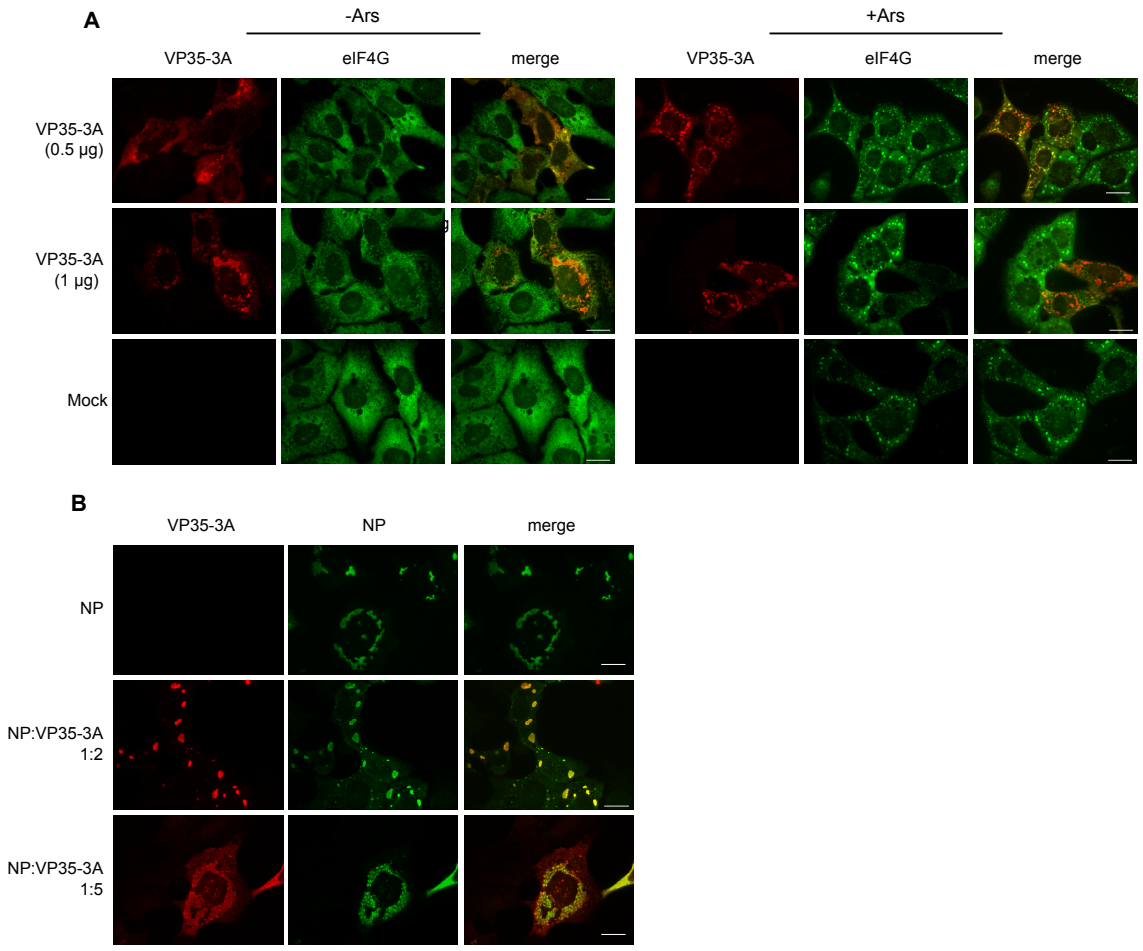

Figure 27. VP35's dsRNA binding ability is not required to disrupt SG formation. A) U2OS cells were transfected with either 0.5 µg or 1 µg of an HA tagged VP35-3A expression plasmid and 2 days post transfection treated with 0.5 mM Ars or left untreated. VP35-3A distribution was visualized using an HA-specific antibody (red). SG formation was shown using an eIF4G antibody (green). B) U2OS cells were transfected with an expression plasmid encoding EBOV NP (0.5 µg) alone, or in combination with an HA tagged VP35-3A. The VP35-3A expression plasmid was transfected at either a 1

μg or 2.5 μg to a1:2 or 1:5 ratio with NP. NP (red) and HA-specific (green) antibodies were used for IFA. Scale bars = 20 μM.

3.15 VP35 mediated disruption in SG formation is distinct from NP inclusion disruption

We next examined if VP35's ability to disrupt both SGs and NP-induced viral inclusions is driven by the same mechanism. Therefore, a VP35 C-terminal deletion variant that lacks the last 10 amino acids, here referred to as VP35Δ331-340, was used (depicted in Figure 28). Previous work in the lab has shown that this protein variant has negligible NP binding activity and is unable to support polymerase function (unpublished data). However, it retains most of its ability to inhibit the IFN response. U2OS cells were transfected with increasing concentrations of a VP35Δ331-340 expression plasmid. However, VP35Δ331-340 distribution looked nearly identical by IFA regardless of the amount of expression plasmid that was transfected. It is possible that the 10 amino acid deletion of this VP35 mutant construct affects its protein expression in these cells. Because of the difficulties expressing a range of VP35Δ331-340 expression plasmid concentrations, we focused on cells transfected with 1.5 μg of VP35Δ331-340. Two days post transfection cells were treated with Ars and examined by IFA. When VP35Δ331-340 was expressed into U2OS cells it was predominately homogenously distributed throughout the cytoplasm (Figure 29A) but did form irregular aggregates in some cells. Upon Ars treatment, VP35Δ331-340 was able to disrupt SG formation, although we did not observe VP35Δ331-340 colocalizing with or clustering around SGs. As expected, in contrast to wild type VP35, VP35Δ331-340 did not colocalize with NP inclusions when co-expressed with NP (Figure 29B). Furthermore, NP inclusions remained undisturbed with VP35Δ331-340 expression. Although we were unable to more precisely control the expression levels of the VP35Δ331-340 variant, these data suggest that the domain

required for VP35 to disrupt NP inclusion formation is distinct from the domain required to disrupt SG formation.

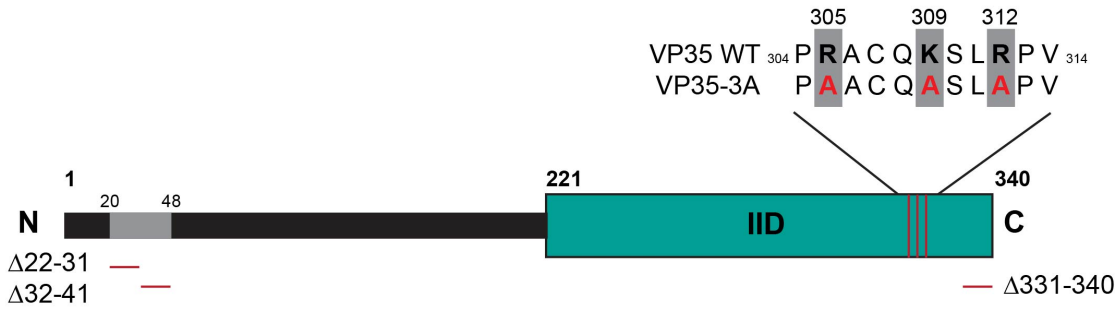

Figure 28. Schematic of VP35 deletion variants.

Cartoon representation of three VP35 deletion variants. These include two N-terminal deletion variants, each with a 10 amino acid deletion, labeled VP35Δ22-31 and VP35Δ32-41, respectively. Amino acids 20-48 comprise an intrinsically disordered region (highlighted in grey). This region is involved in NP binding. The C-terminal 10 amino acid deletion in VP35Δ331-340 ablates NP binding, but retains dsRNA binding and IFN inhibition.

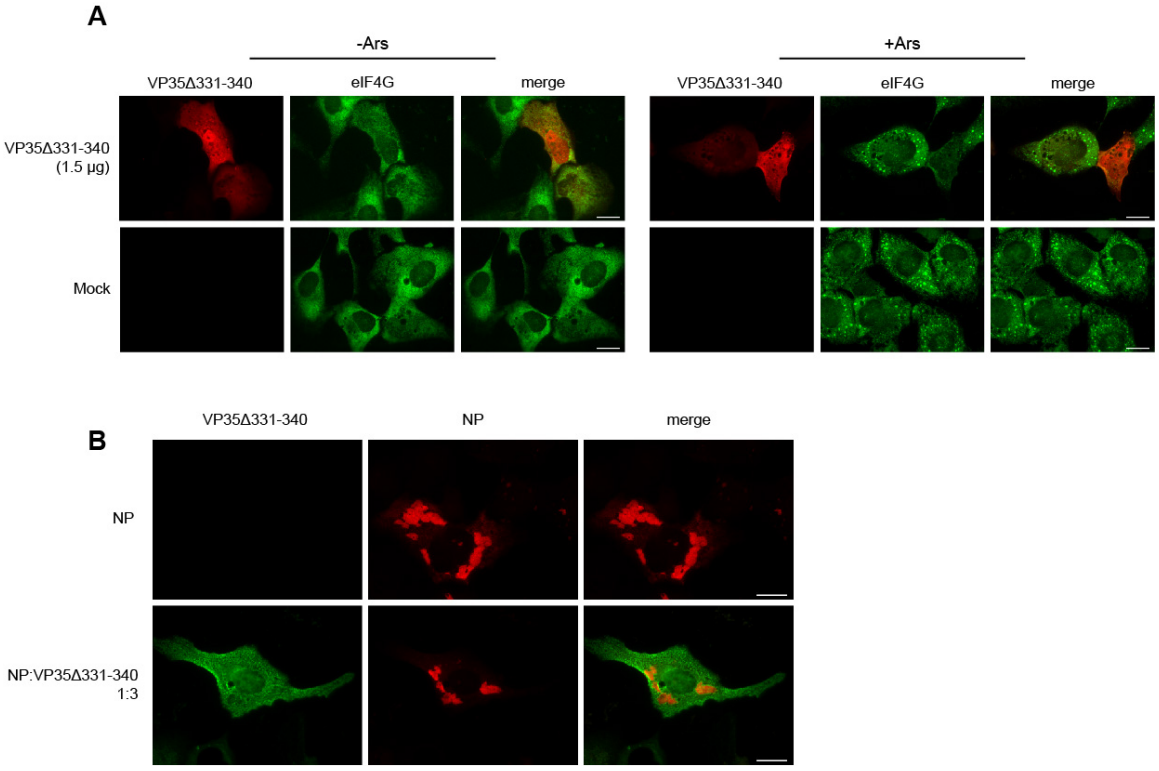

Figure 29. VP35 mediated disruption of SGs is distinct from its disruption of NP based inclusions

A) Huh7 cells were transfected with 1.5 μg of an HA tagged VP35Δ331-340 expression plasmid and 2 days post transfection, treated with 0.5 mM Ars or left untreated. VP35Δ331-340 distribution was visualized using an HA specific antibody (red) and SG formation was shown using an eIF4G antibody (green). B) Huh7 cells were co-transfected with 0.5 μg of NP expression plasmid and 1.5 μg of VP35Δ331-340 expression plasmid in a 1:3 ratio. NP was stained for in red and VP35Δ331-340 was stained for using an HA antibody.

3.16 Examination of an intrinsically disordered region on VP35's function in disrupting SG formation

VP35 has been shown to bind to NP via an intrinsically disordered region (IDR) in the N-terminus corresponding to the amino acids 21-48 (Kirchdoerfer et al., 2015; D. W. Leung et al., 2015). IDRs are often found in proteins involved in RNA granule formation and are thought to be mediators of protein-protein binding and aggregation (Kedersha et al., 2013; Molliex et al., 2015). To determine if the IDR of VP35 plays a role in the disruption in SG formation observed, we used two VP35 deletion variants that possess 10 amino acid deletions in the predicted IDR of VP35. These include deletions of amino acids 21-32, and 32-41, respectively. Expression of these VP35 deletion variants in untreated U2OS cells revealed a distribution pattern that looked nearly identical to wild type VP35 where both showed diffuse cytoplasmic distribution that we assume correlated with lower levels of protein expression (Figure 30, white arrows) and more aggregated distribution at presumably higher levels of expression (Figure 30, yellow arrowheads). Furthermore, upon Ars treatment the VP35 IDR deletion variant could be found redistributed into punctate aggregates that surrounded SGs (Figure 31A and B, i). When the variants were expressed at higher levels and showed a more aggregated distribution in these Ars-treated cells, little to no SG formation was observed (Figure 31A and B, ii). These data suggest that partial deletion of the VP35 IDR did not ablate VP35-mediated SG disruption. However, it is unclear whether removal of the entire IDR had any effect on VP35-mediated disruption in SG formation.

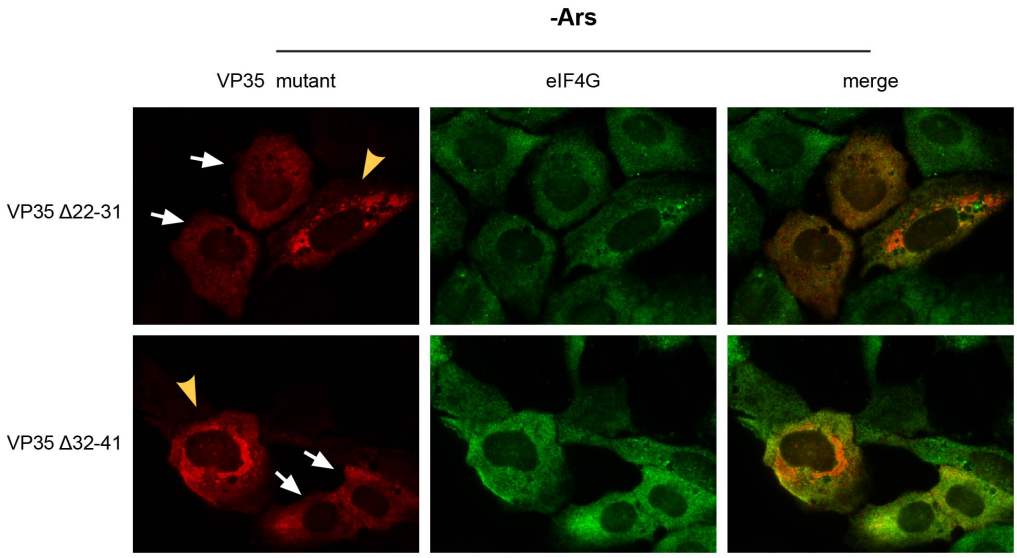

Figure 30. Expression of VP35 IDR deletion variants.

U2OS cells were transfected with 1 μg of expression plasmids encoding HA tagged VP35Δ22-31 (top panels) or VP35Δ32-41 (bottom panels). White arrows indicate cells with demonstrating diffuse distribution of the indicated VP35 variant protein, while yellow arrowheads indicate cells expressing more aggregated distribution of the indicated VP35 variant protein. Cells were stained for eIF4G (green) or HA (red).

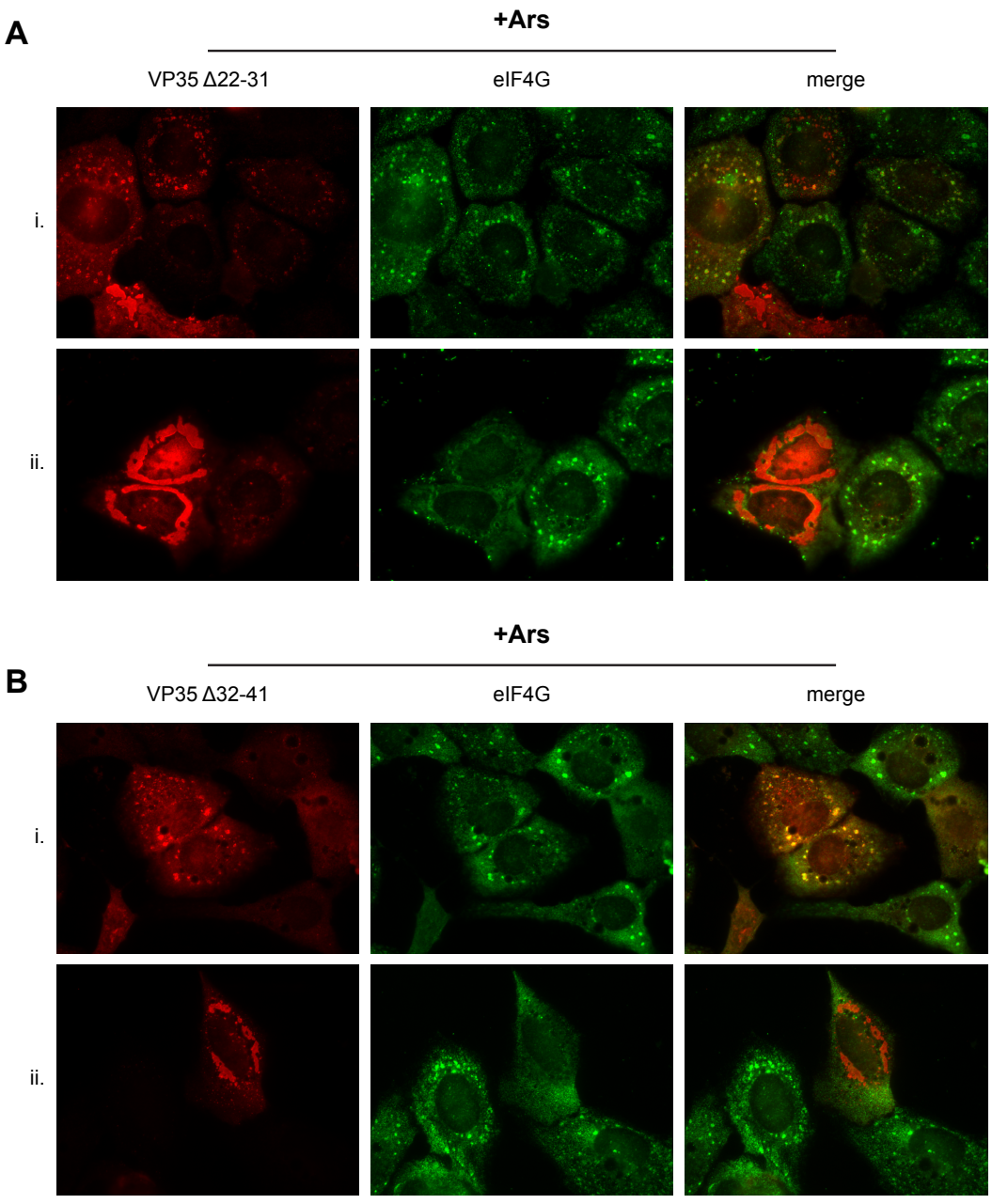

Figure 31. VP35 IDR deletion variants are able to disrupt SG formation.

U2OS cells were transfected with 1 µg of expression plasmids encoding HA tagged VP35Δ22-31 (A) or VP35Δ32-411 (B). Two days post transfections cells were treated with 0.5 mM Ars and examined by IFA. Cells expressing VP35 variants that colocalized

with SGs are shown in top panels (i). Cells with disrupted SG formation expressing VP35 in more aggregated distribution are shown in bottom panels (ii). Cells were stained for eIF4G (green) or HA (red).

Discussion

EBOV does not induce SG formation during infection and may disrupt SG formation independently of eIF2α

The increasing number of viruses shown to disrupt or evade SG formation during infection has led to the recognition of the cellular stress response as an important antiviral mechanism. However, SG formation and the subversion of the cellular stress response have never been characterized during EBOV infection. In the work described in this chapter, we showed for the first time that EBOV does not induce SG formation at any time point p.i. Furthermore, eIF2α was not phosphorylated during the course of infection. This is in line with previous studies demonstrating that both eIF2α and PKR are not phosphorylated at late stages of EBOV infection (Olejnik et al., 2013; Schümann et al., 2009). The absence of SG formation observed might at least in part be due to the already established function of VP35, to antagonize PKR (Olejnik et al., 2013; Schümann et al., 2009). Despite the ability of VP35 to block PKR-induced eIF2α phosphorylation, we showed that if infected cells were treated with Ars to induce oxidative stress, EBOV was unable to prevent phosphorylation of eIF2α or fully block the induction of SGs. This suggests that EBOV may only be capable of blocking PKR-mediated SG formation, and cannot prevent signaling through the other eIF2α kinases such as HRI.

Early in infection a majority of EBOV infected cells formed canonical SGs when exposed to oxidative stress. However, SG formation was significantly decreased late in infection, despite eIF2α phosphorylation. This indicates that EBOV might have evolved a mechanism for disrupting SG formation independently of eIF2α antagonism late during

infection. Alternatively, there might be a concentration dependent requirement of VP35 where early during infection it is able to prevent SG formation induced by viral infection itself, but is unable to prevent further SG formation with the addition of supplemental stress because cells are limited in the amount of VP35 protein present. Blocking SG formation downstream of eIF2α has been shown for other viruses including poliovirus and IAV. In poliovirus-infected cells, the viral 3C protease cleaves G3BP and prevents the assembly of SGs late during infection despite eIF2α phosphorylation (J. P. White et al., 2007; J. P. White & Lloyd, 2011). Disruption of SG formation by IAV downstream of eIF2α phosphorylation is mediated by the viral proteins NP and PA-X (Khaperskyy et al., 2014). PA-X interferes with PABP, ultimately trapping cellular mRNAs within the nucleus. NP was found to disrupt cytoplasmic SG formation when expressed in the absence of other viral proteins, and this function was dependent on the oligomerization capacity of NP (Khaperskyy et al., 2014).

Although it cannot be ruled out that homeostatic cellular processes required for proper SG formation are compromised at late stages of infection, we propose that the observed impairment of SG formation occurs downstream of eIF2α phosphorylation and is mediated by a newly identified function of VP35. When individually expressed in cells, VP35 was in close proximity to and clustered around Ars-induced SGs. Higher expression levels of VP35 in Ars-treated cells resulted in an almost complete loss of SG formation. The same was observed for SGs induced by Hipp and the overexpression of G3BP. VP35's dsRNA binding domain was dispensable for the disruption of SGs, suggesting that this function is mediated by a protein-protein interaction and not through

an RNA intermediate. It is conceivable that VP35 interacts with an unidentified SG component, which then recruits VP35 to SGs upon stress. Subsequently, when VP35 is present at high enough levels, it might prevent the oligomerization of its binding partner, or inhibit binding of other SG components. A number of host proteins have been shown to bind VP35, several of which are found in SGs. VP35 binds to the RNA binding protein DRBP76 (also known as NF90), which is involved in PKR activation and SG formation during viral infection (Shabman et al., 2011). In a proteomic analysis examining cellular proteins associated with filovirus virions, Spurgers et al, found that members of the heterogenous nuclear ribonucleoprotein (hnRNP) family, including hnRNP A2.B1, hnRNP F and hnRNP AB, bind to VP35 (Spurgers et al., 2010). hnRNP proteins interact with other viruses, including poliovirus, dengue virus and Sindbis virus (Brunner, Ertel, Rozovics, & Semler, 2010; Ertel, Brunner, & Semler, 2010) (Dechtawewat, 2015) (Gui, Lu, Adams, Stollar, & Li, 2010). Importantly, a number of hnRNP proteins as well as DRBP76 localize to SGs (Guil, Long, & Cáceres, 2006; Wen et al., 2014) and might act as the link between VP35 and SGs.

RNA granule formation is promoted by low affinity interactions of RNA binding proteins containing IDRs. These regions are characterized by the absence of a defined structural motif such as an alpha helix, and low overall hydrophobicity. Many proteins important for the nucleation of SGs such as TIA-1 and G3BP contain a number of IDRs and areas of low complexity (Calabretta & Richard, 2015; Kedersha et al., 2013). An IDR was identified near the amino terminus of VP35 (Kirchdoerfer et al., 2015; D. W. Leung et al., 2015) and was shown to mediate binding to NP, maintaining NP in a monomeric

state. In line with previous reports, our data show that VP35 is able to disrupt NP-mediated inclusion formation when expressed in high amounts (Noda et al., 2011). Similar to proteins important for SG nucleation, NP serves as a hub for the recruitment of other viral proteins including VP35 (Huang et al., 2002; Shi et al., 2008). The disruption in inclusion formation by VP35 might be related to its IDR-mediated interaction with NP, which impairs NP homo-oligomerization. It is conceivable that through this type of interaction, high levels of VP35 interfere with the nucleation of SGs, possibly through competitive binding, in a manner similar to its disruption of NP-based inclusion formation. Interestingly, two VP35 variants containing non-overlapping 10 amino acid deletions spanning parts of the IDR could still impair SG formation. These deletion variants however only removed portions of the IDR, suggesting that removal of the full length IDR might be necessary to ablate VP35-mediated SG disruption.

SG proteins are sequestered within viral inclusions but are not SG

Although SGs were not induced by EBOV infection, numerous SG proteins were sequestered within viral inclusions late in infection, but these were not canonical SGs. Other viruses including chikungunya, vaccinia virus, Semliki forest virus, and vesicular stomatitis virus, have been shown to redistribute SG associated proteins into distinct cytoplasmic aggregates with altered protein composition or function compared to canonical SGs (Dinh et al., 2013; Fros et al., 2012; Panas et al., 2012; Rozelle et al., 2014; Simpson-Holley et al., 2011). While the inclusion-bound SG-like aggregates we observed during EBOV infection contained many components common to cytoplasmic

SGs such as eIF4G, G3BP and eIF3, they were often larger and less symmetrical in shape compared to canonical SGs and were devoid of the canonical SG marker protein TIA-1. Furthermore, CHX treatment, shown to dissolve canonical SGs, had no effect on the aggregation of these proteins within inclusions. CHX-mediated dissolution of SGs is driven by the stabilization of polysomes, signifying that SG formation requires a pool of messenger ribonucleoprotein (mRNP) complexes independent of ribosomes for their formation and persistence (Buchan, Yoon, & Parker, 2011) (Mollet et al., 2008). The inclusion-bound aggregates did not dissolve with CHX treatment, indicating that these aggregates are composed of translationally silent (viral) mRNAs in complex with mRNA-binding proteins. This is in line with both the antiviral granules observed in vaccinia virus infection and the proviral G3BP aggregates induced in chikungunya virus infection, which were also resistant to dissolution upon CHX treatment (Rozelle et al., 2014; Scholte et al., 2015; Simpson-Holley et al., 2011). Additionally, the inhibition of SG formation mediated through USP10 overexpression had no effect on the aggregation of G3BP within inclusions. This suggests that SG formation is not the impetus for sequestration within inclusions, and that the inclusion bound aggregates do not represent fully formed SGs that are recruited to inclusions, or around which inclusions form.

The presence of inclusion-bound aggregates did not impair the accumulation of newly synthesized proteins within viral inclusion, indicating that they are not detrimental to viral protein translation. This observation, in conjunction with the ability of EBOV to grow to high titers despite the presence SG proteins within inclusions indicates that the inclusion bound granules are not antiviral and might even be proviral. This is in line with

what is known for other viruses including chikungunya virus and West Nile virus, whose replication or viral titers were reduced when the SG components G3BP (for chikungunya virus) and TIAR (for West Nile virus) were depleted in cells (Emara & Brinton, 2007; W Li et al., 2002; Scholte et al., 2015).

While EBOV nucleocapsid proteins in viral inclusions did not colocalize with any of the SG proteins examined, we showed by FISH analysis that the accumulated SG proteins, specifically eIF3, colocalized with both NP positive-sense mRNA and negative-sense genomic RNA. Interestingly HuR, although found within EBOV inclusions, did not colocalize with the other sequestered SG proteins, nor did it colocalize with viral RNA. It was instead found in small granules around the viral RNA clusters. It is possible that we were unable to detect an interaction between viral RNA and HuR because we only probed for NP specific mRNA and genomic RNA, and therefore did not visualize the specific target of HuR. Alternatively, HuR might be involved in the regulation of mRNAs on their way out of the inclusions to the sites of translation, which we posit does not occur within inclusions. TEM analysis showed that ribosomes were not found within viral inclusions, indicating that they are not sites of viral protein translation, which most likely occurs in close proximity to viral inclusions. Therefore, we speculate that one potential function of inclusion-bound SG proteins, many of which are translation initiation factors, may be to prepare viral mRNAs for translation. We hypothesize that the difference in aggregation and distribution between HuR and the other SG proteins within viral inclusions indicates that HuR performs a distinct function compared to the other inclusion bound SG proteins.

The interaction of SG proteins with viral RNAs to promote viral translation or replication is not uncommon. G3BP binds to the 3'UTR of the dengue virus genome and is speculated to enhance viral translation or RNA replication (B. Jain et al., 2014; Ward et al., 2011). Similarly, HuR, which can enhance translation by influencing mRNA stability (Barreau et al., 2005; Brennan & Steitz, 2001), binds to the Sindbis virus 3'UTR. Depletion of HuR from infected cells resulted in a 10-fold repression in viral growth (Sokoloski et al., 2010). Alternatively, binding of SG marker proteins to EBOV RNA within the inclusions might prevent dsRNA formation, which we were unable to detect despite high levels of both positive and negative-sense RNA within inclusions (data not shown).

Viral inclusions create a proviral environment that prevent canonical SG formation

The presence of cellular proteins within viral inclusions might be a common proviral mechanism among those viruses that form cytoplasmic inclusion bodies. Marburg virus, another member of the filovirus family, recruits the cellular protein Tsg101, a component of the endosomal complex required for transport (ESCRT) I, to viral inclusions. The interaction of Tsg101 with viral components found within inclusions was required for efficient viral budding (Dolnik, Kolesnikova, Stevermann, & Becker, 2010; Dolnik et al., 2014; Dolnik, Stevermann, Kolesnikova, & Becker, 2015). The sequestration of cellular proteins within viral inclusions has also been shown for RSV, which recruits HuR into viral inclusions (Lindquist et al., 2010). While the function of HuR within RSV inclusions remains inconclusive, RSV inclusions also sequestered the antiviral signaling molecules MDA5, RIG-I and MAVS, which resulted in attenuation of

the IFN response upon secondary co-infection with Newcastle disease virus (Lifland et al., 2012). This supports the hypothesis that the sequestration of certain cellular proteins within viral inclusions promotes viral infection by disrupting antiviral signaling pathways. Alternatively, the sequestration of proteins involved in cellular antiviral signaling pathways in EBOV viral inclusions might prevent the formation of cellular granules, similar to SGs, with antiviral function. During infection with an NS1 deficient IAV, cytoplasmic SG-like granules, termed antiviral stress granules (avSGs), formed and contained both viral RNA and RIG-I, and promoted RIG-I induced IFN production (Onomoto et al., 2012). Although it is unclear how NS1 is able to prevent avSG formation, its similarities to VP35 suggest that EBOV might also prevent formation of similar granules, potentially though sequestration of avSG factors or by an undetermined function of VP35.

Although we showed that VP35 is able to disrupt SG formation, we also wanted to determine whether the reduction in SG formation observed late during infection in the presence of additional stress was the result of the sequestration of SG proteins within inclusions. Semliki forest virus has been shown to redistribute G3BP into puncta that colocalize with viral RNA and prevent SG formation, allowing the virus to avoid SG-associated translational arrest (McInerney, Kedersha, Kaufman, Anderson, & Liljeström, 2005; Panas et al., 2012). However, this was not the case for EBOV, as infected cells treated with Ars could still form SGs within the cytoplasm, even at one-day post infection. Interestingly, EBOV-infected cells treated with Ars no longer showed any sequestration of SG proteins within the inclusions. We propose that although the

inclusion-bound SG proteins are segregated from the cytoplasmic environment, they are not statically associated with inclusions and are able to recycle in and out of this viral compartment. They remain sensitive to stress signals and therefore upon exposure to additional stress, might remain in the cytoplasm after egress from inclusions and not recycle back into inclusions. The intricacies of SG persistence and disassembly are not wholly understood, however it is thought that SGs are highly dynamic structures that represent the transient accumulation of RNA and RNA binding proteins. Although they can persist for many hours, the proteins that comprise SGs are continuously recycled, where any one individual SG protein may not remain statically associated with a single SG during the entirety of the stress response (Kedersha et al., 2000; Loschi et al., 2009; Nadezhdina, Lomakin, Shpilman, Chudinova, & Ivanov, 2010). Coupled with the dynamic nature of EBOV nucleocapsids (Hoenen et al., 2012b) it is conceivable that the inclusion bound aggregates are not rigidly bound by viral inclusions.

Even though the sequestered SG proteins still responded to stress signals despite being subverted into viral inclusions, SGs did not form within inclusions, suggesting that viral inclusions comprise an environment that is resistant to SG formation. We hypothesize that this may in part be mediated by the disruption in SG formation observed with high expression levels of VP35. Inclusions are rich in VP35 and as such might prevent canonical SG formation despite the abundance of many canonical SG components. The exclusion of certain canonical SG proteins, such as TIA-1 and the small ribosomal subunit, may also preclude canonical SG formation and result in the formation

of a distinct species of RNA granule within inclusions. The mechanism of exclusion of some SG proteins over others remains to be identified.

The dynamic and oscillating nature of stress granules makes them difficult to study outside the realm of microscopy{Brielle:2015kh}. As such, the majority of data represented in this dissertation make use of various forms of microscopy, focusing primarily on fluorescence microscopy. While these techniques allowed for the direct visualization of SG formation during EBOV infection, and were critical in the identification of SG marker proteins within viral inclusions, it is important to highlight that there are both technical and interpretive limitations to these methods. Notably, the data obtained are by nature more qualitative rather than quantitative. While a correlation can be drawn between the amount of fluorescence in any given image and the amount of protein, colocalization or other parameter of interest, it is not a direct measure of such parameters. There are a number of factors that confound a quantitative interpretation of these data, including cell shape or confluency, antibody affinity or concentration, and fluorescence bleed through or photobleaching. Of relevance to this dissertation are the interpretations of the data examining VP35 expression levels and SG formation. The limitations to immunofluorescence analysis therefore make it difficult to precisely define the amount of VP35 expressed in any individual cell, or the amount of colocalization between VP35 and different SG proteins. These limitations however, do not detract from the observations made that VP35 disrupts SG formation at high levels of expression and we remain confident in the data produced and the conclusions we've made from them.

In summary, we have shown for the first time that EBOV does not induce SG formation during infection. However, many SG proteins are sequestered within viral inclusions, which may be mediated by an interaction between viral RNA and SG-associated RNA binding proteins. The inclusion-bound aggregates do not represent canonical SGs, and do not negatively impact protein translation during infection. Furthermore, their sequestration did not prevent the formation of SGs within the cytoplasm upon exposure to subsequent stress. However, late during infection SG formation was reduced in infected cells exposed to exogenous stress such as Ars and Hipp. We have identified a novel function for VP35 by showing that it is able to disrupt SG formation and hypothesize that this function is mediated independently of eIF2α phosphorylation or the stress-signaling pathway. Finally, we showed that viral inclusions are an environment that does not support SG formation, which may in part be due to the high levels of VP35 present.

CHAPTER FOUR: THE ROLE OF POST-TRANSCRIPTIONAL REGULATION OF RNA VIA AU-RICH ELEMENTS DURING EBOLA VIRUS INFECTION

Rationale

A hallmark of EBOV infection is a dysregulated cytokine response that is thought to contribute to EBOV pathogenesis and is characterized by the hypersecretion of proinflammatory cytokines and chemokines (Ebihara et al., 2011; Villinger et al., 1999; Wauquier et al., 2010). However, the mechanisms leading to this dysregulated cytokine response are not well understood. Many cytokines and chemokines are regulated at the mRNA level by AREs, which serve as important mechanisms for fine-tuning the immune response to infection, allowing for immediate and targeted control of gene expression (Kafasla et al., 2014; Vlasova-St Louis & Bohjanen, 2014). These AREs are recognized by ARE-BPs that impact the stability and localization of mRNAs within the cell and thereby influence protein translation. Components of signaling pathways that are important for cytokine responses such as NFκB or IFN signaling can also be regulated at the mRNA level by AREs to influence cytokine production (Anderson, 2010; Kafasla et al., 2014; Palanisamy, Jakymiw, Van Tubergen, D'Silva, & Kirkwood, 2012; Vlasova-St Louis & Bohjanen, 2014). Therefore, altered stability of ARE-containing cellular mRNAs might contribute to the dysregulated cytokine response observed during EBOV infection. Intriguingly, the viral protein VP30 is a ssRNA binding protein that possesses a CCCH motif (John et al., 2007; Modrof et al., 2003), which is a hallmark of numerous cellular ARE-BPs including TTP and BRF1 (Brooks & Blackshear, 2013; Lai et al.,

2000; 2002). We therefore sought to determine if VP30 functions as an ARE-BP and influences the stability of cellular mRNAs, focusing on two cytokines that are known to be dysregulated during EBOV infection, IL-6 and IL-10 (Baize et al., 2002; Bosio et al., 2003; Ebihara et al., 2011; Panchal et al., 2014; Wauquier et al., 2010). We also examined if VP30 has any effect on IKB-α mRNA stability as this molecule is a key regulator of NF-κB signaling (Lawrence, 2009).

The regulation of ARE-containing mRNAs also has implications for viral mRNAs but has not been examined for its effects on EBOV replication or pathogenesis. The presence of viral mRNAs in the cytoplasm of infected cells leaves them prone to recognition by host proteins ARE-BPs, which could negatively impact viral protein translation. These cellular proteins could also potentially enhance viral infection by stabilizing viral mRNA and increasing viral protein production. As such, many viruses interact with ARE-BPs to promote efficient and unimpeded viral infection (Dickson & Wilusz, 2011). The EBOV genome is AU-rich (Brauburger et al., 2014; Neumann et al., 2009) and encodes four viral mRNAs that contain putative AREs within their 3'UTRs. These include the mRNAs for the viral proteins NP, VP35, VP30 and VP24. This prevalence of AU-rich elements suggests that these EBOV mRNAs might be targets of post-transcriptional regulation mediated by ARE-BPs. To explore if EBOV mRNAs can be regulated by cellular ARE-BPs, we examined the interaction of two well characterized ARE-BPs, TTP and HuR, with EBOV ARE-containing mRNAs. Similarly, we examined whether VP30 affects the stability of viral mRNAs as a means of controlling the abundance of viral RNA transcripts or enhancing their translation.

Results

4. 1 Potential role of VP30 as an ARE-BP

As mentioned above in chapter one, EBOV VP30 shares a number of features with ARE-BPs including the CCCH motif. This domain is conserved among the filoviral VP30 proteins and has also been found in the RSV protein M2-1 (Hardy & Wertz, 2000; Modrof et al., 2003; Mühlberger, 2007). A comparison of these zinc finger domains to the CCCH motif of TTP is illustrated in Figure 32. To determine if VP30 is involved in ARE-mediated post-transcriptional regulation of mRNA, we tested its function using a 3'UTR luciferase reporter system. This system involves the use of an expression plasmid that contains the firefly luciferase gene under the control of a CMV promoter with a multiple cloning site (MCS) downstream of the luciferase gene (Figure 33B). Cis-acting regulatory elements can then be inserted into the MCS creating chimeric transcripts. By using luciferase activity as a readout and comparing it to the activity of a luciferase reporter without any added sequences (Figure 33C), it is possible to examine the effects of cis-acting elements on reporter gene activity. We first examined whether VP30 had any effect on potential cellular mRNA targets. We focused on three cellular mRNAs that play a crucial role in the initiation and regulation of an inflammatory response and might play a role in EBOV pathogenesis (Baize et al., 2002; Bosio et al., 2003; Ebihara et al., 2011; Panchal et al., 2014; Wauquier et al., 2010; Wong, Kobinger, & Qiu, 2014). These include the cytokines IL-6, IL-10 and the regulator of NF-κB signaling, IKB-α. The 3'UTRs of these genes were cloned into the pMIR-luciferase reporter plasmid and transfected into 293T cells, with or without an additional VP30 expression plasmid. In

the presence of VP30, there was about a 50% reduction in luciferase activity for the 3'UTR-luciferase reporter constructs containing the IL-6 and IL-10 3'UTR compared to the negative control (Figure 34A). There was no significant difference in luciferase activity for the IKB-α 3'UTR reporter construct transfected in the presence of VP30 compared to the luciferase activity when VP30 was absent. While the 50% decrease in luciferase activity for the IL-6 and IL-10 3'UTR reporters was reproducible, the reduction was less pronounced than that observed for TTP and its known target IL-6, which resulted in 80-90% reduction in luciferase activity. This suggests that the IL-6 and IL-10 mRNAs may not be the real targets of VP30-mediated regulation. Instead, the overexpression of VP30 might lead to off-target effects leading to nonspecific repression in luciferase activity.

We also examined if VP30 was able to regulate the stability of any of the four viral mRNAs that possess putative AREs in their 3'UTRs. To do so, the 3'UTR luciferase reporter constructs containing the 3'UTRs of NP, VP35, VP30 or VP24 were individually transfected into 293T cells with or without a VP30 expression plasmid. Similar to what was observed for the cellular 3'UTR targets examined, VP30 mediated a moderate but reproducible reduction in luciferase activity for all four viral 3'UTR reporter constructs (Figure 34B). However, the ~50% reduction in luciferase reporter activity combined with the overexpression of VP30 makes it inconclusive whether these 3'UTRs represent true targets of VP30.

EBOV VP30	C-X_8-C-X_4-C-X_3-H-X_2
RESTV VP30	C-X_8-C-X_4-C-X_3-H-X_2
MARV VP30	C-X_8-C-X_4-C-X_3-H-X_2
hRSV M2-1	C-X_7-C-X_5-C-X_3-H-X_3
TTP	C-X_8-C-X_5-C-X_3-H-X_3

Figure 32. Comparison of CCCH zinc finger domains

The CCCH zinc finger domain found in EBOV VP30 is conserved among filoviruses and can be found in the M2-1 proteins of pneumoviruses such as RSV. These domains are nearly identical to the zinc finger motifs found in the known ARE-BP TTP.

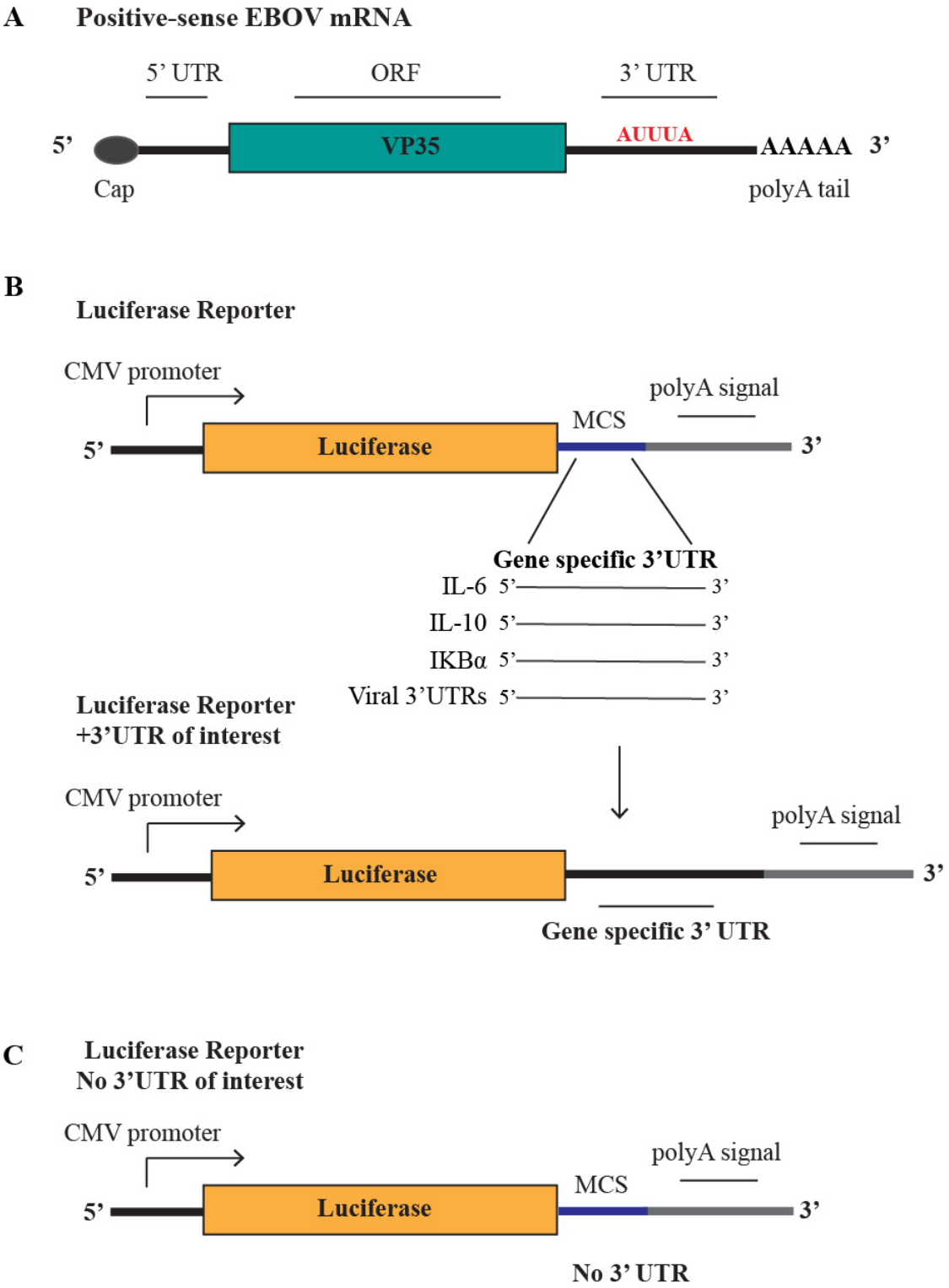

Figure 33. Schematic of pMIR-luciferase reporter system and cloning strategy.

A) EBOV mRNAs are capped and polyadenylated with varying lengths of 5' and 3'UTRs. Four viral transcripts contain putative AREs in their 3'UTRs (example of a canonical ARE highlighted in red). B) The luciferase reporter expression system contains a firefly luciferase gene with a downstream multiple cloning sight (MCS) followed by a polyadenylation signal. The 3'UTRs of cellular genes of interest including *IL-6, IL-10* and *IKBα*, or four viral genes including *NP, VP35, VP30* and *VP24*, were invidually inserted into the pMIR-luciferase reporter expression plasmid downstream of the firefly luciferase gene to create chimeric transcripts containing the gene specific 3'UTRs. C) The luciferase reporter plasmid with no added 3'UTR serves as a negative control.

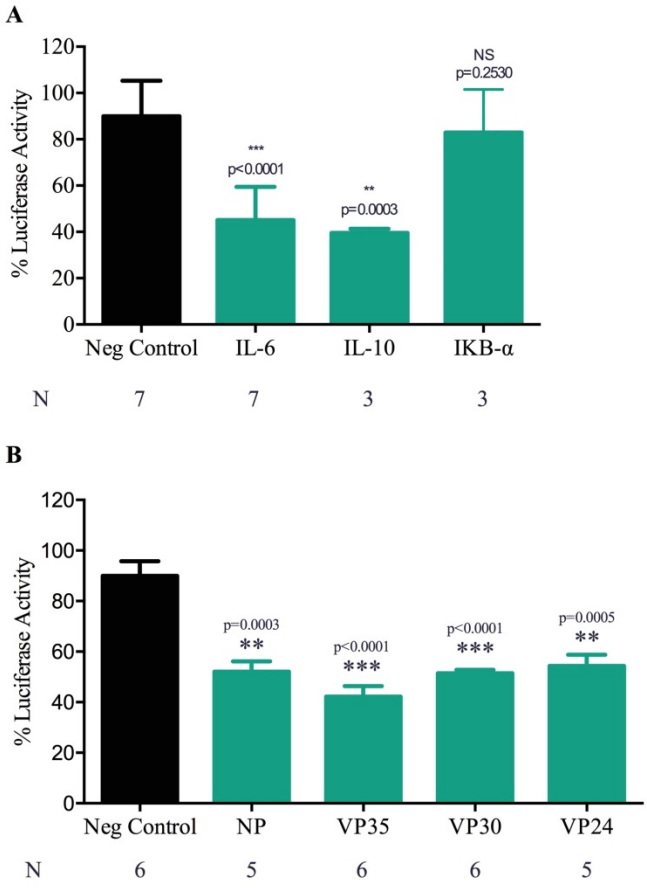

Figure 34. VP30 modestly down regulates luciferase reporter activity via 3'UTRs. 3x10^5 293T cells were seeded per well in 6-well plates and were transfected one day later with 200 ng of the indicated 3'UTR-luciferase reporter constructs and 100 ng of B-gal expression plasmid as a transfection control, with or without an expression plasmid encoding VP30 (100 ng). Lysates were harvested two days post transfection and luciferase and B-gal activity was measured. Reporter constructs in (A) include the 3'UTRs of cellular targets IL-6, IL-10 and IKB-α. Reporter constructs in (B) include the 3'UTRs of viral targets NP, VP35, VP30 and VP24. Luciferase values were normalized

to B-gal activity, converted to milliunits. The normalized luciferase values were then compared to those measured in the absence of VP30 for each construct. Data are representative of experiments repeated at least 3 times. Statistical analysis was performed using GraphPad prism software, using a one-sample t-test. N indicates the number of replicates for each condition. * indicates p value ≤ 0.05, ** indicates p value ≤ 0.01, *** indicates p value ≤ 0.001.

4.2 The 3'UTRs of four EBOV mRNAs contain putative ARES and enhance luciferase reporter activity

Examination of the nucleotide sequences of the seven viral mRNA species made during EBOV transcription revealed that four viral nucleocapsid protein mRNAs, NP, VP35, VP30 and VP24, contain putative AREs within their 3'UTRs, suggesting they might be targets of ARE-BPs. The sequence of each 3'UTR was further examined using the online ARE analysis program AREscore (http://arescore.dkfz.de/arescore.pl) to confirm that these viral 3'UTRs contain putative AREs. The sequences of each viral 3'UTR we examined are outlined in Figure 35, with putative AREs highlighted in red. These are compared to the 3'UTR of IL-6, a well-characterized target of ARE-mediated post-transcriptional regulation, which contains many canonical AREs (Zhao, Liu, & Kirkwood, 2008; Zhao, Liu, D'Silva, & Kirkwood, 2011). To first broadly examine whether these viral 3'UTRs influence mRNA stability, we employed the pMIR-luciferase reporter expression system described above (Figure 33). The 3'UTRs of the respective EBOV mRNAs containing putative AREs were inserted into this luciferase reporter plasmid downstream of the luciferase open reading frame to create luciferase mRNA transcripts containing viral 3'UTRs (Figure 33B). To examine if the EBOV 3'UTRs conferred any difference in luciferase reporter activity, 293T cells were transfected with luciferase reporter plasmids containing the individual EBOV 3'UTRs along with a B-gal reporter plasmid as a transfection control. A reporter plasmid containing no added 3'UTR (negative control) and reporter plasmids containing the 3'UTRs of the IL-6 or IKB-α mRNA, respectively, were used as controls. Cell lysates were harvested 2 days post

transfection and luciferase and B-gal activity was measured (Figure 36). The luciferase reporter activity for each individual 3'UTR-containing reporter plasmid was normalized to B-gal and compared to the luciferase values measured for the negative control. Interestingly, while the IL-6 and IKB-α 3'UTRs did not have a significant impact on luciferase activity compared to the negative control (Figure 36, grey bars), luciferase activity was enhanced in cells transfected with the reporter constructs containing the EBOV 3'UTRs compared to the negative control (Figure 36, green bars). This suggests that the tested EBOV 3'UTRs might be targeted by cellular proteins involved in regulating mRNA stability.

NP

1 AAGCUUUUUU CUUAAUUAUA AAACGAUCGU GUAAAUGUUG GGCAGGCUAG UAGGUAAGUU
61 AUAAAAGCAU AAUGUAAUUU AAUUUAGAUA AAUCGCUAGU UAGAAUAUUG AGUUACAAUU
121 AUGGCUAUAA CUGUGGCUUA ACGCCUAUUU GCAUUAAGAC UCAAAUUGAA CUUUGAAAAA
181 CGGCUAGUAA UAAUAAGCUA GCUUUAAAUU CAAAAAUAAG AAUCACUUUU AUUGUGAUAA
241 UAAUUCACAC CUUAGACAUC AAAAAUUCUU CCUGUUUUCG UUCCUUGACU ACUUAAUGUU
301 AGCUAUUUGU CGGUUGAAUC AUCCCAUUGU UCCAUGCUCA UUCAACUA

VP35

1 UAUUAAGCUU UUUCUUAAUC UUCAUCACUU UUGGUUUGGG UUACUUAAUA ACAAUUGAUU
61 AUAAUACUGU CAGAGAUAUA GCUCCUAUUA CAUUUAUAUU UUAAGCUGCU AGCGAGAUAU
121 GAACAAUUUU AUCUUGGUCG UUUAAUUGAC UUAUAUAUCC AGGGCUGAUA CUCACAAGUG
181 UAUCAUUAAU GUAACGUACC CUAUAGUUCA GCAGUUGAAG CCUCUGCUAU UAUUCGCCUC
241 UUUCGGAGGG AAGGGAGAUU GGCUCAACUA GUGCGC

VP30

1 UUUCUUAAUA UUUUAAGAGA UCAUUAGUAA GUCAUGAAAU ACUUAUUUUU UGAUGGGAUG
61 GAUCGUUGCU ACCUCCUGUA GAGUAAAACA UUAUUUGUGU ACAAGAAUCA CUUUGUGCAA
121 GAGGUAUGCU UGGCAGGUUA UAUUACGAGC GAUACGAGAU UAUGAUUUUC UUUGAUCACU
181 GUUAGGGUUG UAUCAUACCU CUUCAUAUAU UAGGGCAAUC AUGCACAUCU UAUUAAUUUG
241 AAACGAGAGU GAUUAUAGUA CUGAAUAAGU UUUAAAGGAU AUCGUCUUGA UUAAAUAUAU
301 GAUGAUAGGU AUACGGAGUA UUGUGAUCAA GUAGAAGGUU AUAUAGUGUU UUAGUCAGCC
361 UUAUUAAC

VP24

1 UAAGCUUUUU UCUUAAUCUA CUUAUCUAAU GUUAAUUACG AGUAUAGAGU UAGUAAUAUA
61 UAGAAUCUGU GAAACCUAAC ACAUGUGACC UGCGGGUUCA GUUACAAUUA ACCAUUUAGU
121 AUAUAGGAUU UCUGGUGAUA AAAUGCUUAU UCAUAUAAUA AAGCAAUUCU AUGAUGUUGU
181 CUUGGAAUCU CUUGUUUGAG GGAUUCUGAG UCCUGGUUUU UGUAAGGGUG UCAACUUGGA
241 AGCUGGCUUA CAGUGAGGAU UUAUCUGUGG UUAAACAAAU UAUCAAGAAA UAUGAGUAUU
301 UAUUUAUUAU GCUUAUAUAU CUGAUUAUGA AAGCAGAGAU GUCAAGAUAA CUAUUGAGUC
361 AGCAUAUAUG AGUUAGCUCA AUAUGAAGUA UUCUACCUUA GUUAACUAGU GCG

IL-6

1 CAUGGGCACC UCAGAUUGUU GUUGUUAAUG GGCAUUCCUU CUUCUGGUCA GAAACCUGUC
61 CACUGGGCAC AGAACUUAUG UUGUUCUCUA UGGAGAACUA AAAGUAUGAG CGUUAGGACA
121 CUAUUUUAAU UAUUUUUAAU UUAUUAAUAU UUAAAUAUGU GAAGCUGAGU UAAUUUAUGU
181 AAGUCAUAUU UAUAUUUUUA AGAAGUACCA CUUGAAACAU UUUAUGUAUU AGUUUUGAAA
241 UAAUAAUGGA AAGUGGCUAU GCAGUUUGAA UAUCCUUUGU UUCAGAGCCA GAUCAUUUCU
301 UGGAAAGUGU AGGCUUACCU CAAAUAAAUG GCUAACUUAU ACAUAUUUUU AAAGAAAUAU
361 UUAUAUUGUA UUUAUAUAAU GUAUAAAUGG UUUUUAUACC AAUAAAUGGC AUUUU

Figure 35. EBOV 3'UTRs containing putative AREs.

3'UTR sequences with putative AREs (bolded in red) of four EBOV mRNAs. The 3'UTR of the IL-6 mRNA is shown for comparison

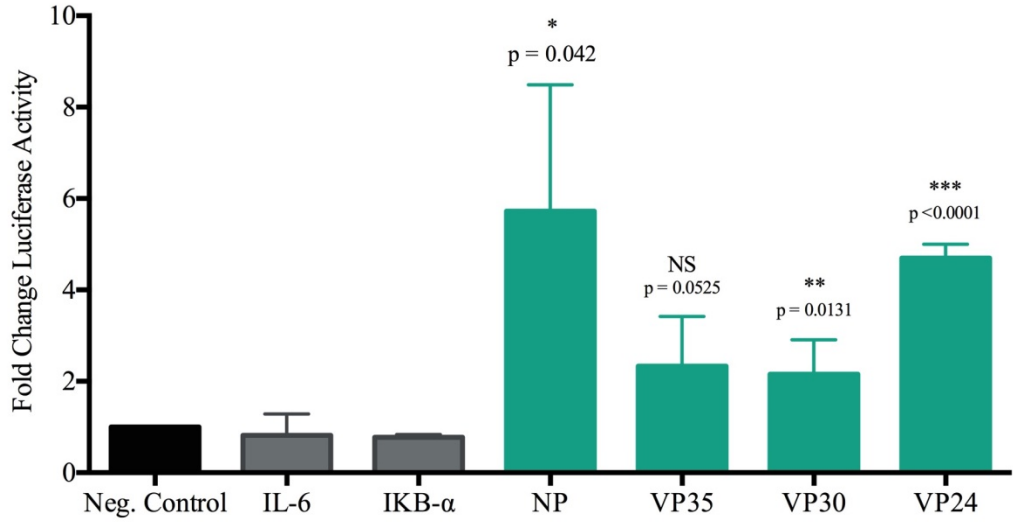

Figure 36. Viral 3'UTRs enhance luciferase reporter activity.

1.5 x10^5 293T cells were seeded per well of a 12-well plate and were transfected one day later with 100 ng of luciferase reporter plasmids containing the indicated 3'UTRs and 100 ng of a B-gal expression plasmid as a transfection control. The luciferase reporter containing no added gene specific 3'UTR served as the negative control (Neg. Control). Cell lysates were harvested 2 days post transfection and measured for luciferase and B-gal activity. Luciferase values were normalized to B-gal activity (converted to milliunits), and the normalized luciferase values for the negative control were set to one. The normalized luciferase values for each individual 3'UTR-luciferase reporter construct were then compared to the negative control. Statistical analysis was performed using the GraphPad Prism software, using a one-sample t-test analysis. N= 5 for all conditions except for the 3'UTR-luciferase reporter containing the IKB-α 3'UTR which was repeated only twice. NS indicates p value that is not significant and $p > 0.05$, * indicates p value ≤ 0.05, ** indicates p value ≤ 0.01, *** indicates p value ≤ 0.001.

4.3 TTP and BRF1 target the 3'UTR of NP

We next analyzed if well-characterized ARE-BPs altered the luciferase activity in cells co-transfected with the EBOV 3'UTR-containing luciferase reporters plasmids. We therefore examined the effects of, TTP, known to destabilize its targets, and HuR, known to stabilize its targets, on the 3'UTR-luciferase reporter system (Barreau et al., 2005). 293T cells were transfected with reporter gene expression plasmids containing the individual EBOV 3'UTRs with or without the co-transfection of HuR (Figure 37A) or TTP (Figure 37B). The TNF-α 3'UTR was used as a positive control in this experiment because the TNF-α mRNA is a known target of HuR and is stabilized by HuR binding (Palanisamy et al., 2012). The IL-10 3'UTR is not targeted by HuR and served as an additional negative control in this assay. A B-gal expression plasmid was co-transfected in all conditions as a transfection control. Lysates were harvested 2 days post transfection and luciferase and B-gal activity were measured. The cells co-transfected with EBOV 3'UTR-luciferase reporter plasmids and the HuR expression plasmid showed little to no difference in luciferase reporter activity compared to those not transfected with HuR. However, the same level of increase in reporter gene expression was observed with the TNF-α 3'UTR positive control. Luciferase activity was only enhanced by about 2-fold in cells co-transfected with the reporter plasmid containing the TNF-α 3'UTR and the HuR expression plasmid, indicating that the overexpression of HuR did not lead to greatly enhanced mRNA stability. As HuR is constitutively expressed in most cell types (Antic & Keene, 1997; Brennan & Steitz, 2001), it is conceivable that the presence of endogenous HuR in these transfected cells might account for the small increase in

luciferase activity for the TNF-α 3'UTR-containing reporter due to HuR saturation. Therefore it is inconclusive whether HuR mediates any effect on the 3'UTRs of EBOV mRNAs.

Interestingly, when the EBOV 3'UTR luciferase reporter plasmids were co-transfected with TTP, the luciferase activity in cells transfected with the reporter plasmid containing the NP 3'UTR was significantly decreased (Figure 37B). This decrease in luciferase activity was comparable to what was observed for the luciferase reporters containing the 3'UTRs of IL-6 and IL-10, which are both well characterized targets of TTP mediated degradation (Brooks & Blackshear, 2013; Palanisamy et al., 2012). The cellular protein butyrate response factor 1 (BRF1) is another well studied member of the TTP protein family involved in ARE-mediated mRNA degradation (Palanisamy et al., 2012; Sanduja, Blanco, & Dixon, 2011). Interestingly, cells transfected with the NP 3'UTR-luciferase reporter plasmid also showed decreased luciferase activity when BRF1 was co-expressed. However, the BRF-1 experiments are preliminary and need to be repeated in order to determine statistical significance. Nevertheless, they suggest that the NP mRNA might be the target of multiple cellular ARE-BPs.

Cells expressing the luciferase reporter plasmids containing the 3'UTRs of VP30 and VP35 showed an intermediate reduction in luciferase activity in the presence of TTP compared to the negative control. Similarly, cells expressing the reporter plasmid containing the 3'UTR of VP24 showed little to no change in luciferase activity when TTP was co-expressed compared to when it was absent. Together, these data suggest that TTP and BRF1 specifically target the NP 3'UTR.

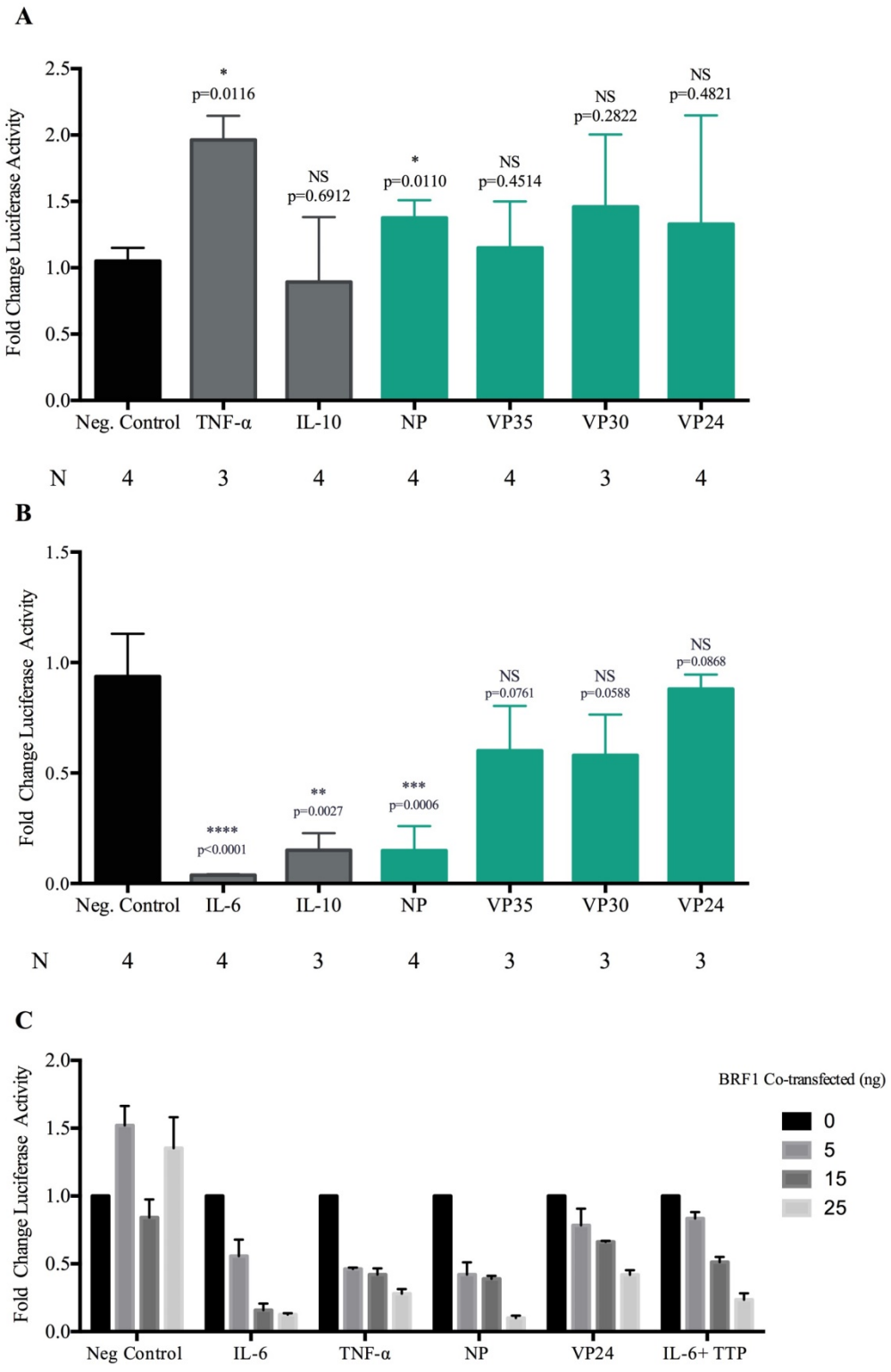

Figure 37. TTP and BRF1 repress NP 3'UTR-luciferase reporter activity.

293T cells were seeded in 12-well plates at a density of 1.5 x 10^5 cells per well and transfected one day later with individual luciferase reporter plasmids containing the indicated 3'UTR or no gene specific 3'UTR (Neg. Control) along with a B-gal expression plasmid as a transfection control. Cells were transfected with 100 ng of these 3'UTR containing luciferase reporter plasmids alone or with an additional expression plasmid containing HuR (A, 100 ng), TTP (B, 25 ng), or BRF1 (C, 5-25 ng) respectively. Cell lysates were harvested two days post transfection and measured for luciferase and B-gal activity. Luciferase values were normalized to B-gal activity, which was converted to milliunits. The normalized luciferase values for the individual 3'UTR-luciferase reporter constructs in the presence of the indicated ARE-BP were divided by the normalized luciferase values for the individual 3'UTR-luciferase reporter constructs in the absence of any ARE-BP. These values were then compared to the negative control, which was set to one. N indicates the number of replicates for each condition. Results in (C) were collected from an experiment performed once in duplicate. Statistical analysis was performed using the GraphPad Prism software, using their one-sample t-test analysis. NS indicates p value that is not significant and $p > 0.05$, * indicates p value ≤ 0.05, ** indicates p value ≤ 0.01, *** indicates p value ≤ 0.001.

4.4 TTP negatively regulates the protein expression and mRNA levels of NP

To further investigate the downregulation of luciferase reporter activity for the NP 3'UTR reporter plasmid mediated by TTP, we next examined the effects of TTP on full length NP protein expression. To do so, NP expression plasmids containing the open reading frame of the NP gene with the full length NP 3'UTR (348 nucleotides), a truncated NP 3' UTR (140 nucleotides) or no 3' UTR (Figure 38) were transfected into 293T cells with or without a TTP expression plasmid. Cells were harvested 2 days post transfection and examined by Western blot analysis for NP protein expression (Figure 39). Cells transfected with the NP expression plasmid containing no 3'UTR showed little to no reduction in NP protein expression when co-transfected with TTP compared to cells transfected without TTP (Figure 39 A and C). However, NP expression was reduced by about 75% in cells transfected with the NP expression construct containing the full-length 3'UTR when TTP was co-expressed. Cells transfected with the NP expression plasmids containing either the full length 3'UTR or no 3'UTR showed little to no difference in NP protein expression when eGFP was co-expressed instead of TTP. While the protein expression of NP was also reduced in cells transfected with the NP expression plasmid containing a truncated 3'UTR in the presence of TTP (Figure 39 B and C), this reduction was not as pronounced as what was observed when cells were co-transfected with TTP and the NP expression plasmid containing a full length 3'UTR.

To determine if the reduction in NP protein expression was recapitulated at the mRNA level, mRNA was collected from cells transfected with the NP expression plasmid containing a full length 3'UTR, with or without co-transfection of TTP, at one

day post transfection. NP mRNA levels were quantified by qRT-PCR using primers that bind to sequences within the ORF of NP mRNA. When TTP was co-expressed with the NP expression plasmid containing the full length 3'UTR, NP mRNA levels were dramatically reduced compared to cells transfected with the NP expression plasmid containing the full length 3'UTR in the absence of TTP. This was recapitulated when cells were transfected with the TTP and the pMIR-luciferase 3'UTR reporter expression plasmid containing the NP 3'UTR and luciferase mRNA levels were measured by qRT-PCR. Collectively, these data suggest that TTP specifically targets the 3'UTR of NP mRNA, which ultimately leads to a reduction in NP protein expression. Shortening of the 3'UTR mitigates the reduction in NP protein expression observed in the presence of TTP, suggesting that the NP 3'UTR contains multiple AREs or other cis-acting elements that are recognized by TTP or TTP-related proteins such as BRF1.

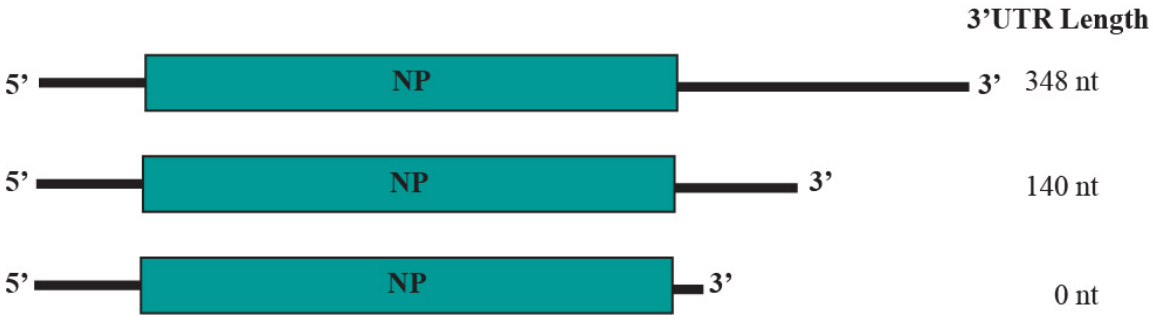

Figure 38. Schematic of NP expression plasmids with varying lengths of 3'UTR

Schematic representation of the mRNA transcripts produced from the expression plasmids containing the full length NP gene with varying 3'UTR lengths. The full length NP 3'UTR is 348 nucleotides (nt) and the truncated 3'UTR is 140 nt in length. The partial 3'UTR contains the 140 nt directly following the NP ORF. The last construct contains no 3'UTR.

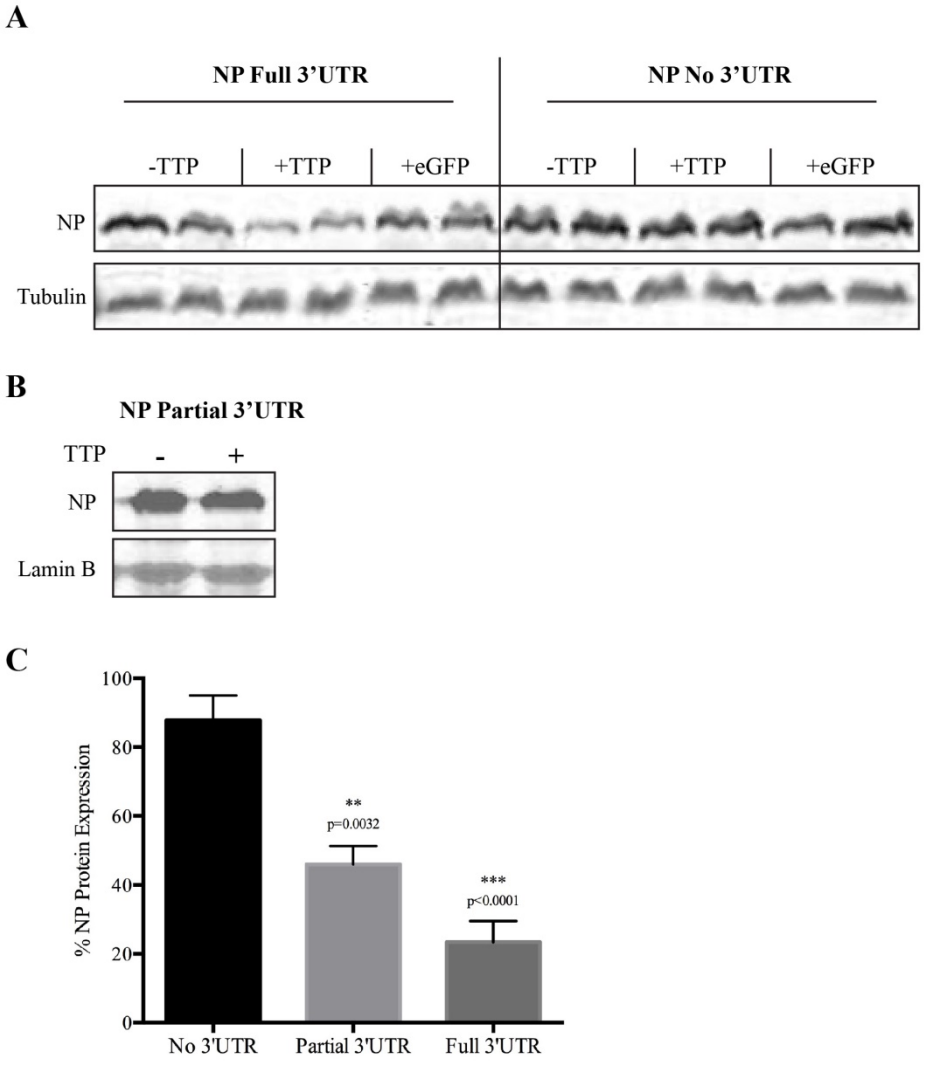

Figure 39. TTP negatively impacts NP protein expression.

A) 3x10^ 5 293T cells were seeded into 6-well plates and transfected one day later with 200 ng expression plasmids containing the NP gene with either a full length 3'UTR, or no 3'UTR. These plasmids were transfected in the absence or presence of 25 ng of a TTP expression plasmid. As a control, NP expression plasmids were co-transfected with 25 ng of an eGFP expression plasmid instead of TTP. Cells were harvested two days post transfection and analyzed by Western blot. This blot is representative of three

independent experiments. Tubulin was used as a control for endogenous cellular protein amount. B) Cells were transfected as in (A) but with an NP expression plasmid containing a truncated 3'UTR in the presence or absence of 25 ng of a TTP expression plasmid. Lamin B was used as a control for endogenous cellular protein amount. This blot is representative of three independent experiments. C) Quantification of NP protein expression in the presence of TTP using NP expression plasmids containing no 3'UTR, a partial 3'UTR, or a full length 3'UTR. Protein bands were quantified using Li-COR Image Studio western blot analysis software. Statistical analysis was performed using GraphPad prism software, using a one-sample t-test. ** indicates p value ≤ 0.01, *** indicates p value ≤ 0.001.

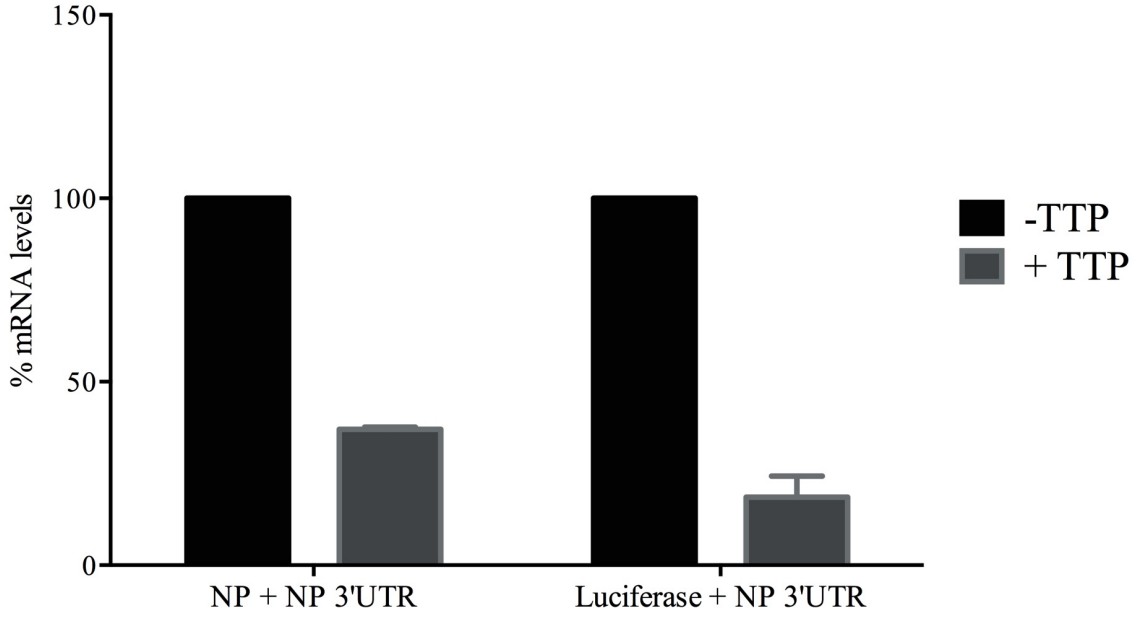

Figure 40. NP mRNA levels are reduced in the presence of TTP

3x10^5 293T cells were seeded in 6-well plates and one day later were transfected with 200 ng of the expression plasmids containing the full length NP 3'UTR downstream of either the full length NP gene or the firefly luciferase gene, with or without the co-transfection of 25 ng of a TTP expression plasmid. 100 ng of eGFP plasmid were also transfected as a transfection control. Cellular RNA was harvested one day post transfection using an RNA isolation method that isolates mRNA and miRNA. NP mRNA levels (left columns) or luciferase mRNA levels (right columns) were measured by qRT-PCR using 5 ng RNA and primers specific for either NP or luciferase. The levels of mRNA were calculated using the $\Delta\Delta C_T$ method with Bio-Rad CFX Manager 1.5 software and were normalized to beta-2-microglobulin. Levels of mRNA measured in the absence of TTP were set to 100%. This experiment was performed twice.

4.5 TTP overexpression impairs minigenome activity.

In order to determine if the targeting effects of TTP on NP had any impact on viral replication or transcription, the EBOV minigenome system was used. This system, is described above in chapter three (Figure 9). 293T cells were transfected with a plasmid containing the 3E5E-eGFP minigenome under the control of the T7 RNA polymerase promoter, along with an expression plasmid encoding the T7 RNA polymerase. In addition, plasmids encoding the EBOV genes NP, VP30, VP35 and L, all under the control of the T7 RNA polymerase promoter, were transfected. All of these support plasmids contain full length 3'UTRs. As expected, when cells were examined two days post-transfection, there was no eGFP expression in the absence of L (Figure 41A). In the presence of L, eGFP was expressed, indicative of proper replication and transcription. When TTP was co-expressed with the minigenome and support plasmids, eGFP expression was significantly reduced. There was also a decrease in eGFP expression when cells were co-transfected with mCherry instead of TTP, indicating that the expression of an additional protein might contribute to the reduction in minigenome activity observed when TTP was co-expressed. However, because the reduction in eGFP expression was much greater in the presence of TTP than mCherry, we propose that the inhibitory effects observed when TTP was overexpressed can be mainly attributed to TTP activity.

To quantify the decrease in minigenome activity in cells overexpressing TTP, an EBOV minigenome containing firefly luciferase as the reporter gene was used. Using luciferase activity as the readout of minigenome activity corroborated what was shown

with the eGFP minigenome. Luciferase activity was significantly reduced when TTP was co-expressed (Figure 41B). Co-transfection of a mCherry again lead to a reduction in minigenome activity, but this inhibitory effect was still less than that observed for TTP. Combined, our data suggest that TTP inhibits EBOV replication by downregulating NP mRNA.

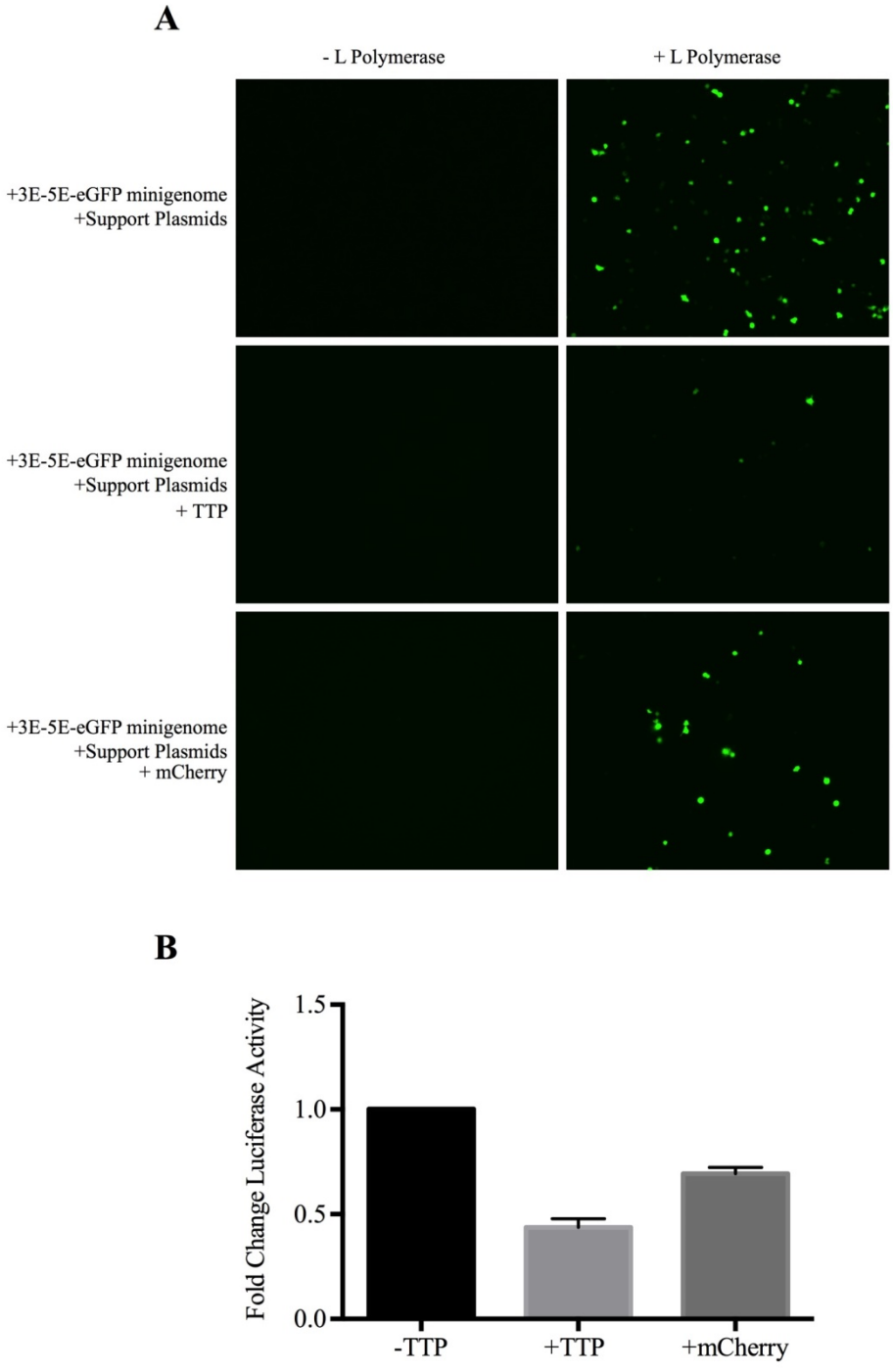

Figure 41. TTP overexpression decreases minigenome activity.

A) 3 x10 ^5 293T cells were seeded in a 6-well plate and transfected one day later with the 3E-5E-eGFP minigenome and appropriate support plasmids all driven by a T7 RNA polymerase promoter. Cells were co-transfected with the expression plasmids for the L polymerase, TTP (50 ng), or mCherry (50 ng) as indicated. Cells were live imaged 2 days post transfection. Experiment was performed twice. B) Cells were transfected as in (A) but with the 3E-5E-luciferase minigenome instead of the 3E-5E-eGFP minigenome. Cells were co-transfected with the B-gal reporter plasmid as a transfection control. Lysates were harvested 2 days post transfection and luciferase and B-gal values were measured. Luciferase activity was normalized to B-gal activity, converted to milliunits. The normalized luciferase values for cells transfected with the minigenome in the absence of TTP were set to one and compared to the normalized luciferase values for cells co-transfected with the minigenome and TTP. Data presented are the luciferase values measured in cells co-transfected with L. This experiment was performed twice

DISCUSSION

VP30 has similarities to TTP

Because of its similarities to other proteins involved in post-transcriptional regulation of mRNA, we examined whether the viral protein VP30 was able to function in a manner similar to other ARE-BPs such as HuR and TTP. VP30 expression consistently and reproducibly led to a moderate decrease of about 50% in luciferase activity from constructs with an ARE-containing 3'UTR. However, VP30 did not appear to specifically target one of the tested cellular or viral UTRs. The slight decrease in reporter gene expression might be due to high VP30 expression levels in the transfected cells. When TTP was expressed at high levels, it was found to exhibit a moderate off-target repressive effect on luciferase activity. This repression was similar to the level of repression observed for VP30. Although it is inconclusive whether VP30 specifically targets any of the 3'UTRs constructs we tested, the observed reduction in luciferase activity, albeit only about 2 fold, suggests that VP30 may in fact function similarly to TTP.

Viral 3'UTRs influence protein expression

Viruses interact with the host RNA regulation machinery in a number of different ways (Charley & Wilusz, 2014; Dickson & Wilusz, 2011). This often entails the avoidance or disruption of the cellular mechanisms that impair viral infection such as RNA interference, innate immune signaling and RNA degradation. Alternatively, many viruses have been shown to exploit these pathways to their own advantage. The EBOV

genome is enriched in A and U residues and as such represents a potential target for specific cellular RNA binding proteins influencing mRNA turnover via AREs. We identified four viral mRNAs containing putative AREs within their 3'UTRs and aimed to determine if these regions are targeted by the RNA regulating machinery, either for stabilization or degradation of the viral mRNAs. When expressed in cells, reporter plasmids containing the viral 3'UTRs showed enhanced luciferase activity compared to the luciferase reporter construct containing no additional 3'UTR. This suggests that the viral 3'UTRs enhanced the stability or promoted the translation of the luciferase gene. The interaction between ARE-BPs and viral RNA is not uncommon. HuR, which is associated with mRNA stability and enhanced translation, has been shown to interact with a number of viruses, and was found sequestered within viral inclusions in EBOV-infected cells. We therefore hypothesized that it might be targeting viral mRNA and ultimately enhancing the translation of viral proteins. However, HuR only induced a modest increase in luciferase activity when co-expressed with luciferase reporter plasmids containing the viral 3'UTRs. This was also the case for a reporter construct containing the TNF-α 3'UTR, a known target of HuR (Barreau et al., 2005; Brennan & Steitz, 2001). It is important to note that HuR is ubiquitously expressed, and most cell lines express HuR efficiently (Brennan & Steitz, 2001). Therefore it is possible that the cells we used for transfection were already saturated with HuR and overexpression of HuR would not lead to enhanced mRNA stability and subsequent increased luciferase reporter activity. Efforts to knockdown HuR in 293T and HeLa cells using an siRNA approach failed. This might be due to the function of HuR as an important regulator of

the cell cycle. Furthermore, it has not been possible to breed HuR knockout mice, supporting the notion that it is difficult to establish a cell system in which HuR expression is abolished or limited (Brennan & Steitz, 2001; Simone & Keene, 2013). Despite these challenges, the localization of HuR within viral inclusions as shown in chapter three suggests that HuR plays a role during viral infection, and we aim to study this in more detail in the future.

TTP negatively targets the NP 3'UTR

TTP and BRF1 are known to destabilize their RNA targets, often through the recruitment of RNA processing and decay enzymes such as deadenylases and exosome components (Brooks & Blackshear, 2013; Carrick & Blackshear, 2007; Lai et al., 2000). Our data suggest that TTP and BRF1 target the 3 'UTR of the EBOV NP mRNA. The luciferase reporter activity for the NP 3'UTR construct co-transfected with TTP was comparable to that observed for the luciferase constructs containing the 3'UTRs of IL-6 and IL-10, two known targets of TTP (Brooks & Blackshear, 2013). This was recapitulated at the RNA level, when luciferase mRNA levels were measured by qRT-PCR. The luciferase activity of the 3'UTR reporter plasmids encoding the three other viral 3'UTRs showed less than a 50% reduction in the presence of TTP. Previous experiments aiming to optimize the luciferase reporter system showed that transfection of higher TTP plasmid amounts led to the unspecific downregulation of luciferase activity from constructs that did not possess an ARE-containing 3'UTR (data not shown). However, TTP transfected at lower concentrations still showed a potent negative

regulatory effect on specific targets, while making little difference to the negative control. This suggests that the slight reduction in luciferase reporter activity for the 3'UTR reporter constructs containing the VP30 and VP35 3'UTRs might be due to a nonspecific or off-target effect of TTP. It is also conceivable that TTP binds to the putative AREs within these 3'UTRs with low affinity, leading to a mild effect.

We further showed that TTP was able to down-regulate full-length NP protein expression. This negative effect was ablated when the 3'UTR of NP was removed, indicating that TTP recognizes specific elements within the NP 3'UTR. Furthermore, TTP was able to down regulate minigenome activity. However, it is unclear if this effect was due to TTP's downregulation of NP protein expression or was mediated by another potential target such as the genomic RNA itself. While we hypothesize that TTP directly targets the NP 3'UTR and promotes NP mRNA degradation, it is also conceivable that TTP mediates this effect in a more indirect way. ARE-BPs often share the same or overlapping targets and thereby can create a gradient of regulatory control based on the abundance of certain ARE-BPs over others (Barreau et al., 2005; Kafasla et al., 2014). TTP might compete for binding to other cellular RNA targets, thereby freeing up an unknown ARE-BP that is then able to bind to the NP 3'UTR. It is also feasible that the increase in TTP expression in this system might be indirectly affecting luciferase activity via an off-target effect. TTP might down regulate the expression of a stability factor that recognizes the NP 3'UTR, which would then promote the turnover of the NP mRNA. Future studies will be aimed at more precisely defining the mechanism of TTP-mediated downregulation of NP protein expression and minigenome activity.

We hypothesized in chapter three that viral inclusions promote viral replication through the recruitment of cellular factors that are beneficial to this process. TTP did not colocalize with viral RNA species within viral inclusions (Figure 12), which supports the hypothesis that inclusions are important proviral environments. However, TTP expression is not nearly as ubiquitous as that of HuR (Carrick & Blackshear, 2007), making it possible that the cell lines we used were not ideal for examining TTP localization during infection. As a key regulator of inflammatory responses, TTP is upregulated in immune cells such as monocytes and macrophages upon activation (Brooks & Blackshear, 2013). These are also thought to be primary target cells of EBOV infection (Feldmann & Geisbert, 2011b; Messaoudi et al., 2015). Therefore it would be interesting to examine whether TTP can be found associated with inclusions or RNA in cells that express higher or more physiological levels of TTP such as macrophages.

While the sequestration of certain cellular proteins might promote EBOV replication or translation, the exclusion of other cellular proteins, such as TTP, might provide an equally important function for EBOV. TIA-1, which was also excluded from EBOV inclusions, is a critical component of SGs but is also an ARE-BP that has been shown to target viral RNA and promote mRNA degradation (Albornoz, Carletti, Corazza, & Marcello, 2014). Although it is unclear how certain cellular proteins are sequestered within inclusions while others are excluded, because many ARE-BPs have overlapping targets, it is possible that the sequestration of HuR, or another related protein, allows HuR to outcompete or prevent TTP or TIA-1 from binding viral RNA.

In summary, we have shown that the 3'UTR of NP is subject to regulation by at least one cellular protein involved in the control of mRNA stability. This protein, TTP, was able to downregulate the protein expression of NP only when it possessed at least a partial 3'UTR. TTP also significantly impaired EBOV minigenome activity, although it is unclear whether this function was mediated solely through its targeting of NP. While HuR was not found to mediate any substantial effect on viral 3'UTRs, its sequestration within viral inclusions fosters the notion that HuR plays some undetermined role during EBOV infection. Finally, we have shown that VP30 possesses characteristics common to ARE-BPs like TTP. We were unable to find a specific RNA target, but propose that a real target has yet to be identified

.

CHAPTER FIVE: CONCLUDING REMARKS

Overview

The ongoing outbreak of Ebola virus disease in West Africa has had significant and widespread global health consequences, highlighting the importance of understanding its highly pathogenic causative agent. Since its discovery, considerable research efforts have focused on understanding the interaction between EBOV and the host immune response. These studies have shown that EBOV causes significant immune dysfunction and possesses a number of immune evasion strategies, which contribute to its relatively uninhibited viral spread. One aspect of this aberrant immune response is the uncontrolled release of proinflammatory cytokines and chemokines, leading to a cytokine storm that has been associated with fatal infection(Baize et al., 2002; Bird et al., 2015; Ebihara et al., 2011; Mohamadzadeh et al., 2006; Wauquier et al., 2010). Furthermore, the evasion of innate antiviral immunity is typified by the disruption in type I IFN production and signaling(Audet & Kobinger, 2015; Basler, 2015). Other immune evasion mechanisms include the antagonism of various sensors of viral infection including RIG-I (Cárdenas et al., 2006) and PKR (Feng, Cerveny, Yan, & He, 2007a; Schümann et al., 2009). The extent to which EBOV is able to disrupt, evade or inhibit a robust antiviral response is not wholly understood, and this emphasizes the importance of more precisely defining these mechanisms. Identifying cellular factors that the virus interacts with or antiviral pathways that the virus is unable to evade is valuable for the development of effective antiviral strategies.

Two cellular processes predominantly involved in maintaining homeostasis are increasingly becoming appreciated as mediators of innate antiviral responses. These include the translational repression associated with SG formation during the cellular stress response and the post-transcriptional regulation of mRNA via AREs and their associated RBPs(Dickson & Wilusz, 2011; Onomoto et al., 2014). However, there have been no studies examining the effects of SG formation or post-transcriptional regulation of viral RNA during EBOV infection. Here we examined these two cellular systems in more depth in the context of EBOV infection.

Summary of Major Findings

In Chapter Three we explored the interaction between EBOV and the cellular stress response. The key findings we made are:

- SGs were not induced at any time point during the course of EBOV infection. This is supported by the absence of eIF2α phosphorylation both early and late in infection.
- Despite the observed absence of SGs, EBOV was unable to fully prevent SG formation induced by other stresses including Ars, heat, or Hipp treatment.
- SG proteins were found sequestered within viral inclusions late in infection, and colocalized with both positive sense mRNA and negative sense genomic RNA within inclusions. These inclusion bound granules were not canonical SGs, however, and did not impair protein translation during infection.
- Canonical SGs did not form within inclusions.

- When additional stress was applied to EBOV infected cells late in infection, SG proteins were no longer found sequestered within inclusions. Furthermore, there was a reduction in cytoplasmic SG formation compared to early stages of infection.
- A newly identified function of the viral IFN antagonist VP35 was discovered. VP35 disrupted SG formation when expressed at high levels. Mutational analysis revealed that this function was independent of VP35's IFN inhibitory domain.

In Chapter Four we examined if the 3'UTRs of viral mRNAs containing putative AREs are targets of post-transcriptional regulation. Furthermore, we tested if VP30 functions as an ARE-BP and targets these specific viral 3'UTRs or the 3'UTRs of selected cellular mRNAs with links to the dysregulated cytokine response observed during infection. The key findings are:

- In cells expressing VP30, the luciferase activity of the reporter gene constructs containing the IL-6 or IL-10 3'UTR was modestly decreased, while the luciferase activity of the IKB-α 3'UTR reporter construct was not affected. Coexpression of VP30 with the reporter constructs containing the EBOV 3'UTRs led to a 2-fold reduction in luciferase activity. A similar modest decrease in reporter gene activity was also observed when TTP was overexpressed at higher levels along with non-specific target 3'UTRs, making it is conceivable that VP30 has an mRNA destabilizing activity, but the true targets remain to be identified

- Using online bioinformatics tools, it was predicted that the 3'UTRs of four EBOV mRNAs, NP, VP35, VP30 and VP24, contain AREs.
- Cells transfected with luciferase reporter plasmids containing the 3'UTRs of the four EBOV genes showed increased luciferase activity compared to the luciferase reporter without any gene specific 3'UTR, suggesting that the viral UTRs enhance protein expression.
- Overexpression of HuR, a stabilizing ARE-BP that was found in EBOV inclusions, led to slightly enhanced luciferase activity for the reporter constructs containing the investigated EBOV 3'UTRs. However, endogenous HuR leading to potential saturation effects makes it inconclusive whether the viral 3'UTRs are real targets of HuR.
- Overexpression of TTP and BRF1, both destabilizing ARE-BPs, led to a significant decrease in luciferase reporter activity for the 3'UTR-luciferase reporter construct containing the NP 3'UTR. In addition, NP mRNA amounts and protein expression levels were reduced in cells overexpressing TTP. This effect was dependent on the presence of the NP 3'UTR. Overexpression of TTP also led to decreased EBOV minigenome activity. Combined, these results suggest that the NP 3'UTR is a target for TTP and BRF1.
-

Overarching Implications and Significance

This body of work focused on characterizing the dynamics between EBOV and two specific yet interconnected mechanisms of cellular RNA regulation implicated in

host antiviral responses. While much work remains to be done in order to more precisely characterize these events, this work demonstrates for the first time that EBOV is intimately involved in these processes. By gaining a better understanding of the intracellular events that take place during EBOV infection, we continue to improve and design more appropriate treatments and vaccines.

While we show that EBOV does not induce the stress response during infection, we also show that it was unable to fully prevent the induction of SGs mediated by exogenous stress. This provides insight into potential weaknesses of EBOV and suggests the possibility of therapeutic intervention. By inducing translational arrest via stress response pathways that EBOV is unable to block or disrupt, it would be possible to shut down EBOV translation and obstruct viral replication. Similar work was done for IAV, which has also been shown to prevent SG formation during the entirety of infection. Although IAV could prevent PKR mediated SG formation, it was remained sensitive to strong inducers of SG formation early during infection. When the drug Pateamine A was used to induce SG formation and translational arrest early during infection, viral RNA and protein levels were significantly reduced (Khaperskyy et al., 2014). While treating a systemic infection with therapeutics designed to induce SGs and shutdown protein translation seems risky, a number of promising chemotherapeutic agents have been shown to induce SGs with minimal toxicity suggesting that it may be possible (Anderson, Kedersha, & Ivanov, 2015). Furthermore, the widely used anti-inflammatory drug indomethacin induces PKR activation independently of dsRNA or IFN and was shown to inhibit VSV protein translation and replication without harming the cells (Amici et al.,

2015). Therefore, drugs like Pateamine A and indomethacin might prove beneficial as prophylactic or therapeutic intervention against EBOV infection.

A common thread between the two chapters of this dissertation is the interaction between EBOV and the RNA regulatory proteins TTP and HuR. We show that HuR was found sequestered within viral inclusions but showed a distinct aggregation pattern compared to the other SG proteins identified. Similarly, while many of the inclusion-bound aggregate proteins colocalized with viral RNA, HuR was instead found in clusters surrounding, or in very close proximity to viral RNA. TTP on the other hand, which we show was able to target and negative regulate the expression of EBOV NP, was excluded from viral inclusions. These data suggest that viral inclusions recruit host factors that are beneficial for viral replication and provide a protective environment for viral RNA. Furthermore, it is conceivable that cellular proteins that negatively impact viral replication are excluded from viral inclusions. Understanding the mechanisms underlying the specific recruitment of certain host factors over others may also help in the development of therapeutics that target viral inclusions, whose proper function is critical for viral replication and pathogenesis.

Future Directions

Our studies identified three critical observations of cellular events that take place during EBOV infection that open the door to important future studies. First, we showed that SG formation did not occur during infection, but that EBOV was unable to fully prevent the induction of SG formation when exogenous stress was applied. Therefore, it

would be interesting to characterize the effects of stress-induced translational repression on EBOV replication using drugs such as Ars or Hipp, which do not signal through PKR. Furthermore, the precise mechanism of VP35-mediated PKR antagonism, a function we propose is primarily responsible for the absence of SGs during infection, remains unclear. Therefore, future studies should focus on determining the precise mechanism of PKR inhibition. This would provide a potential point for chemotherapeutic or small molecule intervention.

The second important point brought up by this research is the interaction between a diverse panel of cellular SG proteins and EBOV components within viral inclusions. We showed that many SG proteins including eIF4G, eIF3 and PABP were sequestered within viral inclusions and colocalized with viral RNA species. These proteins did not seem to have a negative effect on viral protein translation. However future studies should be done to determine 1) how these proteins are getting into and are aggregating within viral inclusions and 2) if they serve to enhance viral replication. Live cell imaging studies might provide more insight into the dynamics and assembly of these inclusion bound aggregates. It would be interesting to determine more definitively if these aggregates are static complexes, or much like SGs themselves, are more fluid and involve the continuous recycling or shuttling of individual components. Furthermore, it would be valuable to identify if one or many of these proteins functions in a proviral capacity, perhaps by stabilizing viral RNA, or sequestering signaling molecules away from cytoplasmic signaling networks. Similarly, it would be interesting to examine whether all

infected cell types show sequestered proteins within viral inclusions, or if there are potential differences that may better inform us as to the function of these proteins.

Finally, we were able to show that EBOV mRNAs, and potentially genomic RNA, are prone to recognition by RNA regulatory proteins such as TTP. TTP is an important regulatory protein primarily in immune cells such macrophages and dendritic cells (Bros et al., 2010; Carrick & Blackshear, 2007). While we observed that TTP was able to target and negatively regulate the expression of NP and significantly decreased minigenome activity, it is unclear if this effect influences the outcome of viral replication. It would be interesting to determine if EBOV shows enhanced replication in cells deficient in TTP, or conversely if EBOV replication is restricted in cells with high levels of TTP. Although we were unable to determine if HuR was also able to target viral RNAs, we propose that its localization within viral inclusions is highly suggestive of a potential role during EBOV infection. Ablating HuR expression in cells is difficult due to the important role of HuR in cell survival. However, human HuR knockout cell lines were recently established using CRISP-Cas9 technology. These cell lines could be used as tools to determine if the expression of viral mRNAs is altered in the absence of HuR or if viral replication is reduced.

BIBLIOGRAPHY

Agnandji, S. T., Huttner, A., Zinser, M. E., Njuguna, P., Dahlke, C., Fernandes, J. F., et al. (2015). Phase 1 Trials of rVSV Ebola Vaccine in Africa and Europe — Preliminary Report. *The New England Journal of Medicine*, 150401140035006–14.

Akerlund, E., Prescott, J., & Tampellini, L. (2015). Shedding of Ebola Virus in an Asymptomatic Pregnant Woman. *The New England Journal of Medicine*, *372*, 2467–2469.

Albornoz, A., Carletti, T., Corazza, G., & Marcello, A. (2014). The stress granule component TIA-1 binds tick-borne encephalitis virus RNA and is recruited to perinuclear sites of viral replication to inhibit viral translation. *Journal of Virology*, *88*, 6611–6622.

Amici, C., La Frazia, S., Brunelli, C., Balsamo, M., Angelini, M., & Santoro, M. G. (2015). Inhibition of viral protein translation by indomethacin in vesicular stomatitis virus infection: role of eIF2α kinase PKR. *Cellular Microbiology*, *17*, 1391–1404.

Anderson, P. (2010). Post-transcriptional regulons coordinate the initiation and resolution of inflammation. *Nature Reviews. Immunology*, *10*, 24–35.

Anderson, P., & Kedersha, N. (2006). RNA granules. *The Journal of Cell Biology*, *172*, 803–808.

Anderson, P., & Kedersha, N. (2008). Stress granules: the Tao of RNA triage. *Trends in Biochemical Sciences*, *33*, 141–150.

Anderson, P., & Kedersha, N. (2009a). RNA granules: post-transcriptional and epigenetic modulators of gene expression. *Nature Reviews. Molecular Cell Biology*, *10*, 430–436.

Anderson, P., & Kedersha, N. (2009b). Stress granules. *Current Biology : CB*, *19*, R397–8.

Anderson, P., Kedersha, N., & Ivanov, P. (2015). Stress granules, P-bodies and cancer. *Biochimica Et Biophysica Acta*, *1849*, 861–870.

Antic, D., & Keene, J. D. (1997). Embryonic lethal abnormal visual RNA-binding proteins involved in growth, differentiation, and posttranscriptional gene expression. *American Journal of Human Genetics*, *61*, 273–278.

Audet, J., & Kobinger, G. P. (2015). Immune evasion in ebolavirus infections. *Viral Immunology*, *28*, 10–18.

Bah, E. I., Lamah, M.-C., Fletcher, T., Jacob, S. T., Brett-Major, D. M., Sall, A. A., et al.

(2015). Clinical presentation of patients with Ebola virus disease in Conakry, Guinea. *The New England Journal of Medicine*, *372*, 40–47.

Baize, S., Leroy, E. M., Georges, A. J., Georges-Courbot, M.-C., Capron, M., Bedjabaga, I., et al. (2002). Inflammatory responses in Ebola virus-infected patients. *Clinical and Experimental Immunology*, *128*, 163–168.

Baize, S., Leroy, E. M., Georges-Courbot, M.-C., Capron, M., Lansoud-Soukate, J., Debré, P., et al. (1999). Defective humoral responses and extensive intravascular apoptosis are associated with fatal outcome in Ebola virus-infected patients. *Nature Medicine*, *5*, 423–426.

Baize, S., Pannetier, D., Oestereich, L., Rieger, T., Koivogui, L., Magassouba, N., et al. (2014). Emergence of Zaire Ebola virus disease in Guinea. *The New England Journal of Medicine*, *371*, 1418–1425.

Bale, S., Julien, J.-P., Bornholdt, Z. A., Krois, A. S., Wilson, I. A., & Saphire, E. O. (2013). Ebolavirus VP35 coats the backbone of double-stranded RNA for interferon antagonism. *Journal of Virology*, *87*, 10385–10388.

Barreau, C., Paillard, L., & Osborne, H. B. (2005). AU-rich elements and associated factors: are there unifying principles? *Nucleic Acids Research*, *33*, 7138–7150.

Barrette, R. W., Metwally, S. A., Rowland, J. M., Xu, L., Zaki, S. R., Nichol, S. T., et al. (2009). Discovery of swine as a host for the Reston ebolavirus. *Science (New York, N.Y.)*, *325*, 204–206.

Bartoli, K. M., Bishop, D. L., & Saunders, W. S. (2011). The role of molecular microtubule motors and the microtubule cytoskeleton in stress granule dynamics. *International Journal of Cell Biology*, *2011*, 939848.

Basler, C. F. (2015). Innate immune evasion by filoviruses. *Virology*, *479-480*, 122–130.

Basler, C. F., Mikulasova, A., Martinez-Sobrido, L., Paragas, J., Mühlberger, E., Bray, M., et al. (2003). The Ebola virus VP35 protein inhibits activation of interferon regulatory factor 3. *Journal of Virology*, *77*, 7945–7956.

Basler, C. F., Wang, X., Mühlberger, E., Volchkov, V., Paragas, J., Klenk, H. D., et al. (2000). The Ebola virus VP35 protein functions as a type I IFN antagonist. *Proceedings of the National Academy of Sciences of the United States of America*, *97*, 12289–12294.

Becker, S., Rinne, C., Hofsäss, U., Klenk, H. D., & Mühlberger, E. (1998). Interactions of Marburg virus nucleocapsid proteins. *Virology*, *249*, 406–417.

Beisang, D., & Bohjanen, P. R. (2012). Perspectives on the ARE as it turns 25 years old. *Wiley Interdisciplinary Reviews. RNA*, *3*, 719–731.

Biedenkopf, N., Hartlieb, B., Hoenen, T., & Becker, S. (2013). Phosphorylation of Ebola virus VP30 influences the composition of the viral nucleocapsid complex: impact on viral transcription and replication. *The Journal of Biological Chemistry*, *288*, 11165–11174.

Bird, B. H., Spengler, J. R., Chakrabarti, A. K., Khristova, M. L., Sealy, T. K., Coleman-McCray, J. D., et al. (2015). Humanized Mouse Model of Ebola Virus Disease Mimics the Immune Responses in Human Disease. *The Journal of Infectious Diseases*, *213*, 703–711.

Boehmann, Y., Enterlein, S., Randolf, A., & Mühlberger, E. (2005). A reconstituted replication and transcription system for Ebola virus Reston and comparison with Ebola virus Zaire. *Virology*, *332*, 406–417.

Bordeleau, M.-E., Mori, A., Oberer, M., Lindqvist, L., Chard, L. S., Higa, T., et al. (2006). Functional characterization of IRESes by an inhibitor of the RNA helicase eIF4A. *Nature Chemical Biology*, *2*, 213–220.

Bosio, C. M., Aman, M. J., Grogan, C., Hogan, R., Ruthel, G., Negley, D., et al. (2003). Ebola and Marburg viruses replicate in monocyte-derived dendritic cells without inducing the production of cytokines and full maturation. *The Journal of Infectious Diseases*, *188*, 1630–1638.

Bowen, E. T., Lloyd, G., Harris, W. J., Platt, G. S., Baskerville, A., & Vella, E. E. (1977). Viral haemorrhagic fever in southern Sudan and northern Zaire. Preliminary studies on the aetiological agent. *Lancet (London, England)*, *1*, 571–573.

Bradfute, S. B., Swanson, P. E., Smith, M. A., Watanabe, E., McDunn, J. E., Hotchkiss, R. S., & Bavari, S. (2010). Mechanisms and consequences of ebolavirus-induced lymphocyte apoptosis. *Journal of Immunology (Baltimore, Md. : 1950)*, *184*, 327–335.

Brauburger, K., Boehmann, Y., Tsuda, Y., Hoenen, T., Olejnik, J., Schümann, M., et al. (2014). Analysis of the highly diverse gene borders in Ebola virus reveals a distinct mechanism of transcriptional regulation. *Journal of Virology*, *88*, 12558–12571.

Brennan, C. M., & Steitz, J. A. (2001). HuR and mRNA stability. *Cellular and Molecular Life Sciences : CMLS*, *58*, 266–277.

Brielle, S., Gura, R., & Kaganovich, D. (2015). Imaging stress. *Cell Stress & Chaperones*, *20*, 867–874.

Brooks, S. A., & Blackshear, P. J. (2013). Tristetraprolin (TTP): interactions with mRNA and proteins, and current thoughts on mechanisms of action. *Biochimica Et Biophysica Acta*, *1829*, 666–679.

Brooks, S. A., Connolly, J. E., & Rigby, W. F. C. (2004). The role of mRNA turnover in the regulation of tristetraprolin expression: evidence for an extracellular signal-regulated kinase-specific, AU-rich element-dependent, autoregulatory pathway. *Journal of Immunology (Baltimore, Md. : 1950)*, *172*, 7263–7271.

Bros, M., Wiechmann, N., Besche, V., Art, J., Pautz, A., Grabbe, S., et al. (2010). The RNA binding protein tristetraprolin influences the activation state of murine dendritic cells. *Molecular Immunology*, *47*, 1161–1170.

Brunner, J. E., Ertel, K. J., Rozovics, J. M., & Semler, B. L. (2010). Delayed kinetics of poliovirus RNA synthesis in a human cell line with reduced levels of hnRNP C proteins. *Virology*, *400*, 240–247.

Buchan, J. R., & Parker, R. (2009). Eukaryotic stress granules: the ins and outs of translation. *Molecular Cell*, *36*, 932–941.

Buchan, J. R., Yoon, J.-H., & Parker, R. (2011). Stress-specific composition, assembly and kinetics of stress granules in Saccharomyces cerevisiae. *Journal of Cell Science*, *124*, 228–239.

Calabretta, S., & Richard, S. (2015). Emerging Roles of Disordered Sequences in RNA-Binding Proteins. *Trends in Biochemical Sciences*, *40*, 662–672.

Carrick, D. M., & Blackshear, P. J. (2007). Comparative expression of tristetraprolin (TTP) family member transcripts in normal human tissues and cancer cell lines. *Archives of Biochemistry and Biophysics*, *462*, 278–285.

Cárdenas, W. B., Loo, Y.-M., Gale, M., Hartman, A. L., Kimberlin, C. R., Martinez-Sobrido, L., et al. (2006). Ebola virus VP35 protein binds double-stranded RNA and inhibits alpha/beta interferon production induced by RIG-I signaling. *Journal of Virology*, *80*, 5168–5178.

Centers for Disease Control and Prevention (CDC). (2016). Outbreaks Chronology: Ebola Virus Disease. Retrieved January 21, 2016, from http://www.cdc.gov/vhf/ebola/outbreaks/history/chronology.html

Charley, P. A., & Wilusz, J. (2014). Sponging of cellular proteins by viral RNAs. *Current Opinion in Virology*, *9*, 14–18.

Chen, C. Y., & Shyu, A. B. (1995). AU-rich elements: characterization and importance in mRNA degradation. *Trends in Biochemical Sciences*, *20*, 465–470.

Cherry, J., Karschner, V., Jones, H., & Pekala, P. H. (2006). HuR, an RNA-binding protein, involved in the control of cellular differentiation. *In Vivo (Athens, Greece)*, *20*, 17–23.

Commission, R. O. A. I. (1978). Ebola haemorrhagic fever in Zaire, 1976. *Bulletin of the World Health Organization*, *56*, 271–293.

Conzelmann, K. K. (1998). Nonsegmented negative-strand RNA viruses: genetics and manipulation of viral genomes. *Annual Review of Genetics*, *32*, 123–162.

Courtney, S. C., Scherbik, S. V., Stockman, B. M., & Brinton, M. A. (2012). West nile virus infections suppress early viral RNA synthesis and avoid inducing the cell stress granule response. *Journal of Virology*, *86*, 3647–3657.

Dechtawewat, T. (2015). Role of human heterogeneous nuclear ribonucleoprotein C1/C2 in dengue virus replication, 1–14.

Deen, G. F., Knust, B., Broutet, N., Sesay, F. R., Formenty, P., Ross, C., et al. (2015a). Ebola RNA Persistence in Semen of Ebola Virus Disease Survivors — Preliminary Report. *The New England Journal of Medicine*, 151014140118009–3.

Deen, J., Dondorp, A. M., & White, N. J. (2015b). Treatment of Ebola. *The New England Journal of Medicine*, *372*, 1673–1674.

Dickson, A. M., & Wilusz, J. (2011). Strategies for viral RNA stability: live long and prosper. *Trends in Genetics*, *27*, 286–293.

Dinh, P. X., Beura, L. K., Das, P. B., Panda, D., Das, A., & Pattnaik, A. K. (2013). Induction of stress granule-like structures in vesicular stomatitis virus-infected cells. *Journal of Virology*, *87*, 372–383.

Dolnik, O., Kolesnikova, L., Stevermann, L., & Becker, S. (2010). Tsg101 is recruited by a late domain of the nucleocapsid protein to support budding of Marburg virus-like particles. *Journal of Virology*, *84*, 7847–7856.

Dolnik, O., Kolesnikova, L., Welsch, S., Strecker, T., Schudt, G., & Becker, S. (2014). Interaction with Tsg101 is necessary for the efficient transport and release of nucleocapsids in marburg virus-infected cells. *PLoS Pathogens*, *10*, e1004463.

Dolnik, O., Stevermann, L., Kolesnikova, L., & Becker, S. (2015). Marburg virus inclusions: A virus-induced microcompartment and interface to multivesicular bodies

and the late endosomal compartment. *European Journal of Cell Biology*, *94*, 323–331.

Ebihara, H., Rockx, B., Marzi, A., Feldmann, F., Haddock, E., Brining, D., et al. (2011). Host response dynamics following lethal infection of rhesus macaques with Zaire ebolavirus. *The Journal of Infectious Diseases*, *204 Suppl 3*, S991–9.

Ebola-RD-QA-Updated-July-2015.pdf?ua=1. (n.d.). Ebola-RD-QA-Updated-July-2015.pdf?ua=1. Retrieved January 13, 2016, from http://www.who.int/medicines/Ebola-RD-QA-Updated-July-2015.pdf?ua=1

Editorial team. (2009, January 29). Ebola Reston virus detected pigs in the Philippines. *Euro Surveillance : Bulletin Européen Sur Les Maladies Transmissibles = European Communicable Disease Bulletin*.

Emara, M. M., & Brinton, M. A. (2007). Interaction of TIA-1/TIAR with West Nile and dengue virus products in infected cells interferes with stress granule formation and processing body assembly. *Proceedings of the National Academy of Sciences of the United States of America*, *104*, 9041–9046.

Emond, R. T., Evans, B., Bowen, E. T., & Lloyd, G. (1977). A case of Ebola virus infection. *Br Med J*, *2*, 541–544.

Ertel, K. J., Brunner, J. E., & Semler, B. L. (2010). Mechanistic Consequences of hnRNP C Binding to Both RNA Termini of Poliovirus Negative-Strand RNA Intermediates. *Journal of Virology*, *84*, 4229–4242.

Eulalio, A., Behm-Ansmant, I., & Izaurralde, E. (2007). P bodies: at the crossroads of post-transcriptional pathways. *Nature Reviews. Molecular Cell Biology*, *8*, 9–22.

Examination of the Retina. (2015). Examination of the Retina. *The New England Journal of Medicine*, *373*, 2483–2484.

Fabozzi, G., Nabel, C. S., Dolan, M. A., & Sullivan, N. J. (2011). Ebolavirus proteins suppress the effects of small interfering RNA by direct interaction with the mammalian RNA interference pathway. *Journal of Virology*, *85*, 2512–2523.

Feldmann, H. (2014). Ebola--a growing threat? *The New England Journal of Medicine*, *371*, 1375–1378.

Feldmann, H., & Geisbert, T. W. (2011). Ebola haemorrhagic fever. *Lancet (London, England)*, *377*, 849–862.

Feng, Z., Cerveny, M., Yan, Z., & He, B. (2007). The VP35 protein of Ebola virus

inhibits the antiviral effect mediated by double-stranded RNA-dependent protein kinase PKR. *Journal of Virology*, *81*, 182–192.

Fros, J. J., Domeradzka, N. E., Baggen, J., Geertsema, C., Flipse, J., Vlak, J. M., & Pijlman, G. P. (2012). Chikungunya virus nsP3 blocks stress granule assembly by recruitment of G3BP into cytoplasmic foci. *Journal of Virology*, *86*, 10873–10879.

Gallouzi, I. E., Brennan, C. M., Stenberg, M. G., Swanson, M. S., Eversole, A., Maizels, N., & Steitz, J. A. (2000). HuR binding to cytoplasmic mRNA is perturbed by heat shock. *Proceedings of the National Academy of Sciences of the United States of America*, *97*, 3073–3078.

Gao, G., Guo, X., & Goff, S. P. (2002). Inhibition of retroviral RNA production by ZAP, a CCCH-type zinc finger protein. *Science (New York, N.Y.)*, *297*, 1703–1706.

Garaigorta, U., & Chisari, F. V. (2009). Hepatitis C virus blocks interferon effector function by inducing protein kinase R phosphorylation. *Cell Host & Microbe*, *6*, 513–522.

Garaigorta, U., Heim, M. H., Boyd, B., Wieland, S., & Chisari, F. V. (2012). Hepatitis C virus (HCV) induces formation of stress granules whose proteins regulate HCV RNA replication and virus assembly and egress. *Journal of Virology*, *86*, 11043–11056.

García-Sastre, A. (2001). Inhibition of interferon-mediated antiviral responses by influenza A viruses and other negative-strand RNA viruses. *Virology*, *279*, 375–384.

Garneau, N. L., Wilusz, J., & Wilusz, C. J. (2007). The highways and byways of mRNA decay. *Nature Reviews. Molecular Cell Biology*, *8*, 113–126.

Geisbert, T. W., Hensley, L. E., Larsen, T., Young, H. A., Reed, D. S., Geisbert, J. B., et al. (2003a). Pathogenesis of Ebola hemorrhagic fever in cynomolgus macaques: evidence that dendritic cells are early and sustained targets of infection. *The American Journal of Pathology*, *163*, 2347–2370.

Geisbert, T. W., Jahrling, P. B., Hanes, M. A., & Zack, P. M. (1992). Association of Ebola-related Reston virus particles and antigen with tissue lesions of monkeys imported to the United States. *Journal of Comparative Pathology*, *106*, 137–152.

Geisbert, T. W., Young, H. A., Jahrling, P. B., Davis, K. J., Kagan, E., & Hensley, L. E. (2003b). Mechanisms underlying coagulation abnormalities in ebola hemorrhagic fever: overexpression of tissue factor in primate monocytes/macrophages is a key event. *The Journal of Infectious Diseases*, *188*, 1618–1629.

Ghosh, M., Aguila, H. L., Michaud, J., Ai, Y., Wu, M.-T., Hemmes, A., et al. (2009).

Essential role of the RNA-binding protein HuR in progenitor cell survival in mice. *Journal of Clinical Investigation*, *119*, 3530–3543.

Graf, M., Bojak, A., Deml, L., Bieler, K., Wolf, H., & Wagner, R. (2000). Concerted action of multiple cis-acting sequences is required for Rev dependence of late human immunodeficiency virus type 1 gene expression. *Journal of Virology*, *74*, 10822–10826.

Groseth, A., Charton, J. E., Sauerborn, M., Feldmann, F., Jones, S. M., Hoenen, T., & Feldmann, H. (2009). The Ebola virus ribonucleoprotein complex: a novel VP30-L interaction identified. *Virus Research*, *140*, 8–14.

Gui, H., Lu, C.-W., Adams, S., Stollar, V., & Li, M.-L. (2010). hnRNP A1 interacts with the genomic and subgenomic RNA promoters of Sindbis virus and is required for the synthesis of G and SG RNA. *Journal of Biomedical Science*, *17*, 59.

Guil, S., Long, J. C., & Cáceres, J. F. (2006). hnRNP A1 relocalization to the stress granules reflects a role in the stress response. *Molecular and Cellular Biology*, *26*, 5744–5758.

Gupta, M., Spiropoulou, C., & Rollin, P. E. (2007). Ebola virus infection of human PBMCs causes massive death of macrophages, CD4 and CD8 T cell sub-populations in vitro. *Virology*, *364*, 45–54.

Haasnoot, J., de Vries, W., Geutjes, E.-J., Prins, M., de Haan, P., & Berkhout, B. (2007). The Ebola virus VP35 protein is a suppressor of RNA silencing. *PLoS Pathogens*, *3*, e86.

Halees, A. S., El-Badrawi, R., & Khabar, K. S. A. (2008). ARED Organism: expansion of ARED reveals AU-rich element cluster variations between human and mouse. *Nucleic Acids Research*, *36*, D137–40.

Hardy, R. W., & Wertz, G. W. (2000). The Cys(3)-His(1) motif of the respiratory syncytial virus M2-1 protein is essential for protein function. *Journal of Virology*, *74*, 5880–5885.

Hartlieb, B., Modrof, J., Mühlberger, E., Klenk, H.-D., & Becker, S. (2003). Oligomerization of Ebola virus VP30 is essential for viral transcription and can be inhibited by a synthetic peptide. *The Journal of Biological Chemistry*, *278*, 41830–41836.

Hartman, A. L., Towner, J. S., & Nichol, S. T. (2004). A C-terminal basic amino acid motif of Zaire ebolavirus VP35 is essential for type I interferon antagonism and displays high identity with the RNA-binding domain of another interferon antagonist,

the NS1 protein of influenza A virus. *Virology*, *328*, 177–184.

Heeney, J. L. (2015). Ebola: Hidden reservoirs. *Nature*, *527*, 453–455.

Hinman, M. N., & Lou, H. (2008). Diverse molecular functions of Hu proteins. *Cellular and Molecular Life Sciences : CMLS*, *65*, 3168–3181.

Hoenen, T., & Feldmann, H. (2014). Ebolavirus in West Africa, and the use of experimental therapies or vaccines. *BMC Biology*, *12*, 80.

Hoenen, T., Groseth, A., & Feldmann, H. (2012a). Current ebola vaccines. *Expert Opinion on Biological Therapy*, *12*, 859–872.

Hoenen, T., Shabman, R. S., Groseth, A., Herwig, A., Weber, M., Schudt, G., et al. (2012b). Inclusion bodies are a site of ebolavirus replication. *Journal of Virology*, *86*, 11779–11788.

Huang, Y., Xu, L., Sun, Y., & Nabel, G. J. (2002). The assembly of Ebola virus nucleocapsid requires virion-associated proteins 35 and 24 and posttranslational modification of nucleoprotein. *Molecular Cell*, *10*, 307–316.

Huttner, A., Dayer, J. A., Yerly, S., Combescure, C., Auderset, F., Desmeules, J., et al. (2015). The effect of dose on the safety and immunogenicity of the VSV Ebola candidate vaccine: a randomised double-blind, placebo-controlled phase 1/2 trial. *The Lancet. Infectious Diseases*, *15*, 1156–1166.

Ilinykh, P. A., Tigabu, B., Ivanov, A., Ammosova, T., Obukhov, Y., Garron, T., et al. (2014). Role of protein phosphatase 1 in dephosphorylation of Ebola virus VP30 protein and its targeting for the inhibition of viral transcription. *The Journal of Biological Chemistry*, *289*, 22723–22738.

Ivanova, A. A., Velichko, A. K., Kantidze, O. L., & Razin, S. V. (2015). Heat stress induces formation of cytoplasmic granules containing HSC70 protein. *Doklady. Biochemistry and Biophysics*, *463*, 213–215.

Jain, B., Chaturvedi, U. C., & Jain, A. (2014). Role of intracellular events in the pathogenesis of dengue; an overview. *Microbial Pathogenesis*, *69-70*, 45–52.

Jeong, M. S., Kim, E. J., & Jang, S. B. (2010). Expression and RNA-binding of human zinc-finger antiviral protein. *Biochemical and Biophysical Research Communications*, *396*, 696–702.

John, S. P., Wang, T., Steffen, S., Longhi, S., Schmaljohn, C. S., & Jonsson, C. B. (2007). Ebola virus VP30 is an RNA binding protein. *Journal of Virology*, *81*, 8967–

8976.

Jones, K. E., Patel, N. G., Levy, M. A., Storeygard, A., Balk, D., Gittleman, J. L., & Daszak, P. (2008). Global trends in emerging infectious diseases. *Nature*, *451*, 990–993.

Kafasla, P., Skliris, A., & Kontoyiannis, D. L. (2014). Post-transcriptional coordination of immunological responses by RNA-binding proteins. *Nature Immunology*, *15*, 492–502.

Kedersha, N., & Anderson, P. (2002). Stress granules: sites of mRNA triage that regulate mRNA stability and translatability. *Biochemical Society Transactions*, *30*, 963–969.

Kedersha, N., & Anderson, P. (2009). Regulation of translation by stress granules and processing bodies. *Progress in Molecular Biology and Translational Science*, *90*, 155–185.

Kedersha, N., Cho, M. R., Li, W., Yacono, P. W., Chen, S., Gilks, N., et al. (2000). Dynamic shuttling of TIA-1 accompanies the recruitment of mRNA to mammalian stress granules. *The Journal of Cell Biology*, *151*, 1257–1268.

Kedersha, N., Ivanov, P., & Anderson, P. (2013). Stress granules and cell signaling: more than just a passing phase? *Trends in Biochemical Sciences*, *38*, 494–506.

Kedersha, N., Stoecklin, G., Ayodele, M., Yacono, P., Lykke-Andersen, J., Fritzler, M. J., et al. (2005). Stress granules and processing bodies are dynamically linked sites of mRNP remodeling. *The Journal of Cell Biology*, *169*, 871–884.

Kelly, J. D., Richardson, E. T., & Barry, M. (2015). Persistent Ebola Virus in the Eye. *The New England Journal of Medicine*, *373*, 1981–1982.

Khaperskyy, D. A., Emara, M. M., Johnston, B. P., Anderson, P., Hatchette, T. F., & McCormick, C. (2014). Influenza a virus host shutoff disables antiviral stress-induced translation arrest. *PLoS Pathogens*, *10*, e1004217.

Khaperskyy, D. A., Hatchette, T. F., & McCormick, C. (2012). Influenza A virus inhibits cytoplasmic stress granule formation. *FASEB Journal : Official Publication of the Federation of American Societies for Experimental Biology*, *26*, 1629–1639.

Kimberlin, C. R., Bornholdt, Z. A., Li, S., Woods, V. L., MacRae, I. J., & Saphire, E. O. (2010). Ebolavirus VP35 uses a bimodal strategy to bind dsRNA for innate immune suppression. *Proceedings of the National Academy of Sciences of the United States of America*, *107*, 314–319.

Kirchdoerfer, R. N., Abelson, D. M., Li, S., Wood, M. R., & Saphire, E. O. (2015).

Assembly of the Ebola Virus Nucleoprotein from a Chaperoned VP35 Complex. *Cell Reports*, *12*, 140–149.

Kissling, R. E., Robinson, R. Q., Murphy, F. A., & Whitfield, S. G. (1968). Agent of disease contracted from green monkeys. *Science (New York, N.Y.)*, *160*, 888–890.

Kraft, C. S., Hewlett, A. L., Koepsell, S., Winkler, A. M., Kratochvil, C. J., Larson, L., et al. (2015). The Use of TKM-100802 and Convalescent Plasma in 2 Patients With Ebola Virus Disease in the United States. *Clinical Infectious Diseases : an Official Publication of the Infectious Diseases Society of America*, *61*, 496–502.

Krug, R. M., Yuan, W., Noah, D. L., & Latham, A. G. (2003). Intracellular warfare between human influenza viruses and human cells: the roles of the viral NS1 protein. *Virology*, *309*, 181–189.

Kuhn, J. H. (2008). Filoviruses. A compendium of 40 years of epidemiological, clinical, and laboratory studies. *Archives of Virology. Supplementum*, *20*, 13–360.

Kuhn, J. H., Andersen, K. G., Baize, S., Bào, Y., Bavari, S., Berthet, N., et al. (2014a). Nomenclature- and database-compatible names for the two Ebola virus variants that emerged in Guinea and the Democratic Republic of the Congo in 2014. *Viruses*, *6*, 4760–4799.

Kuhn, J. H., Bào, Y., Bavari, S., Becker, S., Bradfute, S., Brauburger, K., et al. (2014b). Virus nomenclature below the species level: a standardized nomenclature for filovirus strains and variants rescued from cDNA. *Archives of Virology*, *159*, 1229–1237.

Lai, W. S., Carballo, E., Thorn, J. M., Kennington, E. A., & Blackshear, P. J. (2000). Interactions of CCCH zinc finger proteins with mRNA. Binding of tristetraprolin-related zinc finger proteins to Au-rich elements and destabilization of mRNA. *The Journal of Biological Chemistry*, *275*, 17827–17837.

Lai, W. S., Kennington, E. A., & Blackshear, P. J. (2002). Interactions of CCCH zinc finger proteins with mRNA: non-binding tristetraprolin mutants exert an inhibitory effect on degradation of AU-rich element-containing mRNAs. *The Journal of Biological Chemistry*, *277*, 9606–9613.

Lal, A., Kawai, T., Yang, X., Mazan-Mamczarz, K., & Gorospe, M. (2005). Antiapoptotic function of RNA-binding protein HuR effected through prothymosin alpha. *The EMBO Journal*, *24*, 1852–1862.

Lal, A., Mazan-Mamczarz, K., Kawai, T., Yang, X., Martindale, J. L., & Gorospe, M. (2004). Concurrent versus individual binding of HuR and AUF1 to common labile

target mRNAs. *The EMBO Journal*, *23*, 3092–3102.

Lawrence, T. (2009). The nuclear factor NF-kappaB pathway in inflammation. *Cold Spring Harbor Perspectives in Biology*, *1*, a001651–a001651.

Le Guenno, B., Formenty, P., & Boesch, C. (1999). Ebola virus outbreaks in the Ivory Coast and Liberia, 1994-1995. *Current Topics in Microbiology and Immunology*, *235*, 77–84.

Le Guenno, B., Formenty, P., Formentry, P., Wyers, M., Gounon, P., Walker, F., & Boesch, C. (1995). Isolation and partial characterisation of a new strain of Ebola virus. *Lancet (London, England)*, *345*, 1271–1274.

Lebedeva, S., Jens, M., Theil, K., Schwanhäusser, B., Selbach, M., Landthaler, M., & Rajewsky, N. (2011). Transcriptome-wide analysis of regulatory interactions of the RNA-binding protein HuR. *Molecular Cell*, *43*, 340–352.

Leroy, E. M., Epelboin, A., Mondonge, V., Pourrut, X., Gonzalez, J.-P., Muyembe-Tamfum, J.-J., & Formenty, P. (2009). Human Ebola outbreak resulting from direct exposure to fruit bats in Luebo, Democratic Republic of Congo, 2007. *Vector Borne and Zoonotic Diseases (Larchmont, N.Y.)*, *9*, 723–728.

Leroy, E. M., Kumulungui, B., Pourrut, X., Rouquet, P., Hassanin, A., Yaba, P., et al. (2005). Fruit bats as reservoirs of Ebola virus. *Nature*, *438*, 575–576.

Leung, D. W., Borek, D., Luthra, P., Binning, J. M., Anantpadma, M., Liu, G., et al. (2015). An Intrinsically Disordered Peptide from Ebola Virus VP35 Controls Viral RNA Synthesis by Modulating Nucleoprotein-RNA Interactions. *Cell Reports*, *11*, 376–389.

Leung, D. W., Ginder, N. D., Fulton, D. B., Nix, J., Basler, C. F., Honzatko, R. B., & Amarasinghe, G. K. (2009). Structure of the Ebola VP35 interferon inhibitory domain. *Proceedings of the National Academy of Sciences of the United States of America*, *106*, 411–416.

Leung, D. W., Prins, K. C., Basler, C. F., & Amarasinghe, G. K. (2010). Ebolavirus VP35 is a multifunctional virulence factor. *Virulence*, *1*, 526–531.

Li, Shoudong, Min, J.-Y., Krug, R. M., & Sen, G. C. (2006). Binding of the influenza A virus NS1 protein to PKR mediates the inhibition of its activation by either PACT or double-stranded RNA. *Virology*, *349*, 13–21.

Li, W, Li, Y., Kedersha, N., Anderson, P., Emara, M., Swiderek, K. M., et al. (2002). Cell proteins TIA-1 and TIAR interact with the 3' stem-loop of the West Nile virus

complementary minus-strand RNA and facilitate virus replication. *Journal of Virology*, *76*, 11989–12000.

Lifland, A. W., Jung, J., Alonas, E., Zurla, C., Crowe, J. E., & Santangelo, P. J. (2012). Human respiratory syncytial virus nucleoprotein and inclusion bodies antagonize the innate immune response mediated by MDA5 and MAVS. *Journal of Virology*, *86*, 8245–8258.

Lindquist, M. E., Lifland, A. W., Utley, T. J., Santangelo, P. J., & Crowe, J. E. (2010). Respiratory syncytial virus induces host RNA stress granules to facilitate viral replication. *Journal of Virology*, *84*, 12274–12284.

Linero, F. N., Thomas, M. G., Boccaccio, G. L., & Scolaro, L. A. (2011). Junin virus infection impairs stress-granule formation in Vero cells treated with arsenite via inhibition of eIF2α phosphorylation. *The Journal of General Virology*, *92*, 2889–2899.

Loschi, M., Leishman, C. C., Berardone, N., & Boccaccio, G. L. (2009). Dynein and kinesin regulate stress-granule and P-body dynamics. *Journal of Cell Science*, *122*, 3973–3982.

Lu, L., Han, A. P., & Chen, J. J. (2001). Translation initiation control by heme-regulated eukaryotic initiation factor 2alpha kinase in erythroid cells under cytoplasmic stresses. *Molecular and Cellular Biology*, *21*, 7971–7980.

Lubaki, N. M., Ilinykh, P., Pietzsch, C., Tigabu, B., Freiberg, A. N., Koup, R. A., & Bukreyev, A. (2013). The lack of maturation of Ebola virus-infected dendritic cells results from the cooperative effect of at least two viral domains. *Journal of Virology*, *87*, 7471–7485.

Luthra, P., Jordan, D. S., Leung, D. W., Amarasinghe, G. K., & Basler, C. F. (2015). Ebola virus VP35 interaction with dynein LC8 regulates viral RNA synthesis. *Journal of Virology*, *89*, 5148–5153.

Luthra, P., Ramanan, P., Mire, C. E., Weisend, C., Tsuda, Y., Yen, B., et al. (2013). Mutual antagonism between the Ebola virus VP35 protein and the RIG-I activator PACT determines infection outcome. *Cell Host & Microbe*, *14*, 74–84.

Lyon, G. M., Mehta, A. K., Varkey, J. B., Brantly, K., Plyler, L., McElroy, A. K., et al. (2014). Clinical Care of Two Patients with Ebola Virus Disease in the United States. *The New England Journal of Medicine*, *371*, 2402–2409.

Maeda, M., Sawa, H., Tobiume, M., Tokunaga, K., Hasegawa, H., Ichinohe, T., et al. (2006). Tristetraprolin inhibits HIV-1 production by binding to genomic RNA.

Microbes and Infection / Institut Pasteur, *8*, 2647–2656.

Mahanty, S., Hutchinson, K., Agarwal, S., McRae, M., Rollin, P. E., & Pulendran, B. (2003). Cutting edge: impairment of dendritic cells and adaptive immunity by Ebola and Lassa viruses. *Journal of Immunology (Baltimore, Md. : 1950)*, *170*, 2797–2801.

Mahtani, K. R., Brook, M., Dean, J. L., Sully, G., Saklatvala, J., & Clark, A. R. (2001). Mitogen-activated protein kinase p38 controls the expression and posttranslational modification of tristetraprolin, a regulator of tumor necrosis factor alpha mRNA stability. *Molecular and Cellular Biology*, *21*, 6461–6469.

Martinez, M. J., Biedenkopf, N., Volchkova, V., Hartlieb, B., Alazard-Dany, N., Reynard, O., et al. (2008). Role of Ebola virus VP30 in transcription reinitiation. *Journal of Virology*, *82*, 12569–12573.

Martinez, M. J., Volchkova, V. A., Raoul, H., Alazard-Dany, N., Reynard, O., & Volchkov, V. E. (2011). Role of VP30 phosphorylation in the Ebola virus replication cycle. *The Journal of Infectious Diseases*, *204 Suppl 3*, S934–40.

Marzi, A., & Feldmann, H. (2014). Ebola virus vaccines: an overview of current approaches. *Expert Review of Vaccines*, *13*, 521–531.

Marzi, A., Robertson, S. J., Haddock, E., Feldmann, F., Hanley, P. W., Scott, D. P., et al. (2015). EBOLA VACCINE. VSV-EBOV rapidly protects macaques against infection with the 2014/15 Ebola virus outbreak strain. *Science (New York, N.Y.)*, *349*, 739–742.

Marzi, A., Yoshida, R., Miyamoto, H., Ishijima, M., Suzuki, Y., Higuchi, M., et al. (2012). Protective efficacy of neutralizing monoclonal antibodies in a nonhuman primate model of Ebola hemorrhagic fever. *PloS One*, *7*, e36192.

Masuda, K., Abdelmohsen, K., & Gorospe, M. (2009). RNA-binding proteins implicated in the hypoxic response. *Journal of Cellular and Molecular Medicine*, *13*, 2759–2769.

Mate, S. E., Kugelman, J. R., Nyenswah, T. G., Ladner, J. T., Wiley, M. R., Cordier-Lassalle, T., et al. (2015). Molecular Evidence of Sexual Transmission of Ebola Virus. *The New England Journal of Medicine*, *373*, 2448–2454.

Mateo, M., Reid, S. P., Leung, L. W., Basler, C. F., & Volchkov, V. E. (2010). Ebolavirus VP24 binding to karyopherins is required for inhibition of interferon signaling. *Journal of Virology*, *84*, 1169–1175.

Matthews, J. D., & Frey, T. K. (2012). Analysis of subcellular G3BP redistribution

during rubella virus infection. *The Journal of General Virology*, *93*, 267–274.

Mattia, J. G., Vandy, M. J., Chang, J. C., Platt, D. E., Dierberg, K., Bausch, D. G., et al. (2015). Early clinical sequelae of Ebola virus disease in Sierra Leone: a cross-sectional study. *The Lancet. Infectious Diseases*. doi:10.1016/S1473-3099(15)00489-2

Mazroui, R., Sukarieh, R., Bordeleau, M.-E., Kaufman, R. J., Northcote, P., Tanaka, J., et al. (2006). Inhibition of ribosome recruitment induces stress granule formation independently of eukaryotic initiation factor 2alpha phosphorylation. *Molecular Biology of the Cell*, *17*, 4212–4219.

McInerney, G. M., Kedersha, N. L., Kaufman, R. J., Anderson, P., & Liljeström, P. (2005). Importance of eIF2alpha phosphorylation and stress granule assembly in alphavirus translation regulation. *Molecular Biology of the Cell*, *16*, 3753–3763.

MD, M. D. T., MD, P. S. O. S., MD, K. E. L., MD, F. C. H., MD, F. D., MD, M. D., et al. (2015a). Articles Use of ChAd3-EBO-Z Ebola virus vaccine in Malian and US adults, and boosting of Malian adults with MVA-BN-Filo: a phase 1, single-blind, randomised trial, a phase 1b, open-label and double-blind, dose-escalation trial, and a nested, randomised, double-blind, placebo-controlled trial. *The Lancet. Infectious Diseases*, *16*, 31–42.

MD, T. W., Kann, G., MD, P. S. B., MD, C. S., MD, H.-R. B., de Leuw MD, P., et al. (2015b). Severe Ebola virus disease with vascular leakage and multiorgan failure: treatment of a patient in intensive care. *Lancet (London, England)*, *385*, 1428–1435.

Mehta, A. K., Lyon, G. M., & Varkey, J. B. (2015). Treatment of Ebola. *The New England Journal of Medicine*, *372*, 1674–1674.

Messaoudi, I., Amarasinghe, G. K., & Basler, C. F. (2015). Filovirus pathogenesis and immune evasion: insights from Ebola virus and Marburg virus. *Nature Reviews. Microbiology*, *13*, 663–676.

Miranda, M. E. G., & Miranda, N. L. J. (2011). Reston ebolavirus in humans and animals in the Philippines: a review. *The Journal of Infectious Diseases*, *204 Suppl 3*, S757–60.

Modrof, J., Becker, S., & Mühlberger, E. (2003). Ebola virus transcription activator VP30 is a zinc-binding protein. *Journal of Virology*, *77*, 3334–3338.

Modrof, J., Mühlberger, E., Klenk, H.-D., & Becker, S. (2002). Phosphorylation of VP30 impairs ebola virus transcription. *The Journal of Biological Chemistry*, *277*, 33099–33104.

Mohamadzadeh, M., Chen, L., Olinger, G. G., Pratt, W. D., & Schmaljohn, A. L. (2006). Filoviruses and the balance of innate, adaptive, and inflammatory responses. *Viral Immunology*, *19*, 602–612.

Mok, B. W.-Y., Song, W., Wang, P., Tai, H., Chen, Y., Zheng, M., et al. (2012). The NS1 protein of influenza A virus interacts with cellular processing bodies and stress granules through RNA-associated protein 55 (RAP55) during virus infection. *Journal of Virology*, *86*, 12695–12707.

Mollet, S., Cougot, N., Wilczynska, A., Dautry, F., Kress, M., Bertrand, E., & Weil, D. (2008). Translationally repressed mRNA transiently cycles through stress granules during stress. *Molecular Biology of the Cell*, *19*, 4469–4479.

Molliex, A., Temirov, J., Lee, J., Coughlin, M., Kanagaraj, A. P., Kim, H. J., et al. (2015). Phase Separation by Low Complexity Domains Promotes Stress Granule Assembly and Drives Pathological Fibrillization. *Cell*, *163*, 123–133.

Montero, H., & Trujillo-Alonso, V. (2011). Stress granules in the viral replication cycle. *Viruses*, *3*, 2328–2338.

Mühlberger, E. (2007). Filovirus replication and transcription. *Future Virology*, *2*, 205–215.

Mühlberger, E., Weik, M., Volchkov, V. E., Klenk, H. D., & Becker, S. (1999). Comparison of the transcription and replication strategies of marburg virus and Ebola virus by using artificial replication systems. *Journal of Virology*, *73*, 2333–2342.

Müller, S., Möller, P., Bick, M. J., Wurr, S., Becker, S., Günther, S., & Kümmerer, B. M. (2007). Inhibition of filovirus replication by the zinc finger antiviral protein. *Journal of Virology*, *81*, 2391–2400.

Nadar, M., Chan, M.-Y., Huang, S.-W., Huang, C.-C., Tseng, J. T., & Tsai, C.-H. (2011). HuR binding to AU-rich elements present in the 3' untranslated region of Classical swine fever virus. *Virology Journal*, *8*, 340.

Nadezhdina, E. S., Lomakin, A. J., Shpilman, A. A., Chudinova, E. M., & Ivanov, P. A. (2010). Microtubules govern stress granule mobility and dynamics. *Biochimica Et Biophysica Acta*, *1803*, 361–371.

Nanbo, A., Watanabe, S., Halfmann, P., & Kawaoka, Y. (2013a). The spatio-temporal distribution dynamics of Ebola virus proteins and RNA in infected cells. *Scientific Reports*, *3*. doi:10.1038/srep01206

Nanbo, A., Watanabe, S., Halfmann, P., & Kawaoka, Y. (2013b). The spatio-temporal distribution dynamics of Ebola virus proteins and RNA in infected cells. *Scientific Reports*, *3*, 1206.

Negredo, A., Palacios, G., Vázquez-Morón, S., González, F., Dopazo, H., Molero, F., et al. (2011). Discovery of an Ebolavirus-Like Filovirus in Europe. *PLoS Pathogens*, *7*, e1002304–8.

Neumann, G., Watanabe, S., & Kawaoka, Y. (2009). Characterization of Ebolavirus regulatory genomic regions. *Virus Research*, *144*, 1–7.

NIAID. (2015, February 25). NIAID Emerging Infectious Diseases/Pathogens. Retrieved January 21, 2016, from https://www.niaid.nih.gov/topics/biodefenserelated/biodefense/pages/cata.aspx

Noda, T., Aoyama, K., Sagara, H., Kida, H., & Kawaoka, Y. (2005). Nucleocapsid-like structures of Ebola virus reconstructed using electron tomography. *The Journal of Veterinary Medical Science / the Japanese Society of Veterinary Science*, *67*, 325–328.

Noda, T., Ebihara, H., Muramoto, Y., Fujii, K., Takada, A., Sagara, H., et al. (2006). Assembly and budding of Ebolavirus. *PLoS Pathogens*, *2*, e99.

Noda, T., Hagiwara, K., Sagara, H., & Kawaoka, Y. (2010). Characterization of the Ebola virus nucleoprotein-RNA complex. *The Journal of General Virology*, *91*, 1478–1483.

Noda, T., Kolesnikova, L., Becker, S., & Kawaoka, Y. (2011). The importance of the NP: VP35 ratio in Ebola virus nucleocapsid formation. *The Journal of Infectious Diseases*, *204 Suppl 3*, S878–83.

Olejnik, J., Alonso, J., Schmidt, K. M., Yan, Z., Wang, W., Marzi, A., et al. (2013). Ebola virus does not block apoptotic signaling pathways. *Journal of Virology*, *87*, 5384–5396.

Onomoto, K., Jogi, M., Yoo, J.-S., Narita, R., Morimoto, S., Takemura, A., et al. (2012). Critical role of an antiviral stress granule containing RIG-I and PKR in viral detection and innate immunity. *PloS One*, *7*, e43031.

Onomoto, K., Yoneyama, M., Fung, G., Kato, H., & Fujita, T. (2014). Antiviral innate immunity and stress granule responses. *Trends in Immunology*, *35*, 420–428.

Palanisamy, V., Jakymiw, A., Van Tubergen, E. A., D'Silva, N. J., & Kirkwood, K. L. (2012). Control of Cytokine mRNA Expression by RNA-binding Proteins and

microRNAs. *Journal of Dental Research*, *91*, 651–658.

Panas, M. D., Kedersha, N., & McInerney, G. M. (2015a). Methods for the characterization of stress granules in virus infected cells. *Methods (San Diego, Calif.)*. doi:10.1016/j.ymeth.2015.04.009

Panas, M. D., Schulte, T., Thaa, B., Sandalova, T., Kedersha, N., Achour, A., & McInerney, G. M. (2015b). Viral and cellular proteins containing FGDF motifs bind G3BP to block stress granule formation. *PLoS Pathogens*, *11*, e1004659.

Panas, M. D., Varjak, M., Lulla, A., Eng, K. E., Merits, A., Karlsson Hedestam, G. B., & McInerney, G. M. (2012). Sequestration of G3BP coupled with efficient translation inhibits stress granules in Semliki Forest virus infection. *Molecular Biology of the Cell*, *23*, 4701–4712.

Panchal, R. G., Mourich, D. V., Bradfute, S., Hauck, L. L., Warfield, K. L., Iversen, P. L., & Bavari, S. (2014). Induced IL-10 splice altering approach to antiviral drug discovery. *Nucleic Acid Therapeutics*, *24*, 179–185.

Prins, K. C., Binning, J. M., Shabman, R. S., Leung, D. W., Amarasinghe, G. K., & Basler, C. F. (2010). Basic residues within the ebolavirus VP35 protein are required for its viral polymerase cofactor function. *Journal of Virology*, *84*, 10581–10591.

Prins, K. C., Cárdenas, W. B., & Basler, C. F. (2009). Ebola virus protein VP35 impairs the function of interferon regulatory factor-activating kinases IKKepsilon and TBK-1. *Journal of Virology*, *83*, 3069–3077.

ProMED-mail post. (2016). ProMED-mail post, 1–2.

Qiu, X., Audet, J., Wong, G., Fernando, L., Bello, A., Pillet, S., et al. (2013). Sustained protection against Ebola virus infection following treatment of infected nonhuman primates with ZMAb. *Scientific Reports*, *3*, 3365.

Rahmeh, A. A., Morin, B., Schenk, A. D., Liang, B., Heinrich, B. S., Brusic, V., et al. (2012). Critical phosphoprotein elements that regulate polymerase architecture and function in vesicular stomatitis virus. *Proceedings of the National Academy of Sciences of the United States of America*, *109*, 14628–14633.

Reed, D. S., Hensley, L. E., Geisbert, J. B., Jahrling, P. B., & Geisbert, T. W. (2004). Depletion of peripheral blood T lymphocytes and NK cells during the course of ebola hemorrhagic Fever in cynomolgus macaques. *Viral Immunology*, *17*, 390–400.

Reid, S. P., Leung, L. W., Hartman, A. L., Martinez, O., Shaw, M. L., Carbonnelle, C., et al. (2006). Ebola virus VP24 binds karyopherin alpha1 and blocks STAT1 nuclear

accumulation. *Journal of Virology*, *80*, 5156–5167.

Rollin, P. E., Williams, R. J., Bressler, D. S., Pearson, S., Cottingham, M., Pucak, G., et al. (1999). Ebola (subtype Reston) virus among quarantined nonhuman primates recently imported from the Philippines to the United States. *The Journal of Infectious Diseases*, *179 Suppl 1*, S108–14.

Roretz, von, C., Marco, S. D., Mazroui, R., & Gallouzi, I.-E. (2010). Turnover of AU-rich-containing mRNAs during stress: a matter of survival. *Wiley Interdisciplinary Reviews. RNA*, *2*, 336–347.

Rozelle, D. K., Filone, C. M., Kedersha, N., & Connor, J. H. (2014). Activation of stress response pathways promotes formation of antiviral granules and restricts virus replication. *Molecular and Cellular Biology*, *34*, 2003–2016.

rpt4. (2008). Managing Potential Laboratory Exposure to Ebola Virus by Using a Patient Biocontainment Care Unit, 1–7.

Ryabchikova, E. I., & Price, B. (2004). Ebola and Marburg viruses: a view of infection using electron microscopy. *Emerging Infectious Diseases* (Vol. 10, pp. 1517–1517).

Ryabchikova, E., Kolesnikova, L., Smolina, M., Tkachev, V., Pereboeva, L., Baranova, S., et al. (1996). Ebola virus infection in guinea pigs: presumable role of granulomatous inflammation in pathogenesis. *Archives of Virology*, *141*, 909–921.

Sanduja, S., Blanco, F. F., & Dixon, D. A. (2011). The roles of TTP and BRF proteins in regulated mRNA decay. *Wiley Interdisciplinary Reviews. RNA*, *2*, 42–57.

Savinova, O., & Jagus, R. (1997). Use of vertical slab isoelectric focusing and immunoblotting to evaluate steady-state phosphorylation of eIF2 alpha in cultured cells. *Methods (San Diego, Calif.)*, *11*, 419–425.

Scholte, F. E. M., Tas, A., Albulescu, I. C., Žusinaite, E., Merits, A., Snijder, E. J., & van Hemert, M. J. (2015). Stress granule components G3BP1 and G3BP2 play a proviral role early in Chikungunya virus replication. *Journal of Virology*, *89*, 4457–4469.

Schudt, G., Dolnik, O., Kolesnikova, L., Biedenkopf, N., Herwig, A., & Becker, S. (2015). Transport of Ebolavirus Nucleocapsids Is Dependent on Actin Polymerization: Live-Cell Imaging Analysis of Ebolavirus-Infected Cells. *The Journal of Infectious Diseases*, *212 Suppl 2*, S160–6.

Schümann, M., Gantke, T., & Mühlberger, E. (2009). Ebola virus VP35 antagonizes PKR activity through its C-terminal interferon inhibitory domain. *Journal of Virology*, *83*, 8993–8997.

Shabman, R. S., Hoenen, T., Groseth, A., Jabado, O., Binning, J. M., Amarasinghe, G. K., et al. (2013). An upstream open reading frame modulates ebola virus polymerase translation and virus replication. *PLoS Pathogens*, *9*, e1003147.

Shabman, R. S., Jabado, O. J., Mire, C. E., Stockwell, T. B., Edwards, M., Mahajan, M., et al. (2014). Deep sequencing identifies noncanonical editing of Ebola and Marburg virus RNAs in infected cells. *mBio*, *5*, e02011.

Shabman, R. S., Leung, D. W., Johnson, J., Glennon, N., Gulcicek, E. E., Stone, K. L., et al. (2011). DRBP76 associates with Ebola virus VP35 and suppresses viral polymerase function. *The Journal of Infectious Diseases*, *204 Suppl 3*, S911–8.

Shaw, G., & Kamen, R. (1986). A conserved AU sequence from the 3' untranslated region of GM-CSF mRNA mediates selective mRNA degradation. *Cell*, *46*, 659–667.

Shi, W., Huang, Y., Sutton-Smith, M., Tissot, B., Panico, M., Morris, H. R., et al. (2008). A Filovirus-Unique Region of Ebola Virus Nucleoprotein Confers Aberrant Migration and Mediates Its Incorporation into Virions. *Journal of Virology*, *82*, 6190–6199.

Simone, L. E., & Keene, J. D. (2013). Mechanisms coordinating ELAV/Hu mRNA regulons. *Current Opinion in Genetics & Development*, *23*, 35–43.

Simpson-Holley, M., Kedersha, N., Dower, K., Rubins, K. H., Anderson, P., Hensley, L. E., & Connor, J. H. (2011). Formation of antiviral cytoplasmic granules during orthopoxvirus infection. *Journal of Virology*, *85*, 1581–1593.

Slenczka, W., & Klenk, H.-D. (2007). Forty years of marburg virus. *The Journal of Infectious Diseases*, *196 Suppl 2*, S131–5.

Sokoloski, K. J., Dickson, A. M., Chaskey, E. L., Garneau, N. L., Wilusz, C. J., & Wilusz, J. (2010). Sindbis virus usurps the cellular HuR protein to stabilize its transcripts and promote productive infections in mammalian and mosquito cells. *Cell Host & Microbe*, *8*, 196–207.

Souquere, S., Mollet, S., Kress, M., Dautry, F., Pierron, G., & Weil, D. (2009). Unravelling the ultrastructure of stress granules and associated P-bodies in human cells. *Journal of Cell Science*, *122*, 3619–3626.

Spurgers, K. B., Alefantis, T., Peyser, B. D., Ruthel, G. T., Bergeron, A. A., Costantino, J. A., et al. (2010). Identification of essential filovirion-associated host factors by serial proteomic analysis and RNAi screen. *Molecular & Cellular Proteomics : MCP*, *9*, 2690–2703.

Stanley, D. A., Honko, A. N., Asiedu, C., Trefry, J. C., Lau-Kilby, A. W., Johnson, J. C., et al. (2014). Chimpanzee adenovirus vaccine generates acute and durable protective immunity against ebolavirus challenge. *Nature Medicine*, *20*, 1126–1129.

Stoecklin, G., Stubbs, T., Kedersha, N., Wax, S., Rigby, W. F. C., Blackwell, T. K., & Anderson, P. (2004). MK2-induced tristetraprolin:14-3-3 complexes prevent stress granule association and ARE-mRNA decay. *The EMBO Journal*, *23*, 1313–1324.

Sun, L., Stoecklin, G., Van Way, S., Hinkovska-Galcheva, V., Guo, R.-F., Anderson, P., & Shanley, T. P. (2007). Tristetraprolin (TTP)-14-3-3 complex formation protects TTP from dephosphorylation by protein phosphatase 2a and stabilizes tumor necrosis factor-alpha mRNA. *The Journal of Biological Chemistry*, *282*, 3766–3777.

Tang, R. S., Nguyen, N., Cheng, X., & Jin, H. (2001). Requirement of cysteines and length of the human respiratory syncytial virus M2-1 protein for protein function and virus viability. *Journal of Virology*, *75*, 11328–11335.

Taylor, G. A., Carballo, E., Lee, D. M., Lai, W. S., Thompson, M. J., Patel, D. D., et al. (1996). A pathogenetic role for TNF alpha in the syndrome of cachexia, arthritis, and autoimmunity resulting from tristetraprolin (TTP) deficiency. *Immunity*, *4*, 445–454.

Team, R. O. A. W. I. S. (1978). Ebola haemorrhagic fever in Sudan, 1976. Report of a WHO/International Study Team. *Bulletin of the World Health Organization*, *56*, 247–270.

Teixeira, D., Sheth, U., Valencia-Sanchez, M. A., Brengues, M., & Parker, R. (2005). Processing bodies require RNA for assembly and contain nontranslating mRNAs. *RNA (New York, N.Y.)*, *11*, 371–382.

Thakor, N., & Holcik, M. (2012). IRES-mediated translation of cellular messenger RNA operates in eIF2α- independent manner during stress. *Nucleic Acids Research*, *40*, 541–552.

Thomas, M. G., Loschi, M., Desbats, M. A., & Boccaccio, G. L. (2011). RNA granules: the good, the bad and the ugly. *Cellular Signalling*, *23*, 324–334.

Towner, J. S., Pourrut, X., Albariño, C. G., Nkogue, C. N., Bird, B. H., Grard, G., et al. (2007). Marburg virus infection detected in a common African bat. *PloS One*, *2*, e764.

Towner, J. S., Sealy, T. K., Khristova, M. L., Albariño, C. G., Conlan, S., Reeder, S. A., et al. (2008). Newly Discovered Ebola Virus Associated with Hemorrhagic Fever Outbreak in Uganda. *PLoS Pathogens*, *4*, e1000212–6.

Trunschke, M., Conrad, D., Enterlein, S., Olejnik, J., Brauburger, K., & Mühlberger, E. (2013). The L-VP35 and L-L interaction domains reside in the amino terminus of the Ebola virus L protein and are potential targets for antivirals. *Virology*, *441*, 135–145.

Valiente-Echeverría, F., Melnychuk, L., & Mouland, A. J. (2012). Viral modulation of stress granules. *Virus Research*, *169*, 430–437.

van Griensven, J., De Weiggheleire, A., Delamou, A., Smith, P. G., Edwards, T., Vandekerckhove, P., et al. (2016a). The Use of Ebola Convalescent Plasma to Treat Ebola Virus Disease in Resource-Constrained Settings: A Perspective From the Field. *Clinical Infectious Diseases : an Official Publication of the Infectious Diseases Society of America*, *62*, 69–74.

van Griensven, J., Edwards, T., de Lamballerie, X., Semple, M. G., Gallian, P., Baize, S., et al. (2016b). Evaluation of Convalescent Plasma for Ebola Virus Disease in Guinea. *The New England Journal of Medicine*, *374*, 33–42.

Varkey, J. B., Shantha, J. G., Crozier, I., Kraft, C. S., Lyon, G. M., Mehta, A. K., et al. (2015). Persistence of Ebola Virus in Ocular Fluid during Convalescence. *The New England Journal of Medicine*, *372*, 2423–2427.

Villinger, F., Rollin, P. E., Brar, S. S., Chikkala, N. F., Winter, J., Sundstrom, J. B., et al. (1999). Markedly elevated levels of interferon (IFN)-gamma, IFN-alpha, interleukin (IL)-2, IL-10, and tumor necrosis factor-alpha associated with fatal Ebola virus infection. *The Journal of Infectious Diseases*, *179 Suppl 1*, S188–91.

Vlasova-St Louis, I., & Bohjanen, P. R. (2014). Post-Transcriptional Regulation of Cytokine Signaling by AU-Rich and GU-Rich Elements. *Journal of Interferon & Cytokine Research*, *34*, 233–241.

Wang, X., Lv, F., & Gao, G. (2010). Mutagenesis analysis of the zinc-finger antiviral protein. *Retrovirology*, *7*, 19.

Ward, A. M., Bidet, K., Yinglin, A., Ler, S. G., Hogue, K., Blackstock, W., et al. (2011). Quantitative mass spectrometry of DENV-2 RNA-interacting proteins reveals that the DEAD-box RNA helicase DDX6 binds the DB1 and DB2 3' UTR structures. *RNA Biology*, *8*, 1173–1186.

Wauquier, N., Becquart, P., Padilla, C., Baize, S., & Leroy, E. M. (2010). Human fatal zaire ebola virus infection is associated with an aberrant innate immunity and with massive lymphocyte apoptosis. *PLoS Neglected Tropical Diseases*, *4*, e837.

Weik, M., Enterlein, S., Schlenz, K., & Mühlberger, E. (2005). The Ebola virus genomic replication promoter is bipartite and follows the rule of six. *Journal of Virology*, *79*,

10660–10671.

Weik, M., Modrof, J., Klenk, H.-D., Becker, S., & Mühlberger, E. (2002). Ebola virus VP30-mediated transcription is regulated by RNA secondary structure formation. *Journal of Virology*, *76*, 8532–8539.

Wen, X., Huang, X., Mok, B. W.-Y., Chen, Y., Zheng, M., Lau, S.-Y., et al. (2014). NF90 exerts antiviral activity through regulation of PKR phosphorylation and stress granules in infected cells. *Journal of Immunology (Baltimore, Md. : 1950)*, *192*, 3753–3764.

Whelan, S. P. J., Barr, J. N., & Wertz, G. W. (2004). Transcription and replication of nonsegmented negative-strand RNA viruses. *Current Topics in Microbiology and Immunology*, *283*, 61–119.

White, J. P., & Lloyd, R. E. (2011). Poliovirus unlinks TIA1 aggregation and mRNA stress granule formation. *Journal of Virology*, *85*, 12442–12454.

White, J. P., & Lloyd, R. E. (2012). Regulation of stress granules in virus systems. *Trends in Microbiology*, *20*, 175–183.

White, J. P., Cardenas, A. M., Marissen, W. E., & Lloyd, R. E. (2007). Inhibition of cytoplasmic mRNA stress granule formation by a viral proteinase. *Cell Host & Microbe*, *2*, 295–305.

Wong, G., Kobinger, G. P., & Qiu, X. (2014). Characterization of host immune responses in Ebola virus infections. *Expert Review of Clinical Immunology*, *10*, 781–790.

World Health Organization. (2016, January 20). Ebola Siutation Report. Retrieved January 21, 2016, from http://apps.who.int/iris/bitstream/10665/204172/1/ebolasitrep_20Jan2016_eng.pdf?ua=1

Wu, X., & Brewer, G. (2012). The regulation of mRNA stability in mammalian cells: 2.0. *Gene*, *500*, 10–21.

Xia, J., Chen, X., Xu, F., Wang, Y., Shi, Y., Li, Y., et al. (2015). Dengue virus infection induces formation of G3BP1 granules in human lung epithelial cells. *Archives of Virology*, 1–9.

Xu, W., Edwards, M. R., Borek, D. M., Feagins, A. R., Mittal, A., Alinger, J. B., et al. (2014). Ebola virus VP24 targets a unique NLS binding site on karyopherin alpha 5 to selectively compete with nuclear import of phosphorylated STAT1. *Cell Host & Microbe*, *16*, 187–200.

Yamasaki, S., & Anderson, P. (2008). Reprogramming mRNA translation during stress. *Current Opinion in Cell Biology*, *20*, 222–226.

Yeh, S., Varkey, J. B., & Crozier, I. (2015). Persistent Ebola Virus in the Eye. *The New England Journal of Medicine*, *373*, 1982–1983.

Zaki, S. R., & Goldsmith, C. S. (1999). Pathologic features of filovirus infections in humans. *Current Topics in Microbiology and Immunology*, *235*, 97–116.

Zhao, W., Liu, M., & Kirkwood, K. L. (2008). p38alpha stabilizes interleukin-6 mRNA via multiple AU-rich elements. *The Journal of Biological Chemistry*, *283*, 1778–1785.

Zhao, W., Liu, M., D'Silva, N. J., & Kirkwood, K. L. (2011). Tristetraprolin regulates interleukin-6 expression through p38 MAPK-dependent affinity changes with mRNA 3' untranslated region. *Journal of Interferon & Cytokine Research : the Official Journal of the International Society for Interferon and Cytokine Research*, *31*, 629–637.

Zhu, Y., Cherukuri, N. C., Jackel, J. N., Wu, Z., Crary, M., Buckley, K. J., et al. (2012). Characterization of the RNA silencing suppression activity of the Ebola virus VP35 protein in plants and mammalian cells. *Journal of Virology*, *86*, 3038–3049.

CURRICULUM VITAE

EMILY VICTORIA NELSON
(b. 1988)

40 QUEENSBERRY ST, APT 21
BOSTON, MA 02215
(937) 286-5443
nelsonemilyv@gmail.com

EDUCATION

2010-2016 — BOSTON UNIVERSITY SCHOOL OF MEDICINE, Boston, MA
Doctor of Philosophy, Microbiology and Immunology
Advisor: Elke Mühlberger, Ph.D., Associate Professor of Microbiology, Director, Biomolecule Production Core, National Emerging Infectious Diseases Laboratories (NEIDL)

2006-2010 — THE GEORGE WASHINGTON UNIVERSITY, Washington, DC
Bachelor of Science, Biological Sciences
Minor: Public Health

RESEARCH EXPERIENCE

09/2010-Present — BOSTON UNIVERSITY SCHOOL OF MEDICINE, Boston, MA
Doctoral Dissertation Research
Advisor*:* Elke Mühlberger, Ph.D.
Thesis topic: Examination of the cellular stress response and post-transcriptional regulation of RNA during Ebola Virus infection

03/2010- 05/2010 — NATIONAL INSTITUTE OF ALLERGERY AND INFECTIOUS DISEASE, VACCINE RESEARCH CENTER (VRC), Bethesda, MD
Undergraduate Research Volunteer
Advisor: Daniel Douek, M.D., PH.D.,
Research topic: Next-generation sequencing of T cell receptor immune repertoires during HIV infection

05/2008-05/2010 — THE GEORGE WASHINGTON UNIVERSITY
Undergraduate Research Assistant/Howard Hughes Research Fellow
Advisor: John Hawdon, Ph.D.

Research topic: Determining genetic variation among geographically distant hookworm (*N. americanus*) populations

PROFESSIONAL EXPERIENCE

07/2015-08/2015 DUTCH MOBILE EBOLA LABORATORY, Koidu City, Sierra Leone
PARTNERS IN HEALTH
Ebola Virus Diagnostic Scientist

- Performed PCR based Ebola virus diagnostics in a BSL-3 mobile laboratory
- Provided training for local hospital staff on Ebola virus disease, proper sample handling, and laboratory safety
- Also performed rapid test for Malaria on blood samples received

07/2014-Present NATIONAL EMERGING INFECTIOUS DISEASES LABORATORIES
Course Director: Infectious Disease Detectives

- Part of a team that designed and implemented an afterschool curriculum for middle school aged children to teach them about the basics of infectious diseases
- Trained new team members to ensure continuity and efficiency

TEACHING/MENTORING EXPERIENCE

10/2015-12/2014 BOSTON UNIVERSITY SCHOOL OF MEDICINE
Teaching Assistant
Course: Foundations in Biomedical Science

06/2015-08/2014 BOSTON UNIVERSITY
Research Mentor
Research Internship in Science and Engineering (RISE) program

01/2013-05/2014 BOSTON UNIVERSITY SCHOOL OF DENTISTRY
Tutor
Course: Dental Microbiology and Immunology

09/2013-12/2013 BOSTON UNIVERSITY METROPOLITAN COLLEGE
Teaching Assistant: Laboratory Skills
Course: Introduction to Biomedical Sciences

AWARDS AND HONORS

2015 BUSM Graduate Medical Sciences, Travel Award

2014	BUSM Department of Microbiology, Corwin Award for Service to the Department
2014	Boston University Scholars Day, Office of Technology Development Award
2012	Competitive Appointment to NIH T32- Host Pathogens Interactions Training Program
2012	BUSM Graduate Medical Sciences, Travel Award
2010	Competitive Appointment to NIH T32- Immunology Training Program

SERVICE TO THE UNIVERSITY:

2010-2015	Recruitment Day Ambassador *Boston University School of Medicine*
2014-2015	Community Outreach Volunteer, *National Emerging Infectious Disease Laboratories*
2013-2015	Peer Mentor, *Program in Biomedical Sciences (PiBS)*
2013-2014	Journal Club Coordinator, *Department of Microbiology*

PUBLICATIONS

1. **Nelson, E.V**., Schmidt, K.M., Deflubé-Owen, L., Doganay, S., Banadyga, L., Olejnik, J., Ryabchikova, E., Ebihara, H., Kedershan, N., Ha, T., Mühlberger, E., *Ebola Virus Sequesters Stress Granule Proteins during Infection and Prevents Canonical Stress Granule Formation within Viral Inclusions.* 2016. **In Submission**.

2. Schmidt, K.M, **Nelson, E.V.** *Analyzing stress responses to infection*. Methods in Molecular Biology. Springer, 2016. **In preparation**

ABSTRACTS PRESENTED

1. **Nelson, E.V.,** Schmidt, K.M., Deflubé, L., Banadyga, L., Ebihara, H., Mühlberger, E., *The Cellular Stress Response as an Antiviral Mechanism During Ebola Virus Infection*. Negative Strand Virus Meeting. Siena, Italy. June 2015.

2. **Nelson, E.V.,** Schmidt, K. M., Mühlberger, E. *Post-transcriptional Regulation of RNA During Ebola Virus Infection.* Boston University School of Medicine, Henry I. Russek Student Achievement Day. Boston, MA. May 2015.

3. **Nelson, E.V,** Schmidt, K. M., Mühlberger, E. *Post-transcriptional Regulation of RNA During Ebola Virus Infection.* Federation of American Societies for Experimental Biology, Post-transcriptional Control of Gene Expression: Mechanisms of mRNA degradation. Big Sky, MT. July 2014.

4. **Nelson, E.V.,** Schmidt, K. M., Mühlberger, E. *Post-transcriptional Regulation of RNA During Ebola Virus Infection.* Boston University School of Medicine, Henry I. Russek Student Achievement Day. Boston, MA. April 2014.

5. **Nelson, E.V.,** Schmidt, K. M., Mühlberger, E. 2014. *Post-transcriptional Regulation of RNA During Ebola Virus Infection*. Boston University, Scholars Day. Boston, MA. March 2014.

6. **Nelson, E.V.,** Schmidt, K.M., Deflubé, L., Mühlberger, E. 2014. *Post-transcriptional Regulation of RNA During Ebola Virus Infection*. International Symposium on Filoviruses. Galveston, TX. March 2014.

ORAL PRESENATIONS

Nelson, E.V., Schmidt, K. M., Deflubé, L., Mühlberger, E**.** *Examining the Cellular Stress Response during Ebola virus Infection*, Bernhard Nocht Institute for Tropical Medicine, Invited speaker. Hamburg, Germany, November 2015

Nelson, E.V., Schmidt, K. M., Deflubé, L., Mühlberger, E**.** *Diversion of Cellular Stress Response Proteins during Ebola Virus Infection*, Boston University School of Medicine, Department of Microbiology, Molecular Pathogenesis and Host Defense Seminar Series. Boston, MA, October 2014

Nelson, E.V., Schmidt, K. M., Deflubé, L., Mühlberger, E. *Work in Progess: Sequestration of Cellular Stress Proteins during Ebola Virus Infection*. Boston University School of Medicine, Negative Strand Virus Group Meeting. Boston, MA, October 2014

Nelson, E.V., Schmidt, K. M., Mühlberger, E. *Post-transcriptional Regulation of RNA during Ebola Virus Infection*. International Graduate Student Immunology Conference. Marseille, France. August 2013.

Nelson, E.V., Schmidt, K. M., Mühlberger, E. *Post-transcriptional Regulation of RNA during Ebola Virus Infection*. Boston University School of Medicine, Department of Microbiology, Molecular Pathogenesis and Host Defense Seminar Series. Boston, MA, November 2013

Nelson, E.V., Mühlberger, E. *Post-transcriptional Regulation of RNA during Ebola Virus Infection*. Boston University School of Medicine, Department of Microbiology, Molecular Pathogenesis and Host Defense Seminar Series. Boston, MA, February 2013